

Results & Discussion

Results and discussion

➤ **SPECTROPHOTOMETRIC STUDIES OF DRUG COMPLEXES IN SOLUTION**

I- Absorption spectra of sulfamethoxazole with reagents I, III and IV:-

In order to investigate the optimum conditions of drug-reagent complex formation, the following studies should be taken in consideration:

1. Effect of pH:

The effect of pH on the complex formation between sulfamethoxazole and reagents o-chloranil, 2,4 dinitrophenol and picric acid (I, III and IV, respectively) was studied in universal buffer solutions of pH range 3.35-11.15. A portion (1.0 mL) of 5.0×10^{-3} M reagent I or 1.0 mL of 1.0×10^{-2} M reagent III or IV, 1.0 mL of (200 $\mu\text{g/mL}$) drug and 3.0 mL buffer of different pH values were mixed well. The volume was completed to 10 mL with bidistilled water. The absorption spectra were recorded using a blank solution prepared in the same way without drug at the same pH value. Illustrative spectra are shown in Figs. (1-a), (2-a) and (3-a) for reagents I, III and IV respectively. Inspection of these figures shows that the optimum pH values giving maximum absorption recommended for subsequent studies of drug-reagent complexes, are 8.23, 5.25 and 11.15 on using reagents I, III and IV, respectively.

2. Determination of λ_{max} of complex species :

For determining the value of λ at which complex species possesses the maximum absorption, the following spectra must be recorded:

- A- Spectrum of pure drug 1.0 mL of 200 $\mu\text{g/mL}$ at the optimum pH value using buffer solution at the recommended pH value as a blank.
- B- Spectrum of pure reagent 1.0 mL of 5.0×10^{-3} M for reagent I or 1.0 mL of 1.0×10^{-2} M for reagents III and IV at the optimum pH value using the same buffer as a blank.
- C- Spectrum of solution mixture of drug (A) and reagent of (B) at the optimum pH value using the same buffer as a blank.
- D- Spectrum of solution (C) against (B) as a blank.

The absorption spectra are shown in Figs (1-b), (2-b) and (3-b) for reagents I, III and IV, respectively. Such figures show that the formed complex absorbed maximally at 550, 440 and 450 nm for the three reagents, respectively. These optimal wavelengths are chosen for further investigations.

3. Effect of time and temperature:

The effect of time on complex formation was studied by measuring the absorbance of the complexes at optimum pH against a blank solution of the same pH at various time intervals. Also, the effect of temperature was studied for the same solution by incubating the sample and blank in a water bath at different temperatures (25-45 °C). The absorbance was measured after cooling to room temperature.

The experiments showed that complexes are formed simultaneously after mixing drug and reagent and remain stable for about two hours. Also, it

was found that, increasing the temperature up to 45 °C has a slight effect on the absorbance above which the colour began to fade slowly.

4. Effect of sequence of addition:

The effect of sequence of addition on complex formation was studied by measuring the absorbance of solutions prepared by different sequences of addition against a blank solution prepared in the same manner. Experiments showed that the best sequence of addition is drug-buffer-reagent.

5. Effect of reagent concentration:

To study the effect of reagents I, III and IV concentration on the complex formation, the concentration of drug was kept constant at 200 µg/mL while that of reagent was varied regularly. The resulted spectra showed that 1.0 mL of 5.0×10^{-3} M of reagent I and 1.0×10^{-2} M of reagent III or IV is sufficient for complete complexation.

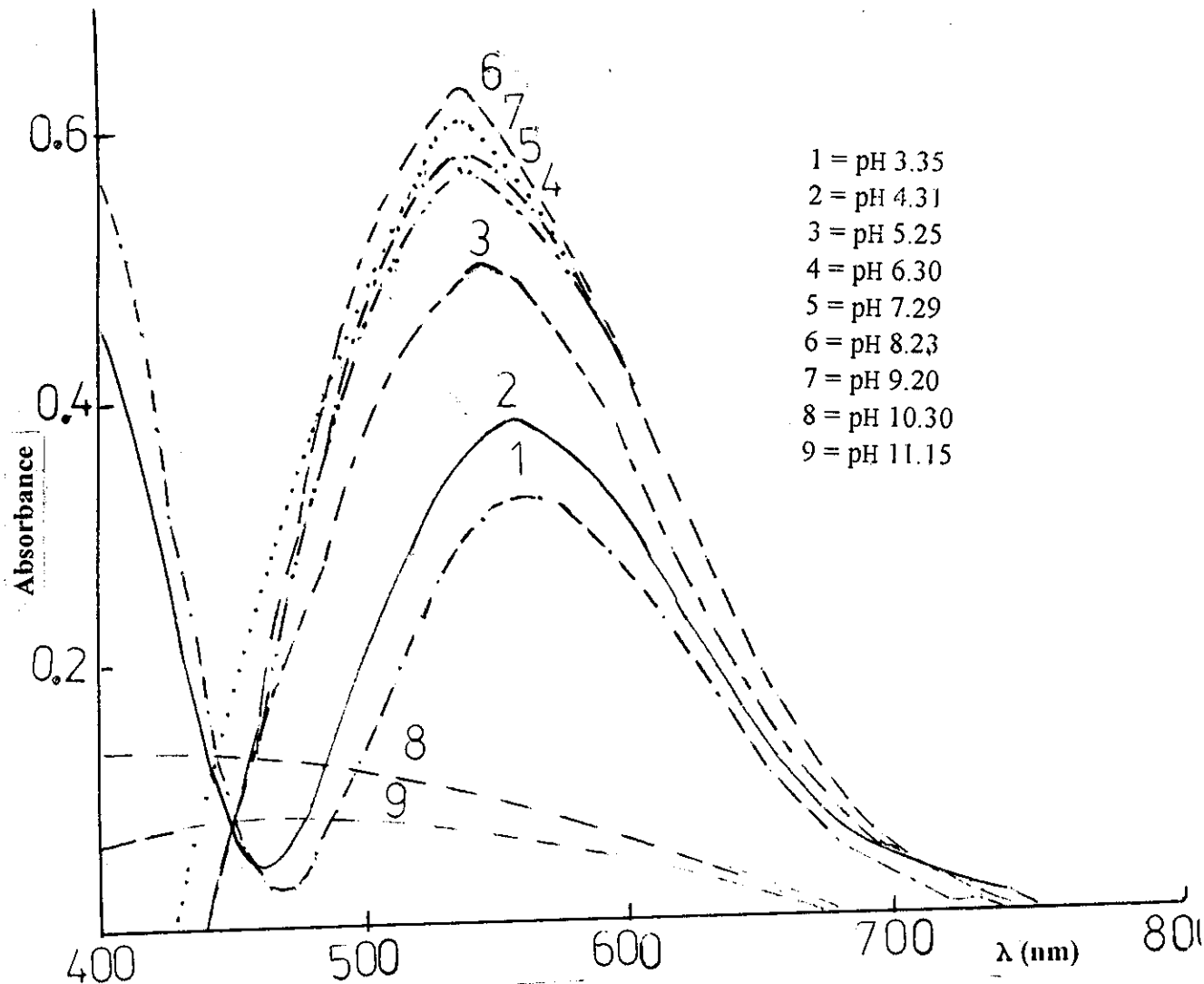


Fig. (1-a) Effect of pH on the absorption spectra of sulfamethoxazole - o-chloranil complex.

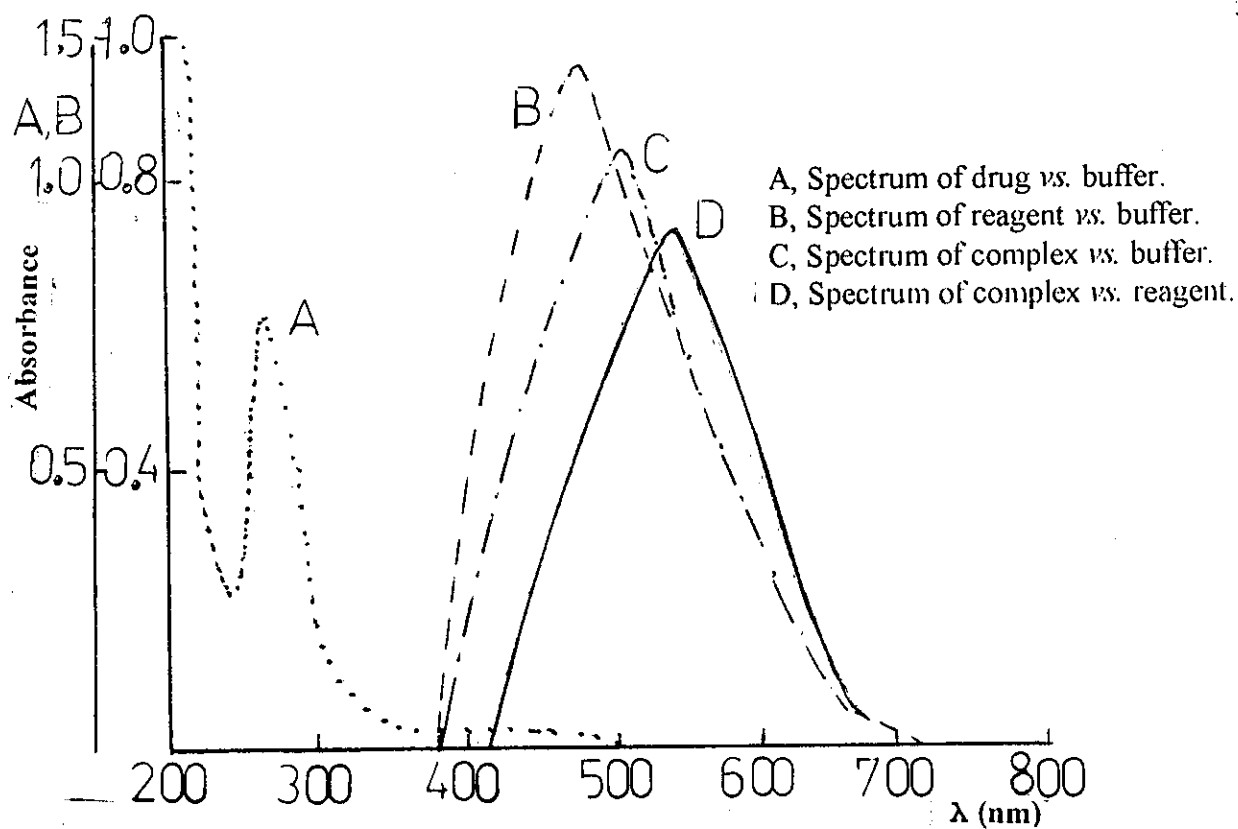


Fig. (1-b) Determination of λ_{max} of sulfamethoxazole- o-chloranil complex at pH 8.23.

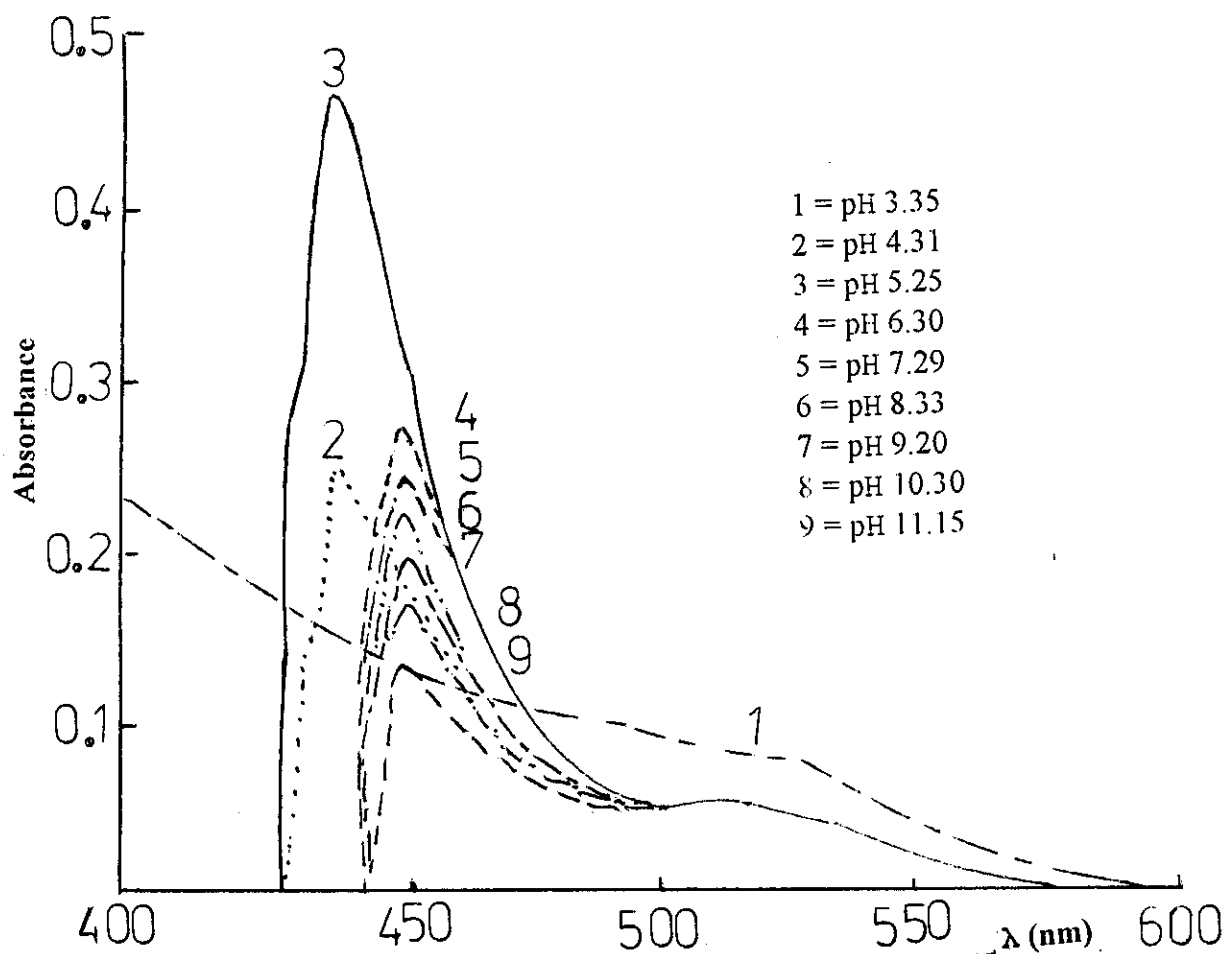


Fig. (2-a) Effect of pH on the absorption spectra of sulfamethoxazole - 2,4 dinitrophenol complex.

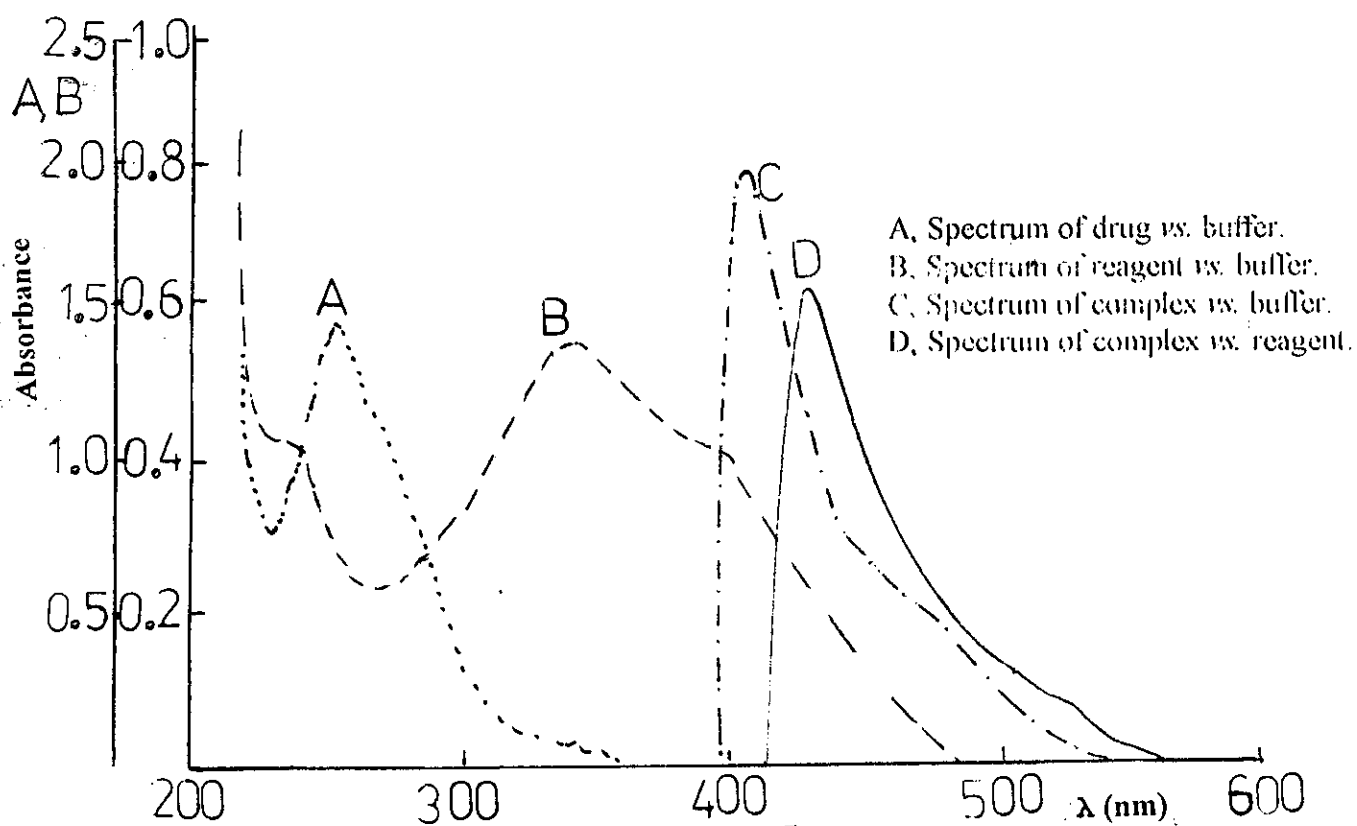


Fig. (2-b) Determination of λ_{max} of sulfamethoxazole- 2,4 dinitrophenol complex at pH 5.25.

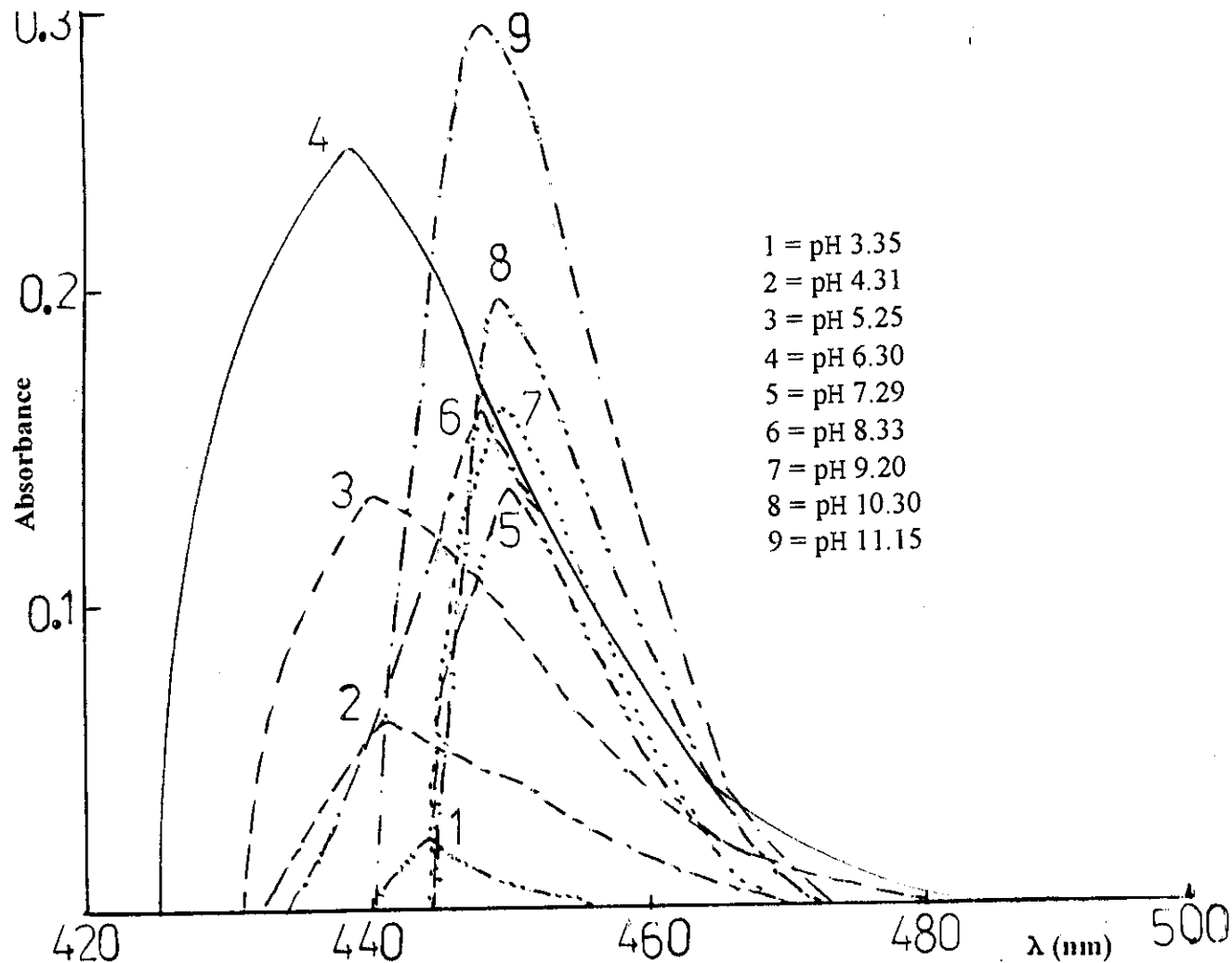


Fig. (3-a) Effect of pH on the absorption spectra of sulfamethoxazole - picric acid complex.

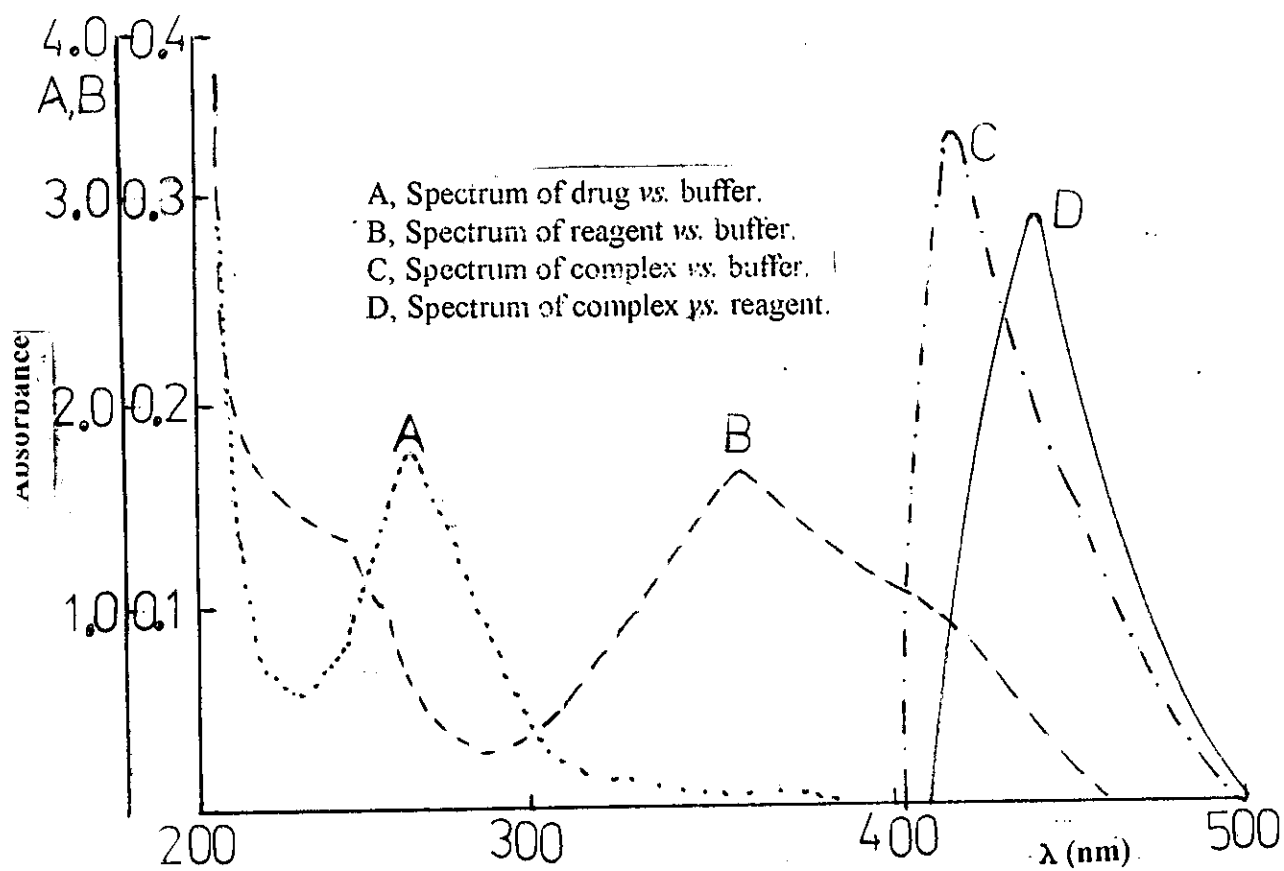


Fig. (3-b) Determination of λ_{max} of sulfamethoxazole- picric acid complex at pH 11.15.

6. Stoichiometry of complexes:

The stoichiometries of the complexes formed between sulfamethoxazole and reagents I, III and IV were determined using the following two methods:

(i) Mole ratio method:

The molar ratio method, described by *Yeo and Jones*⁽³⁸⁾ was used to study the molecular composition of complexes between sulfamethoxazole with reagents I, III and IV. A portion (1.0 mL) of 5.0×10^{-3} M of I or 1.0 mL of 1.0×10^{-2} M of III or IV was mixed with variable volumes of drug, 3.0 mL of buffer at optimum pH, then the volume was completed to 10 mL with bidistilled water. The absorbance was measured at the recommended wavelength against blank solution prepared in the same manner. The absorbance values were plotted against the mole ratio (D/R) as shown in Fig. (4). Experimental results revealed that the complexes formed have 1:1 stoichiometric ratio.

(ii) Continuous variation method:

A modification of *Jopes* continuous variation method⁽³⁹⁾ performed by *Vosburgh and Cooper*⁽⁴⁰⁾ was used for investigating the reaction between the drug and reagents. Different volumes of 5.0×10^{-3} or 1.0×10^{-2} M of drug and reagent were mixed with keeping the total molar concentration constant. 3.0 mL buffer solution of the selected pH was added, then the volume was completed to 10 mL with bidistilled water. The absorbance was measured at the optimum wavelengths and then plotted against the mole fraction of reagent as shown in Fig. (5). Results obtained revealed that the complexes are formed in stoichiometric ratio 1: 1.

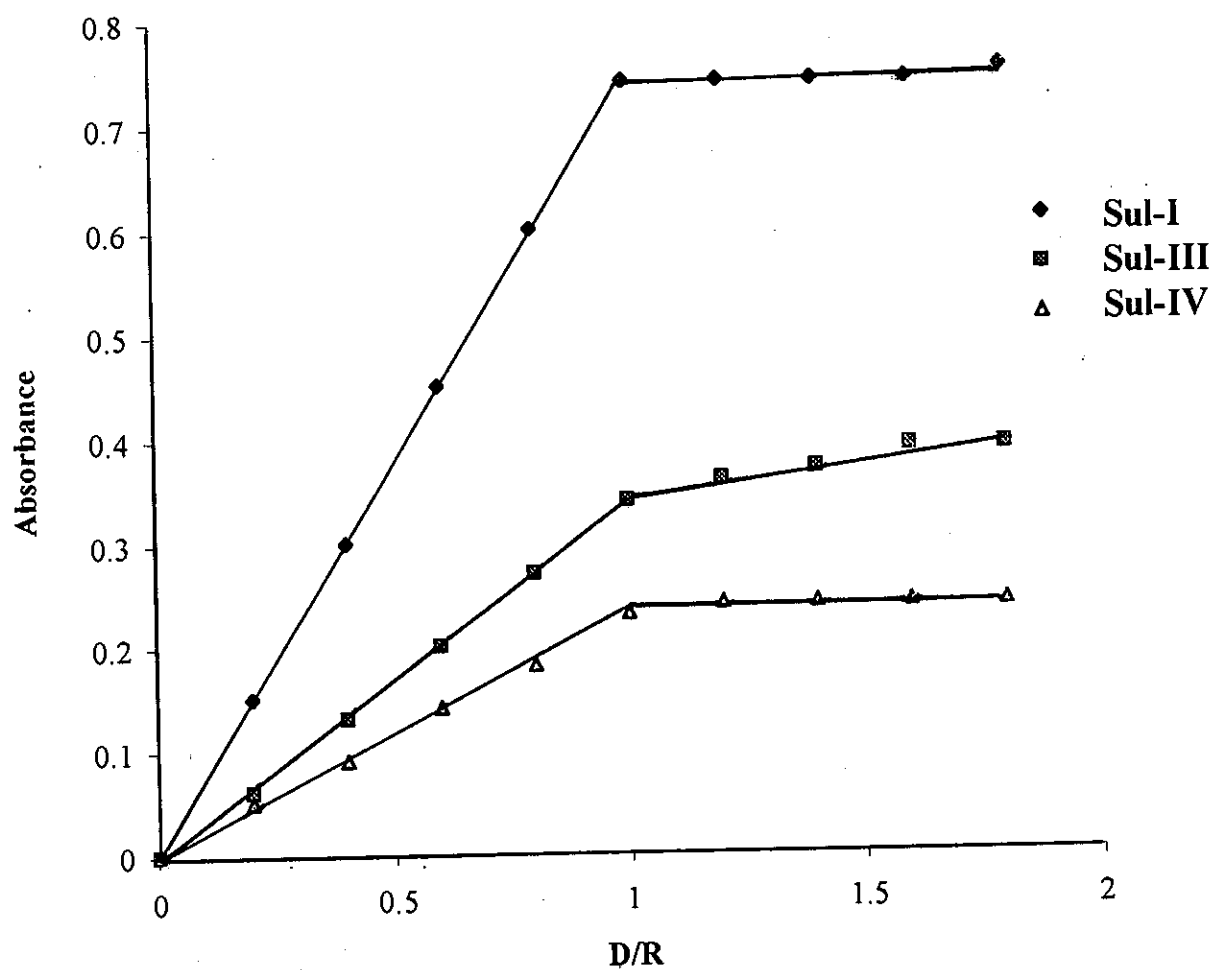


Fig. (4): Mole ratio for sulfamethoxazole with reagents I, III and IV.

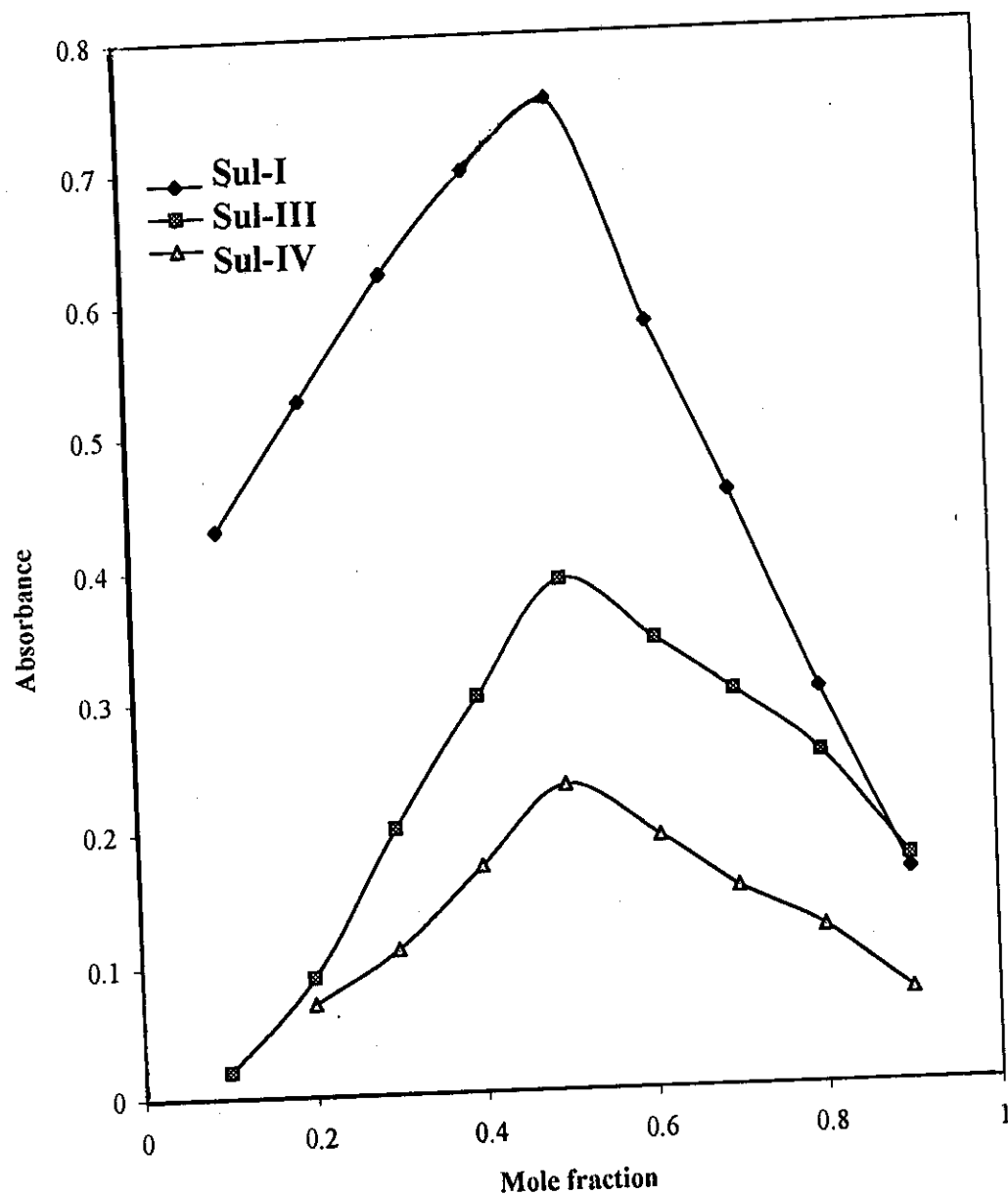


Fig. (5) Continuous variation for sulfamethoxazole with reagents I, III and IV.

7. Stability constants of complexes:

Spectrophotometric methods can be applied for the determination of the stability constant of complexes. The overall formation constants of the concerned complexes were calculated using the data of the mole ratio and continuous variation methods applying the mole ratio equation of *Yeo and Jones*⁽³⁸⁾ as modified by *Issa et al*⁽⁴⁶⁾.

$$K_n = \frac{(A/A_{max})}{[1 - (A/A_{max})]^{n+1} C_D^n n^2}$$

Where:

- A : the absorbance at drug concentration C_D
- A_{max} : the absorbance of maximum value.
- n : the stoichiometric ratio of the complex
- K_n : the stability constant

The calculated stability constants are listed in Table (1), from which it is found that reagent I forms the most stable complex with sulfamethoxazole followed by reagent III and then reagent IV.

Table (1): Stoichiometric ratios and stability constants of sulfamethoxazole complexes obtained from spectrophotometric methods.

Complex	pH	λ_{max} (nm)	<u>Mole ratio</u>		<u>Continuous variation</u>	
			Ratio	Log k	Ratio	Log k
Sul-I	8.23	550	1 : 1	4.05	1 : 1	4.10
Sul-III	5.25	440	1 : 1	2.26	1 : 1	2.27
Sul-IV	11.15	450	1 : 1	1.88	1 : 1	1.64

Where:

I, o-cholranil; III, 2,4 dinitrophenol and IV, picric acid

8. Validity to Beer's law:

Under optimum conditions of pH, reagent concentration, sequence of addition, time and temperature for each of the different complexes, different concentrations of drug ($\mu\text{g/mL}$) were transferred into 10 mL measuring flask. 1.0 mL reagent (5.0×10^{-3} M for I or 1.0×10^{-2} M for III or IV), 3.0 mL of the optimum pH value buffer was added and then completed to volume with bidistilled water. The absorbance was measured at optimum λ_{max} , then plotted against drug concentration as shown in Fig. (6). Limits of Beer's law, the molar absorptivity (ϵ ; $\text{L mol}^{-1}\text{cm}^{-1}$) and *Sandell*⁽⁴⁷⁾ sensitivity results are listed in Table (2) indicating high sensitivity in the microdetermination of the drug.

For more accurate analysis, *Ringbom*⁽⁴⁸⁾ optimum concentration range was determined by calculating the transmittance percent from the following equation:

$$T \% = 10^{-A} \times 100$$

Where:

T % : transmittance percent

A : the absorbance of the complex

By plotting logarithm of drug concentration ($\text{Log}[C_D]$) in $\mu\text{g/mL}$ against T % as in Fig. (7), the linear portion of the S-shaped curve gave an accurate range of analysis. Results are listed in Table (2).

9. Interference:

The effect of the presence of co-existing additives and excipients such as sodium acetate, bicarbonate, magnesium stearate, talc powder, starch, glucose, fructose, sucrose and lactose was studied by adding an excess amount of each of them to a solution containing 10 $\mu\text{g/mL}$ of sulfamethoxazole. Study of the

effect of interfering species showed that such ingredients; up to 10 %, do not interfere in the determination of sulfamethoxazole indicating that complexation does not occur with those additives under reaction conditions.

10. Accuracy and precision:

To determine the accuracy and precision of the proposed method, solutions of certain concentration were prepared and analyzed in six replicates. The percentage standard deviation (RSD %) and the percentage range of error (RE %) at 95 % confidence level were calculated and listed in Table (2). The results can be considered as very satisfactory for the examined concentration levels.

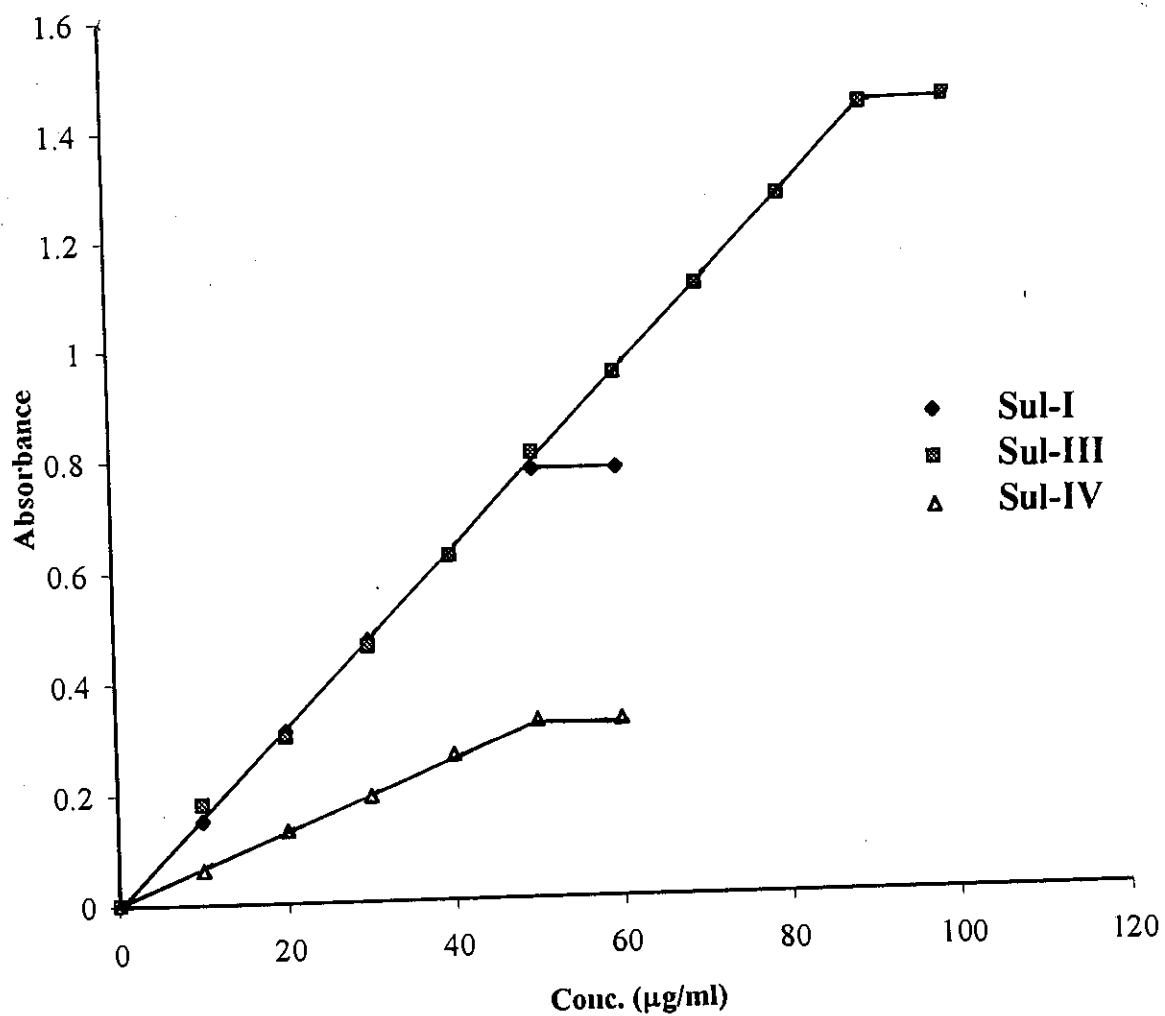


Fig. (6) Beer's assay range for sulfamethoxazole with reagents I, III and IV.

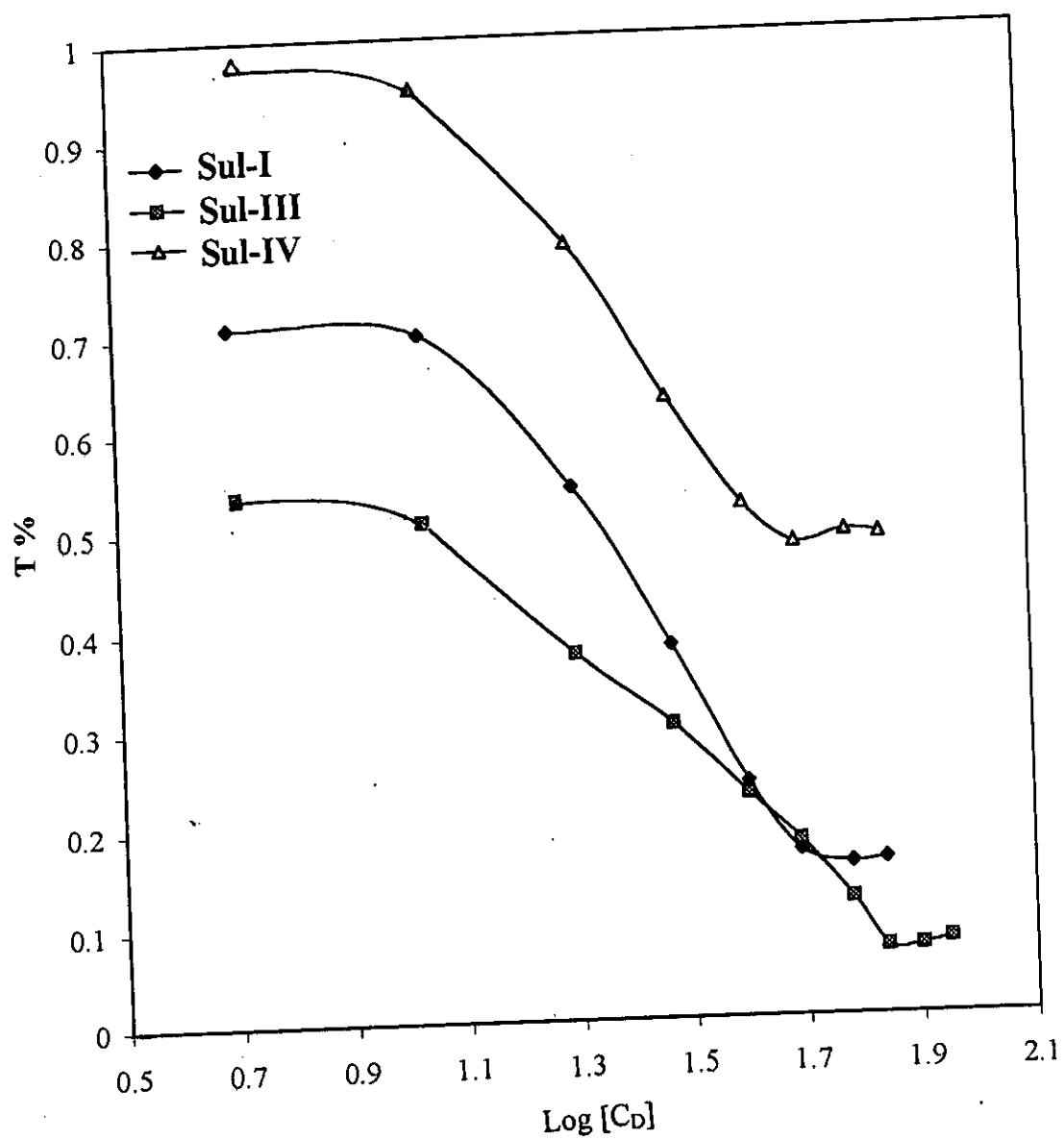


Fig. (7) Ringbom detection limits for sulfamethoxazole with reagents I, III and IV.

Table (3-a): Evaluation of accuracy and precision of the proposed method for Sulfamethoxazole determination in Sutrim tablets.

Reagent	Taken ($\mu\text{g/mL}$)	Found		Recovery %	R.S.D. %	R.E. %	t value	F value
		O	P					
I	30	29.88	29.80	99.33	0.211	0.222	2.25	1.10
III	30	29.88	29.90	99.66	0.298	0.312	0.46	2.20
IV	30	29.88	29.79	99.30	0.272	0.285	2.19	1.82

*Average of six determinations

$$t = 2.57$$

$$F = 5.05$$

O: Official method

P: Proposed method

Table (3-b): Evaluation of accuracy and precision of the proposed method for Sulfamethoxazole determination in Sutrim suspension.

Reagent	Taken ($\mu\text{g/mL}$)	Found		Recovery %	R.S.D. %	R.E. %	t value	F value
		O	P					
I	30	29.95	29.90	99.66	0.251	0.263	0.96	1.95
III	30	29.95	29.89	99.56	0.361	0.361	1.34	1.04
IV	30	29.95	29.85	99.50	0.313	0.313	1.79	1.37

*Average of six determinations

$$t = 2.57$$

$$F = 5.05$$

O: Official method

P: Proposed method

Table (3-c): Evaluation of accuracy and precision of the proposed method for Sulfamethoxazole determination in Septazole tablets.

Reagent	Taken (µg/mL)	Found		Recovery %	R.S.D. %	R.E. %	t value	F value
		O	P					
I	30	30.09	29.99	99.96	0.270	0.283	2.22	1.16
III	30	30.09	30.02	100.06	0.386	0.405	1.24	2.39
IV	30	30.9	30.00	100.00	0.180	0.189	2.38	1.92

*Average of six determinations

$$t = 2.57$$

$$F = 5.05$$

O: Official method

P: Proposed method

Table (3-d): Evaluation of accuracy and precision of the proposed method for Sulfamethoxazole determination in Septazole suspension.

Reagent	Taken ($\mu\text{g/mL}$)	Found		Recovery %	R.S.D. %	R.E. %	t value	F value
		O	P					
I	30	29.99	29.60	98.70	0.254	0.266	1.03	1.93
III	30	29.99	29.89	99.40	0.346	0.363	1.54	1.03
IV	30	29.99	29.75	99.00	0.301	0.315	1.98	1.38

*Average of six determinations

$$t = 2.57$$

$$F = 5.05$$

O: Official method

P: Proposed method

II- Absorption spectra of lincomycin- HCl with reagents II, III and IV:-

In order to investigate the optimum conditions for the formation of drug complexes with the reagents chloranilic acid, 2,4 dinitrophenol and picric acid (II, III and IV, respectively), the following experimental variables were studied:

1. Effect of pH:

The effect of pH on the formation of complexes of lincomycin hydrochloride with reagents II, III and IV was studied in universal buffer solutions of pH range 3.35-11.15. A portion (1.0 mL) of 1.0×10^{-2} M reagent II, III or IV, 1.0 mL of 200 $\mu\text{g/mL}$ drug and 3.0 mL buffer of different pH values were mixed well, then the volume was completed to 10 mL with bidistilled water. The absorption spectra were recorded using a blank solution having the same ingredients except the drug. The optimum pH value; giving maximum absorption, of drug-reagent complexes were 3.35, 4.31 and 7.29 on using reagents II, III and IV, respectively as shown in Figs. (8-a), (9-a) and (10-a). These values are recommended for subsequent studies.

2. Determination of λ_{max} of Complex species :

For determining the value of λ at which complex species possesses the maximum absorption, the following spectra were recorded:

A- Spectrum of pure drug showed no ultraviolet absorption maximum^(49, 50) (220- 400 m μ).

B-Spectrum of pure reagent 1.0 mL of 1.0×10^{-2} M for reagents II, III and IV at the optimum pH value using the same buffer as a blank.

C-Spectrum of solution mixture of drug of (A) and reagent of (B) at the

optimum pH value using the same buffer as a blank.

D-Spectrum of solution (C) against (B) as a blank.

From curves (A-D), Figs. (8-b), (9-b) and (10-b), the recommended λ_{max} for complexes were estimated and found to be 525, 428 and 440 nm for reagents II, III and IV respectively.

3. Effect of time and temperature:

Experiments on the effect of time showed that complexes were formed on adding reagents to the drug and remained constant for 2 hs. Also no change in the absorbance was recorded on increasing the temperature up to 45 °C after which the colour faded slowly.

4. Effect of sequence of addition:

The effect of sequence of addition on complex formation was studied by measuring the absorbances of solutions prepared by different sequences against a blank solution prepared in the same manner. Experiments showed that the best sequence of addition is drug- buffer- reagent.

5. Effect of reagent concentration:

To study the effect of reagents II, III and IV concentration on the complex formation, the concentration of drug was kept constant at 200 µg/mL while that of reagent was varied regularly. The resulted spectra showed that 1.0 mL of 1.0×10^{-2} M of II, III or IV was sufficient to induce a maximum absorbance.

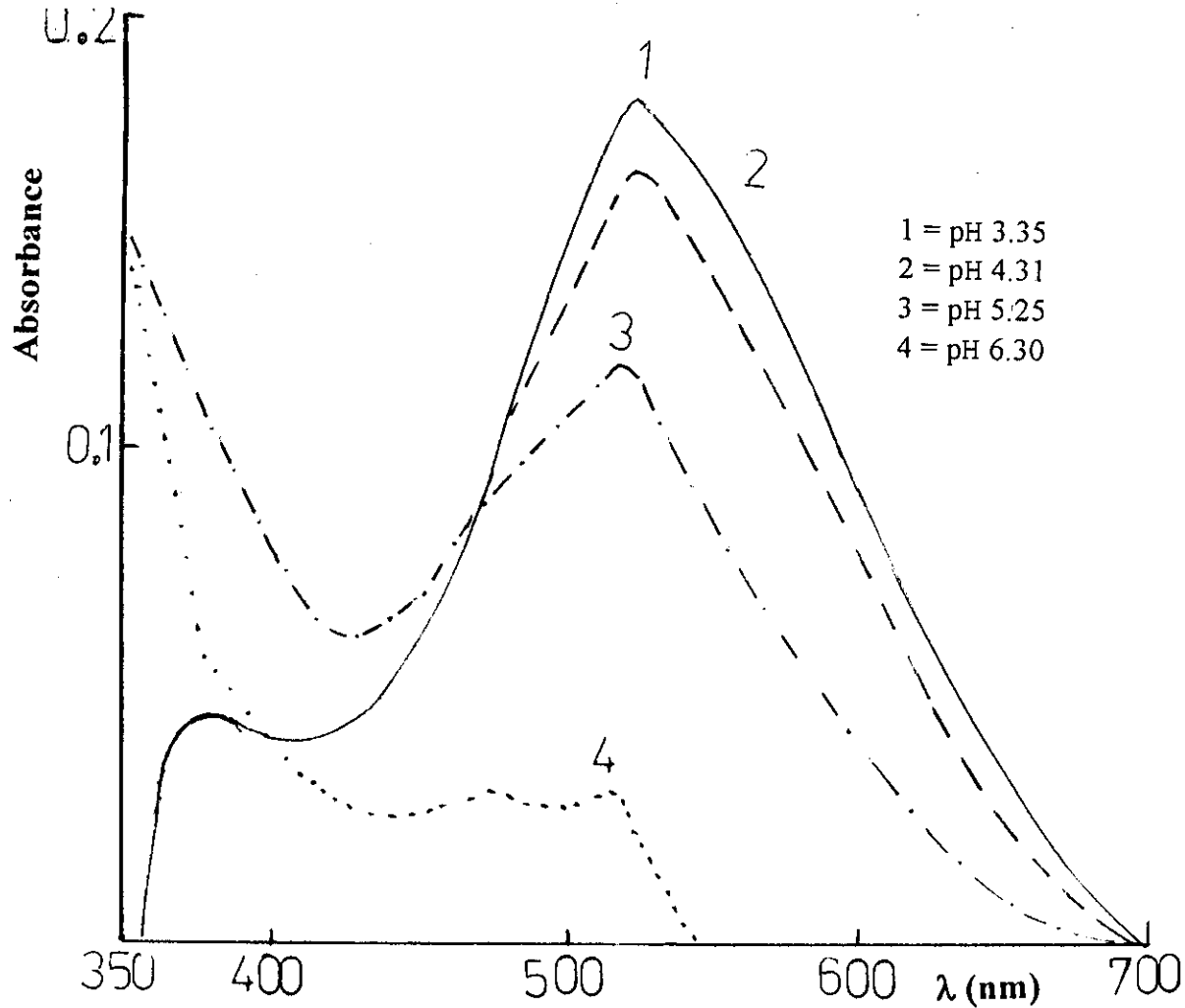


Fig. (8-a) Effect of pH on the absorption spectra of lincomycin HCl-chloranilic acid complex.

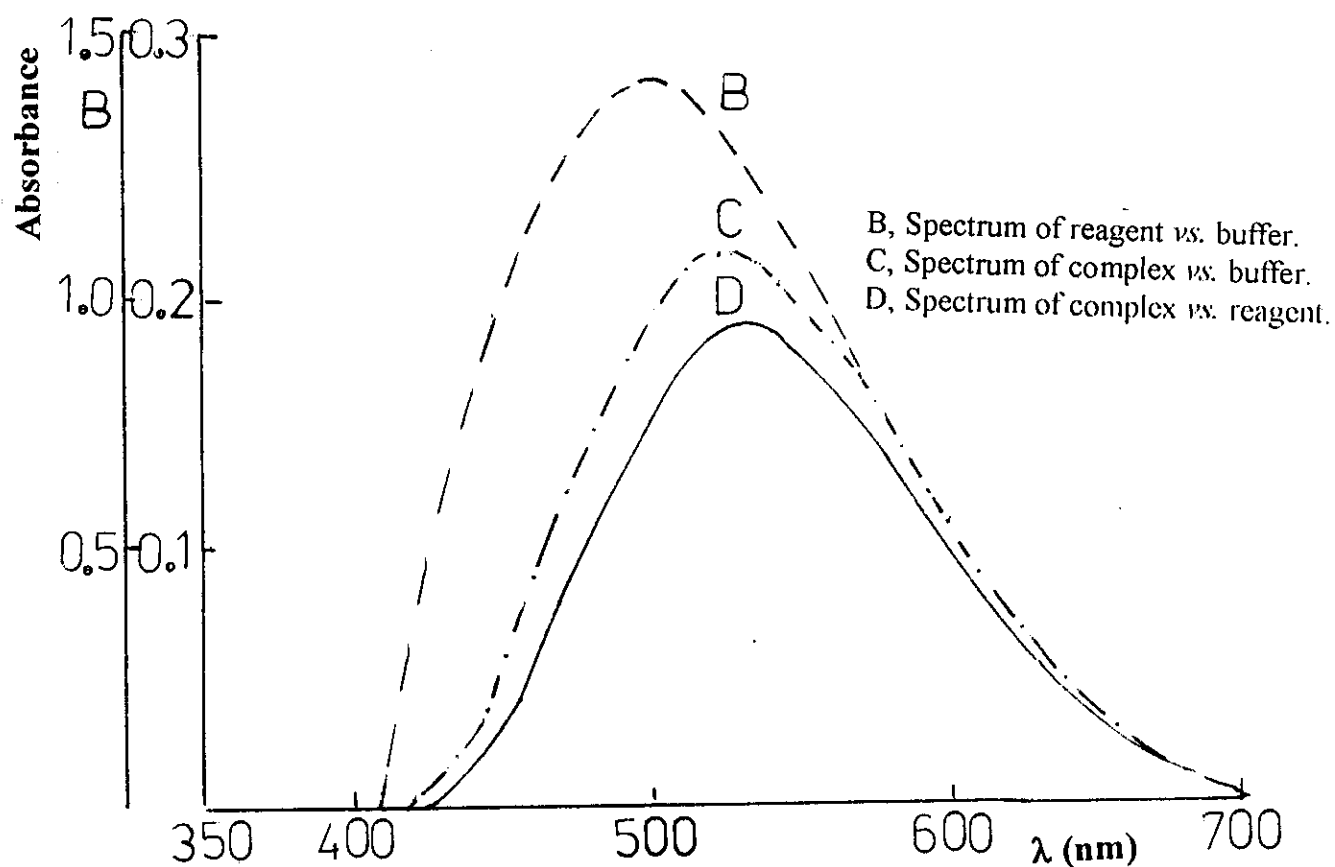


Fig. (8-b) Determination of λ_{max} of lincomycin HCl-chloranilic acid complex at pH 3.35.

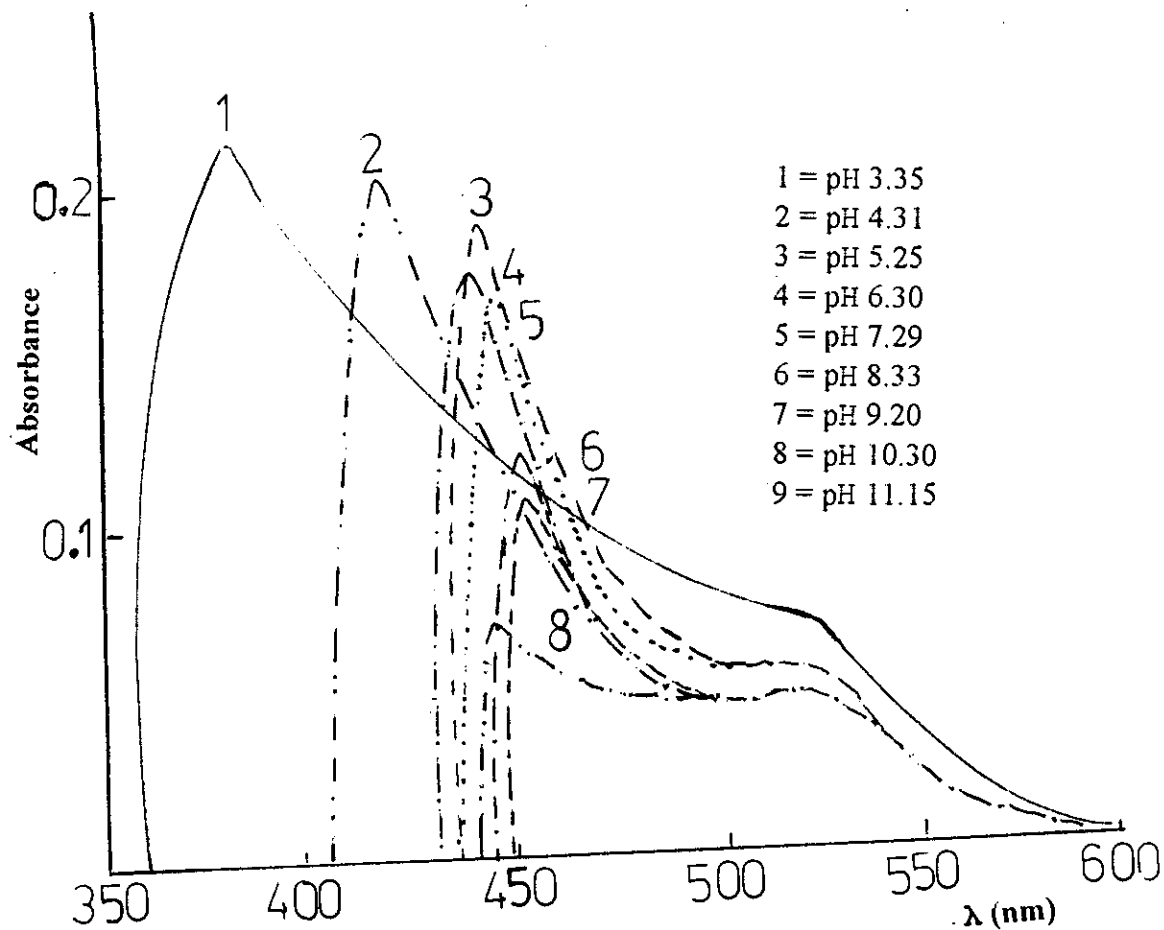


Fig. (9-a) Effect of pH on the absorption spectra of lincomycin HCl-2,4 dinitrophenol complex.

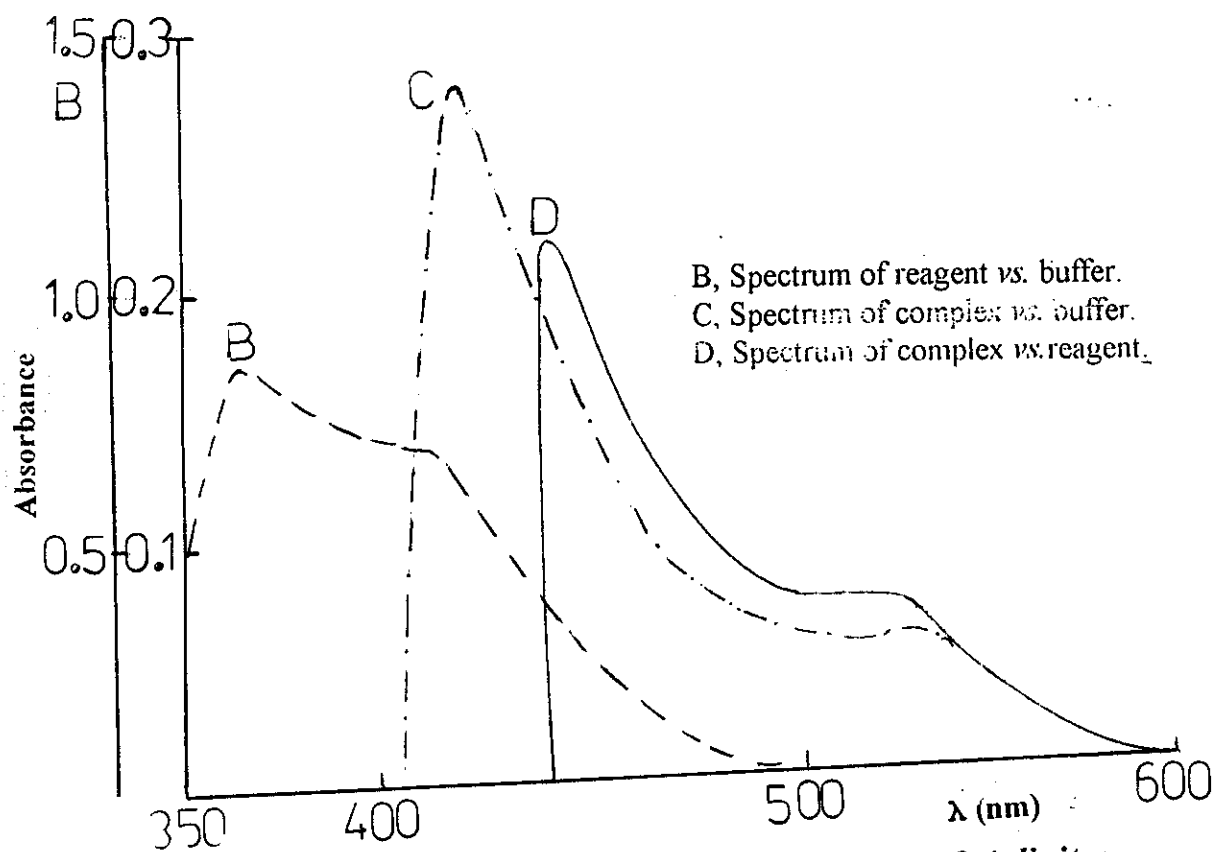


Fig. (9-b) Determination of λ_{max} of lincomycin HCl-2,4 dinitrophenol complex at pH 4.31.

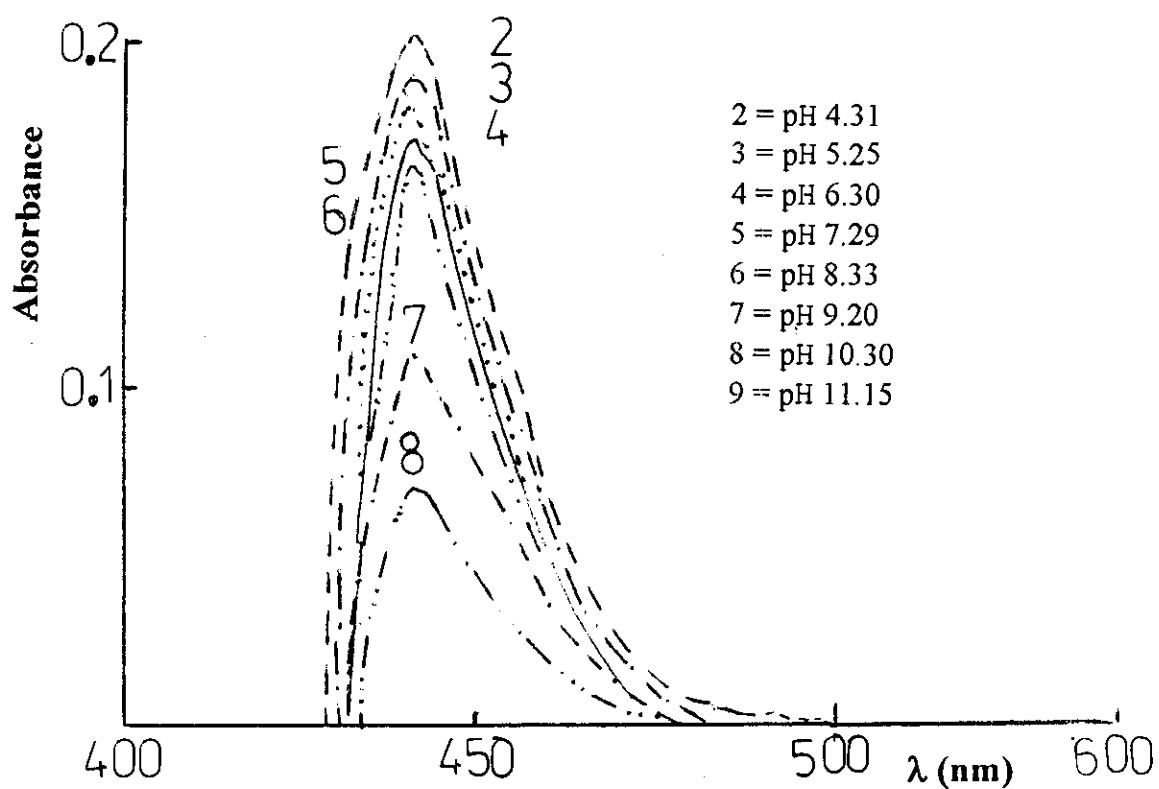


Fig. (10-a) Effect of pH on the absorption spectra of lincomycin HCl-picric acid complex.

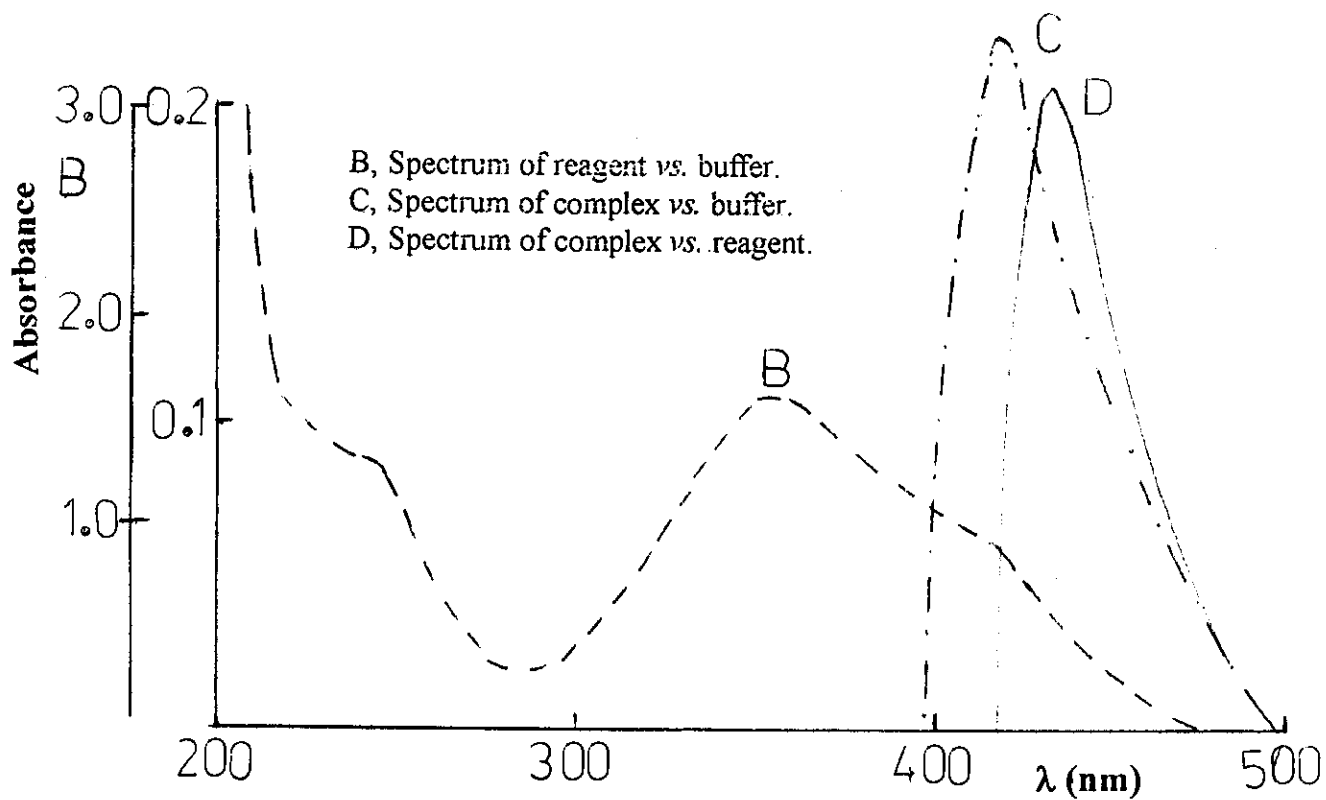


Fig. (10-b) Determination of λ_{max} of lincomycin HCl-picric acid complex at pH 7.29.

6. Stoichiometry of complex:

(i) Mole ratio method:

The mole ratio method was used in studying the molecular composition of complexes between lincomycin hydrochloride and reagents II, III and IV. A portion (1.0- mL) of 1.0×10^{-2} M of II, III or IV was mixed with variable volumes of drug (0.1, 0.2,, 1.0 mL of drug of the same concentration). 3.0 mL of the selected pH buffer was added, then the volume was completed to 10 mL with bidistilled water. The absorbance was then measured at the recommended wavelength against blank solution prepared in the same manner. The absorbance values were plotted against the mole ratio (D/R) as shown in Fig. (11). Experimental results revealed that complexes formed as 1:1 and 2:1 ratio (D/R) with reagent II, 1:1 ratio (D/R) with reagents III and IV.

(ii) Continuous variation method:

Different volumes (0.1, 0.2,, 0.9 mL) of 1.0×10^{-2} M of drug and reagent were mixed while keeping the total molar concentration constant. 3.0 mL of buffer solution at the selected pH value were added, then the volume was completed to 10 mL with bidistilled water. The absorbance was measured and plotted against the mole fraction of reagent as shown in Fig. (12). Results obtained revealed the formation of complexes of two stoichiometric ratios (D/R) 1:1 and 2:1 in case of reagent II, while only one complex of ratio 1:1 on using reagents III and IV. These results confirm those obtained from the mole ratio method.

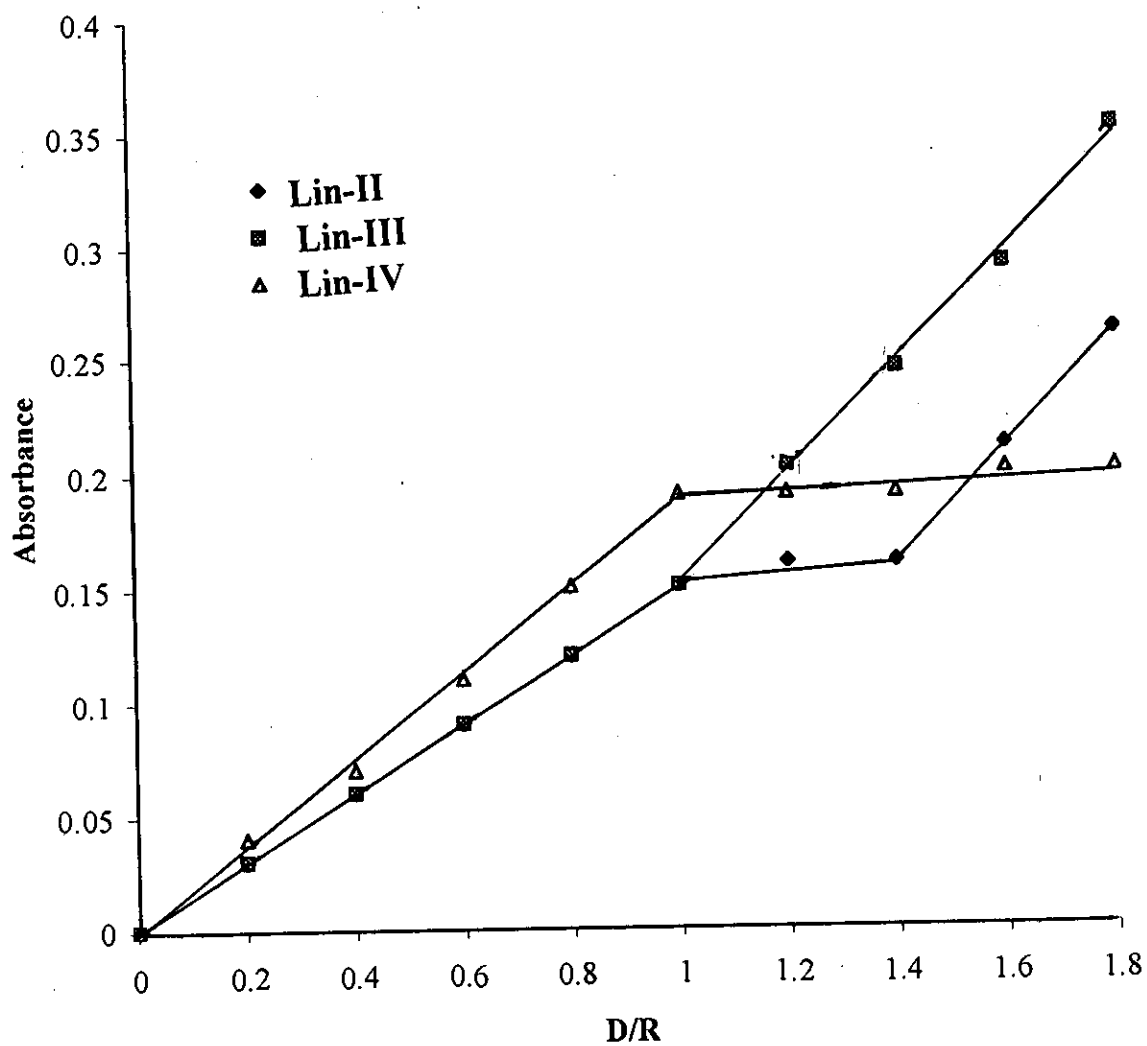


Fig. (11) Mole ratio for lincomycin HCl with reagents II, III and IV.

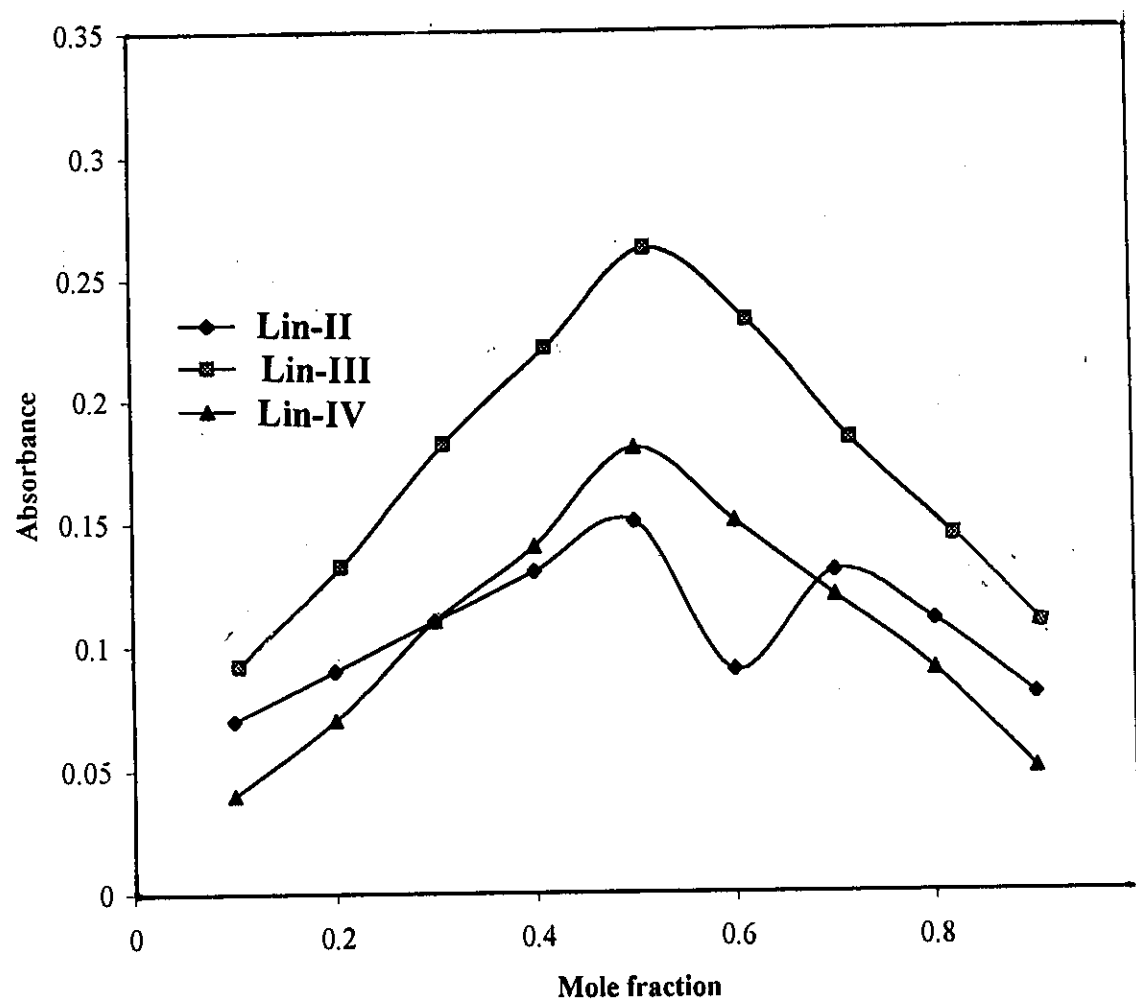


Fig. (12) Continuous variation for lincomycin HCl with reagents II, III and IV.

7. Stability constants of complexes:

The stability constants of complexes were calculated by using data of molar ratio and continuous variation methods applying *Issa et al* equation ⁽⁴⁶⁾ ; the data are recorded in Table (4).

The conditional stability constants of lincomycin (Lin) complexes indicated that the complex of Lin-II is the most stable one followed by complex Lin-III and then that with reagent IV.

Table (4): Stoichiometric ratios and stability constants of lincomycin-HCl complexes obtained from spectrophotometric methods.

Complex	pH	λ_{max} (nm)	<u>Mole ratio</u>			<u>Continuous variation</u>		
			Ratio	Log k	Log K _{Total}	Ratio	Log k	LogK _{Total}
Lin-II	3.35	525	1:1	1.40		1:1	1.49	
			2:1	3.27	4.67	2:1	3.29	4.78
Lin-III	4.31	428	1:1	3.40	3.40	1:1	3.77	3.77
Lin-IV	7.29	440	1:1	1.61	1.61	1:1	1.59	1.59

Where:

II, Chloranilic acid; III, 2,4 dinitrophenol and IV, picric acid

8. Validity to Beer's law:

A calibration graph was constructed using standard solutions of lincomycin in $\mu\text{g/mL}$ and constant concentration of reagents (1.0 mL of 1.0×10^{-2} M for I, II or III). Under optimum conditions of pH, reagent concentration, time and temperature for each of the three complexes, a linear relationship was obtained on plotting the absorbance against drug concentration as shown in Fig. (13). Limits of Beer's law, the molar absorptivity (ϵ ; $\text{L mol}^{-1}\text{cm}^{-1}$) and *Sandell*⁽⁴⁷⁾ sensitivity data are listed in Table (5).

For more accurate results, *Ringbom*⁽⁴⁸⁾ method was applied by plotting $\log[C_D]$ in $\mu\text{g/mL}$ against T % as in Fig. (14). The linear portion of the S-shaped curve gave an accurate range of analysis. Results are listed in Table (5).

9. Interference:

The effect of the presence of additives and excipients e.g., sodium acetate, bicarbonate, magnesium stearate, talc powder, starch, glucose, fructose, sucrose and lactose was studied by adding an excess amount of each of them to a solution containing 10 $\mu\text{g/mL}$ lincomycin. No interference occurred; up to ~ 15 %, in the determination of lincomycin hydrochloride indicating that complexation does not include the additives under reaction conditions.

10. Accuracy and precision:

To determine the accuracy and precision of the proposed method solutions of certain concentration were prepared and analyzed in six replicates. The percentage standard deviation and the percentage range of error at 95 % confidence level were calculated and listed in Table (5). The results are considered as very satisfactory for the examined concentration levels.

Lin-III

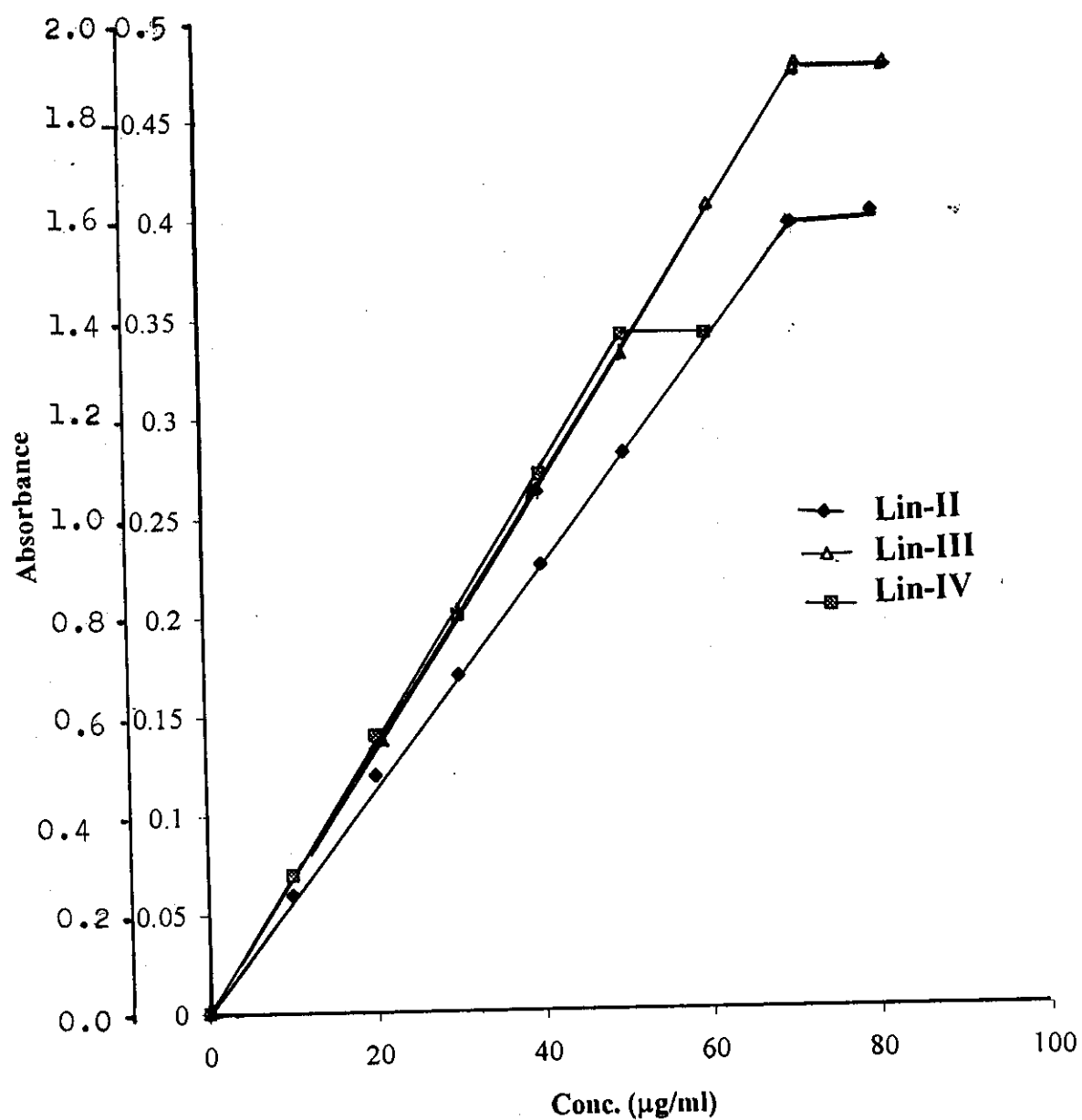


Fig. (13) Beer's assay range for lincomycin HCl with reagents II, III and IV.

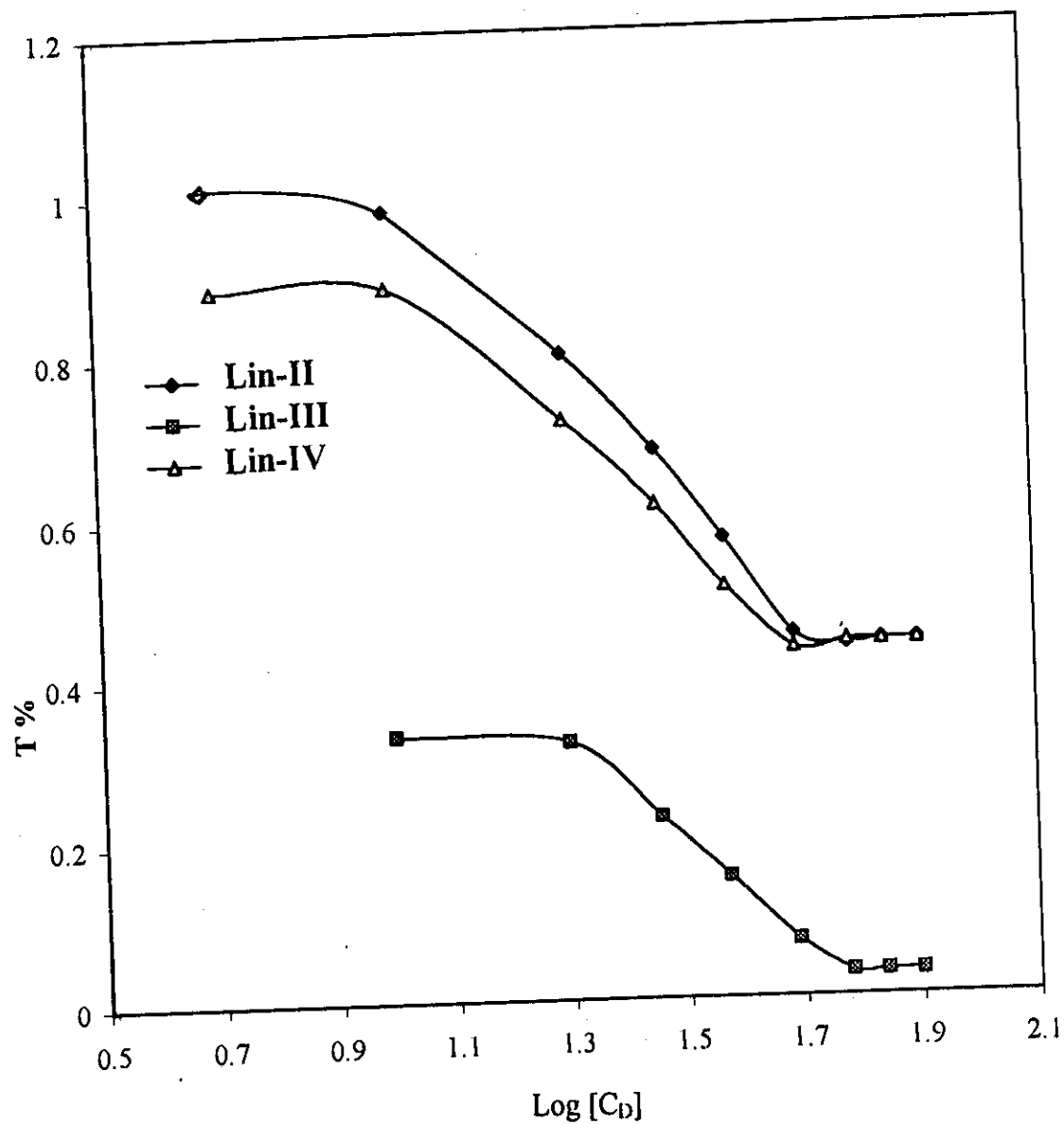


Fig. (14): Ringbom detection limit for lincomycin HCl with reagents II, III and IV.

Table (5): Spectrophotometric cumulative data for lincomycin HCl complexes.

Parameter	Lin-II	Lin-III	Lin-IV
pH	3.35	4.31	7.29
λ_{max} (nm)	525	428	440
Beer's limits ($\mu\text{g mL}^{-1}$)	10-70	10-70	10-50
Ringbom limits ($\mu\text{g mL}^{-1}$)	10-55	20-60	15-45
Molar absorptivity ($\text{L mol}^{-1}\text{cm}^{-1}$)	2.51×10^3	1.24×10^3	3.13×10^3
Sandell sensitivity ($\mu\text{g cm}^{-2}$)	0.183	0.038	0.147
Intercept*(A)	0.008	0.018	0.002
Slope (B)	0.006	0.026	0.007
Correlation coefficient (r)	0.9991	0.9994	0.9995
S. D.	0.069	0.071	0.060
R. S. D. %	0.232	0.239	0.202
R. E. %	0.095	0.098	0.082

Where:

II, Chloranilic acid; III, 2,4 dinitrophenol and IV, Picric acid.

*Linear Regression Equation:

$$Y = A + BX$$

11. Analytical application:

Results from the analysis of lincomycin injection solution by the proposed method were in a good agreement with those of the British Pharmacopoeia (1998) procedure. The relative standard deviation (six determinations) and the percentage recoveries of the proposed method and pharmacopoeia procedure are recorded in Table (6). Results show that the proposed method is highly sensitive and could be easily used in routine analysis for pure drug samples and pharmaceutical preparations.

Table (6): Evaluation of accuracy and precision of the proposed method for Lincomycin-HCl determination in Lincocin injection.

Reagent	Taken ($\mu\text{g/mL}$)	Found		Recovery %	R.S.D. %	R.E. %	t value	F value
		O	P					
I	30	29.86	29.78	99.26	0.252	0.264	1.78	1.16
III	30	29.86	29.80	99.33	0.258	0.271	1.32	1.11
IV	30	29.86	29.77	99.23	0.212	0.222	2.15	1.65

*Average of six determinations

t = 2.57

F = 5.05

O: Official method

P: Proposed method

III- Absorption spectra of mebeverine-HCl with reagents II, III and IV:-

In order to investigate the optimum conditions for complex formation, the following factors were taken into consideration:

1. Effect of pH:

The effect of pH on complex formation between mebeverine hydrochloride and reagents II, III and IV was studied in universal buffer solutions of pH range 3.35-11.15. A portion (1.0 mL) of 1.0×10^{-2} M reagents chloranilic acid, 2,4 dinitrophenol or picric acid (II, III or IV, respectively), 1.0 mL of 200 $\mu\text{g/mL}$ drug and 3.0 mL buffer of different pH values were mixed well, the volume was completed to 10 mL with bidistilled water. The absorption spectra were measured against blank solution prepared as sample except the drug. Inspection of the spectra given in Figs. (17-a), (18-a) and (19-a), the optimum pH values would be 4.21, 4.31 and 7.29 on using reagents II, III and IV respectively.

**N.B.: For the assay of mebeverine- HCl with reagent IV, 1.0 mL of 95 % ethanol was added to each of blank and sample to avoid turbidity.*

2. Determination of λ_{max} of complex species:

To determine the value of λ at which the complex species possesses the maximum absorption, the following spectra were recorded:

- A- Spectrum of pure drug 1.0 mL of 200 $\mu\text{g/mL}$ at the optimum pH value using the same buffer as a blank.
- B- Spectrum of pure reagent 1.0 mL of 1.0×10^{-2} M for reagent II, III and IV at the optimum pH value using the same buffer as a blank.
- C- Spectrum of solution mixture of drug of (A) plus reagent of (B) at the optimum pH value using the same buffer as a blank.

D- Spectrum of solution (C) against (B) as a blank.

From curves (A-D), shown graphically in Figs. (15-b), (16-b) and (17-b), the recommended λ_{\max} for complexes were determined and found to be 525, 428 and 450 nm for reagents II, III and IV, respectively.

3. Effect of time and temperature:

The effect of time on complex formation was studied by measuring the absorbance of the complex at various time intervals. Also the effect of temperature was studied for the same solution by incubating the sample and blank in a water bath at different temperatures (25-45 °C). The absorption was measured after cooling to room temperature. Experiments showed that complexes are formed after mixing drug and reagent and remain stable for 24 hours. Also it is found that, increasing the temperature up to 45 °C has no effect on the absorbance above which the absorbance began to decrease.

4. Effect of sequence of addition:

The effect of sequence of addition on complex formation was studied by measuring the absorbance of solutions prepared by different sequences. Experiments showed that the best sequence of addition is reagent-buffer-drug.

5. Effect of reagent concentration:

To study the effect of reagent (II, III and IV) concentration on the complex formation, the concentration of drug was kept constant (200 µg/mL) while that of reagent was varied regularly. The resulted spectra showed that 1.0 mL of 1.0×10^{-2} M of each reagent is sufficient to give a reasonable maximum absorbance.

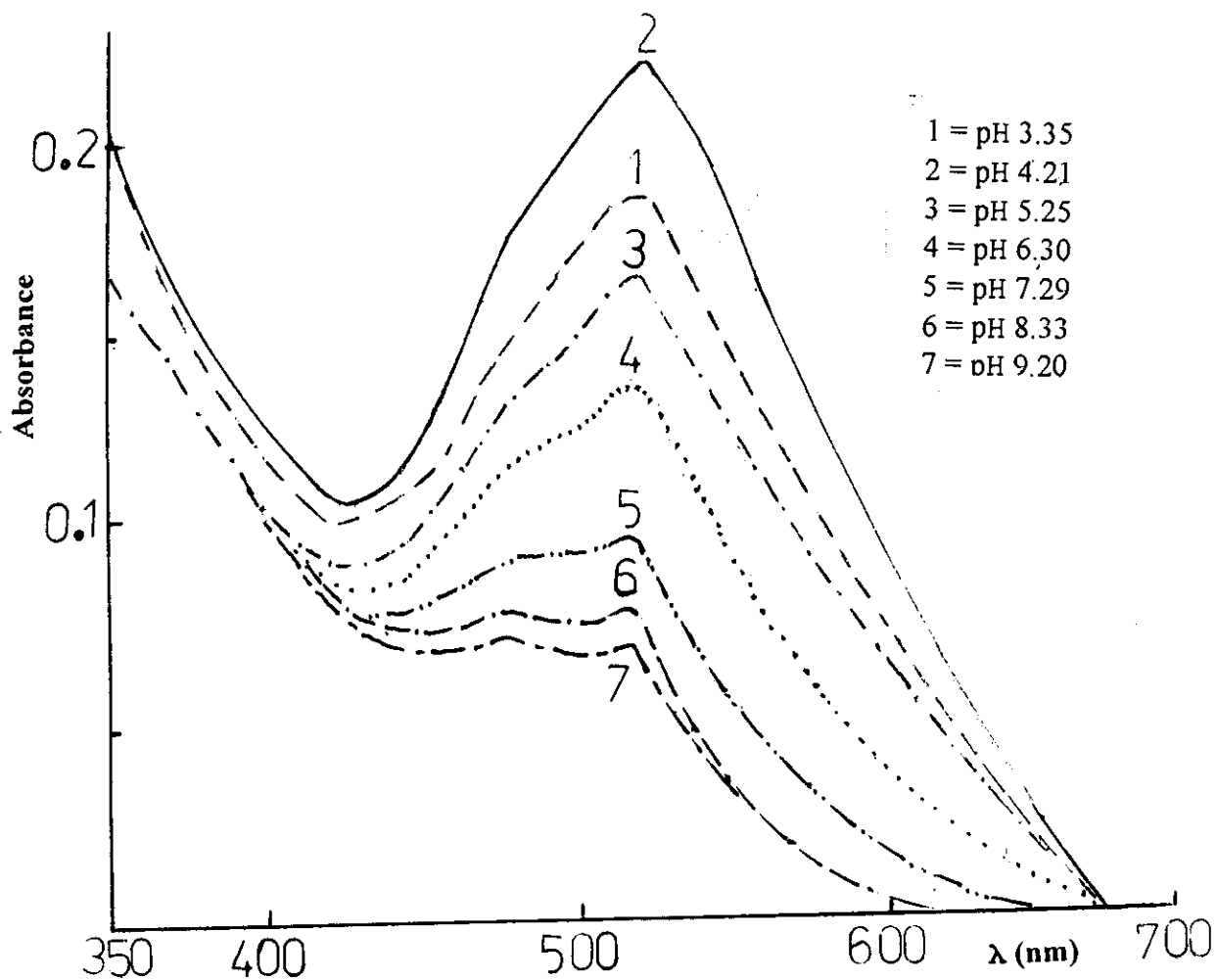


Fig. (15-a) Effect of pH on the absorption spectra of mebeverine HCl-chloranilic acid complex.

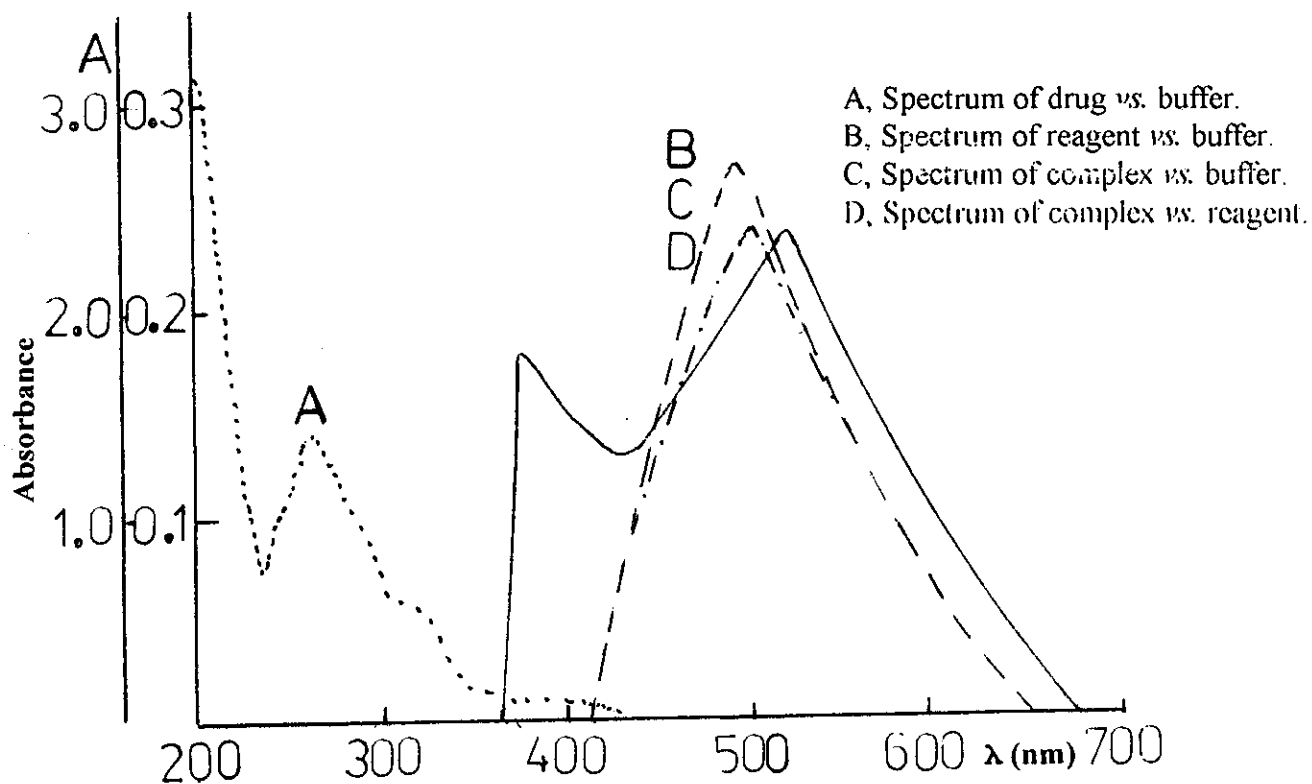


Fig. (15-b) Determination of λ_{\max} of mebeverine HCl-chloranilic acid complex at pH 4.21.

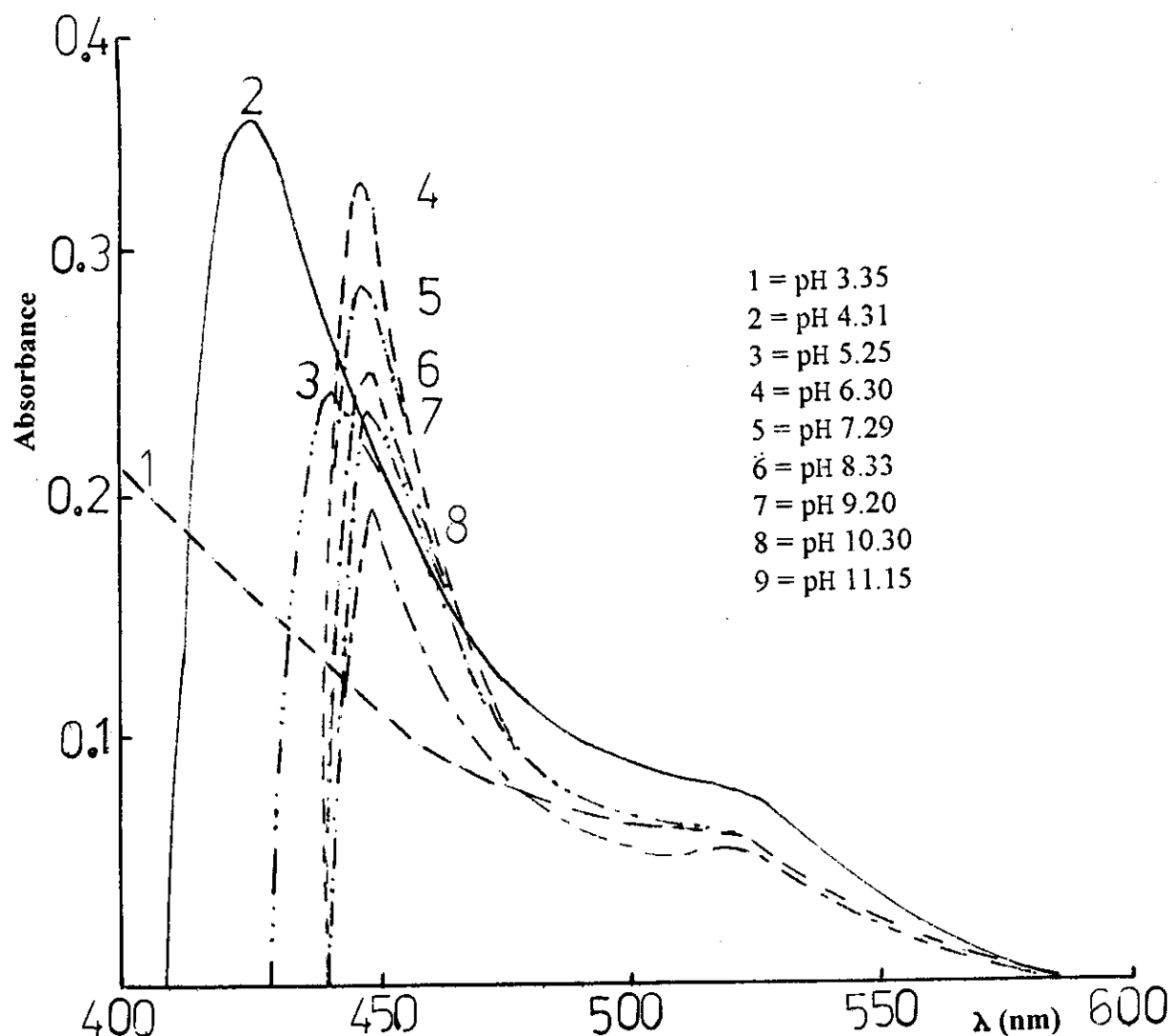


Fig. (16-a) Effect of pH on the absorption spectra of mebeverine HCl-2,4 dinitrophenol complex.

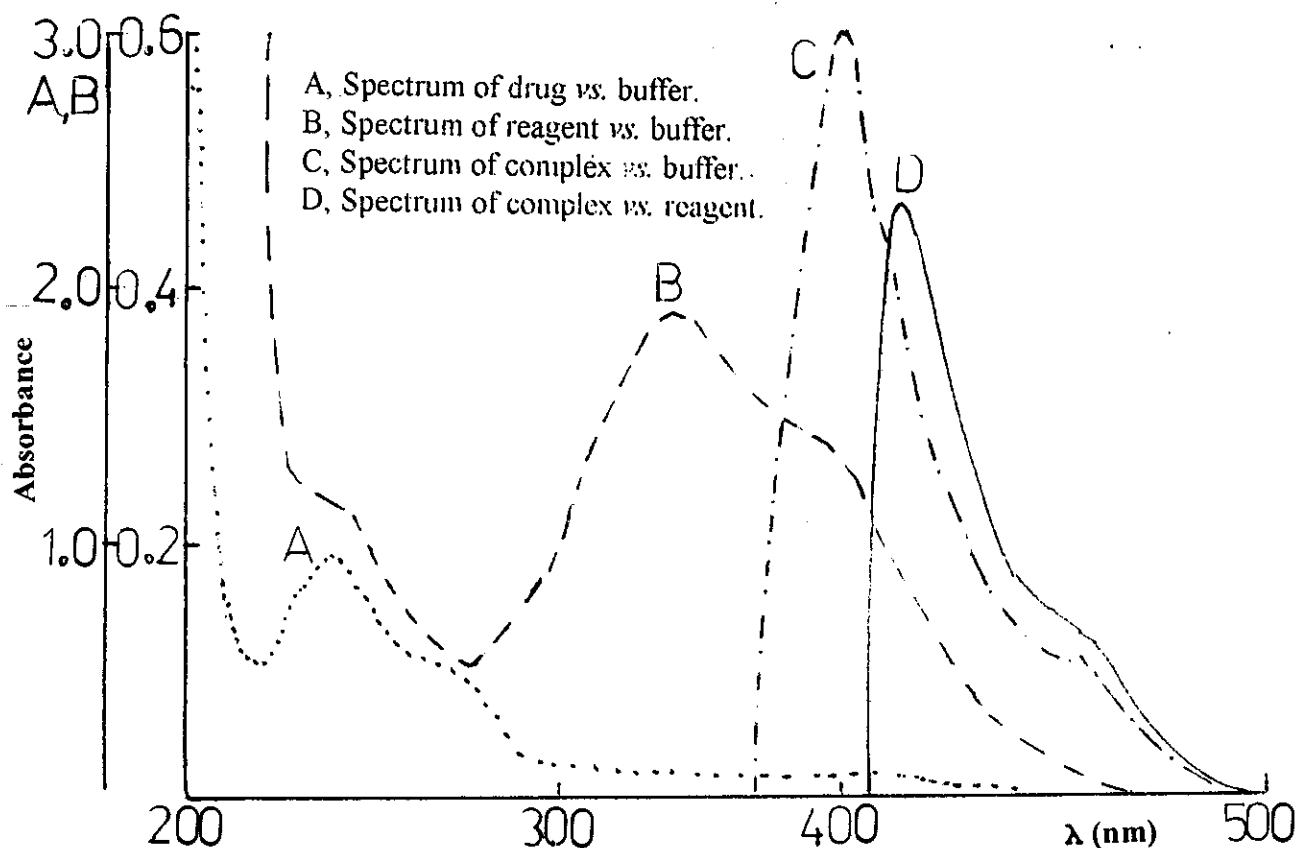


Fig. (16-b) Determination of λ_{\max} of mebeverine HCl-2,4 dinitrophenol complex at pH 4.31.

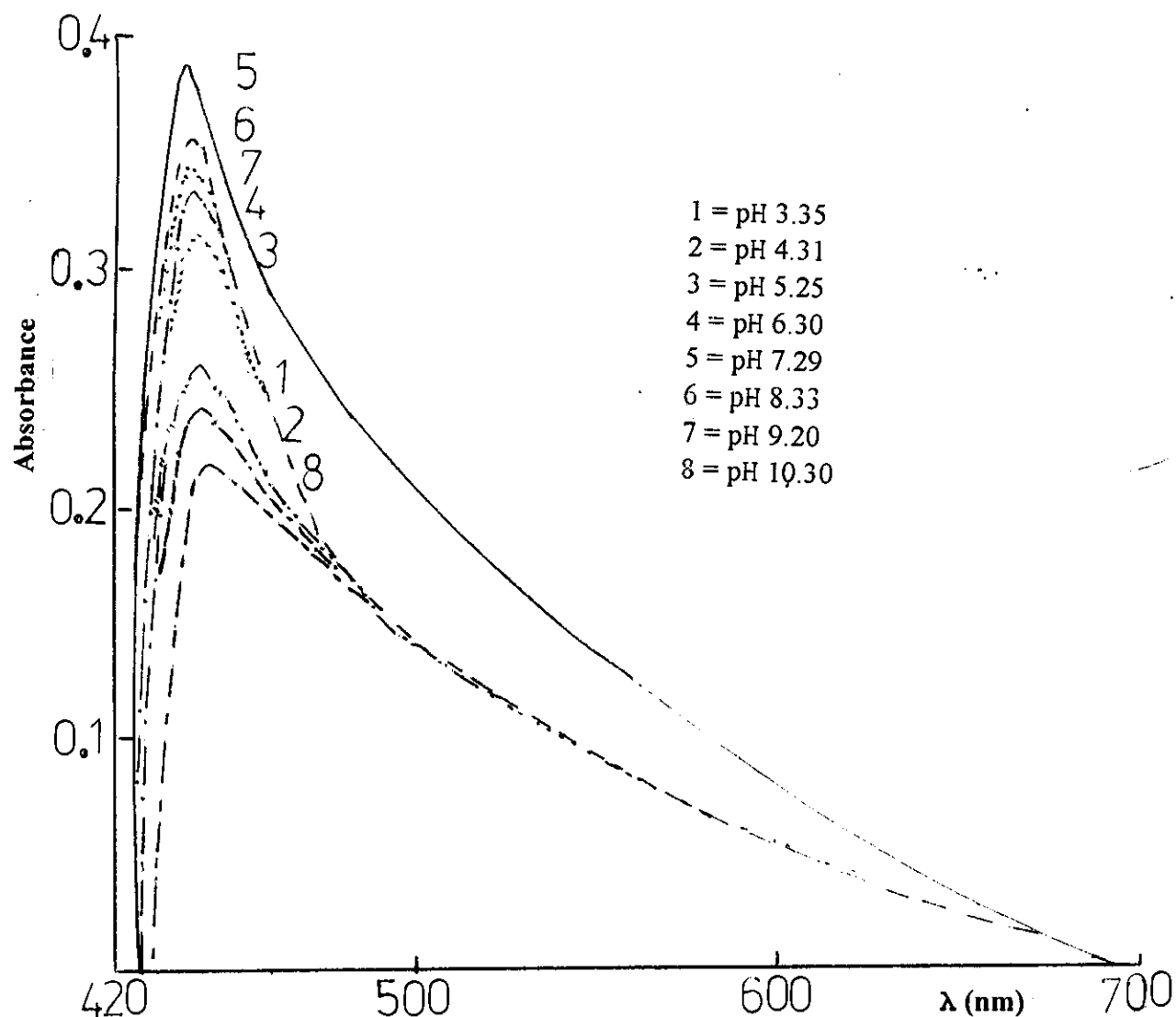


Fig. (17-a) Effect of pH on the absorption spectra of mebeverine HCl-picric acid complex.

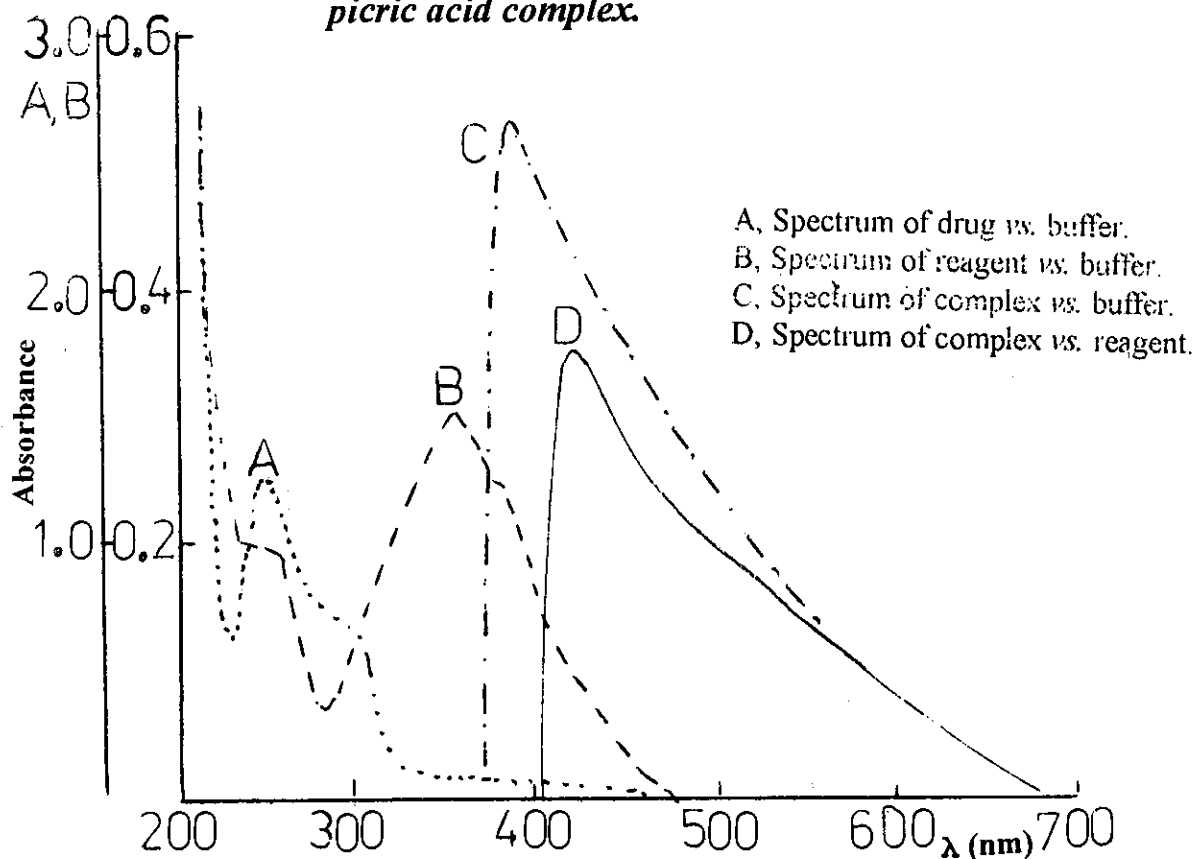


Fig. (17-b) Determination of λ_{\max} of mebeverine HCl-picric acid complex at pH 7.29.

6. Stoichiometry of complex:

(i) Mole ratio method:

A portion (1.0 mL) of 1.0×10^{-2} M of II, III or IV was mixed with different volumes of drug (0.1, 0.2,, 1.0 mL of the same concentration). 3.0 mL of the selected pH buffer was added, then the volume was completed to 10 mL with bidistilled water. The absorbance was then measured at the recommended wavelength against blank solution composed of the same ingredients except that of drug. The absorbance values were plotted against the mole ratio (D/R) as shown in Fig. (18). Experimental results revealed the formation of only (1:1) stoichiometric ratio with the three reagents used.

(ii) Continuous variation method:

Different volumes (0.1, 0.2,, 0.9 mL) of 1.0×10^{-2} M of drug and reagent were mixed while keeping the total molar concentration constant. 3.0 ml of buffer solution of the selected pH value was added, then the volume was completed to 10 mL with bidistilled water. The absorbance was measured and plotted against the mole fraction of reagent as shown in Fig. (19). Results obtained revealed that complexes formed are of the ratio 1:1 confirming those obtained from mole ratio method.

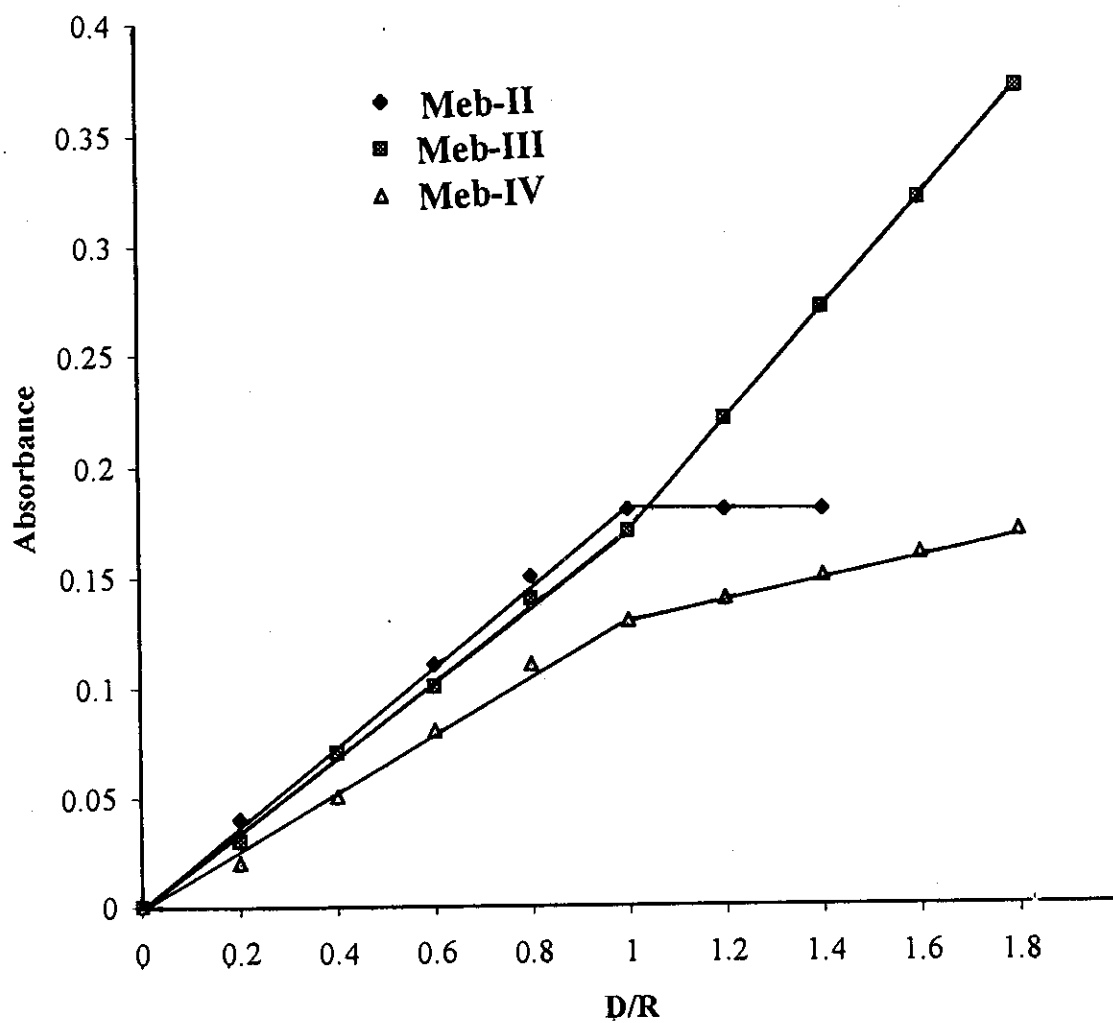


Fig. (18) Mole ratio for mebeverine HCl with reagents II, III and IV.

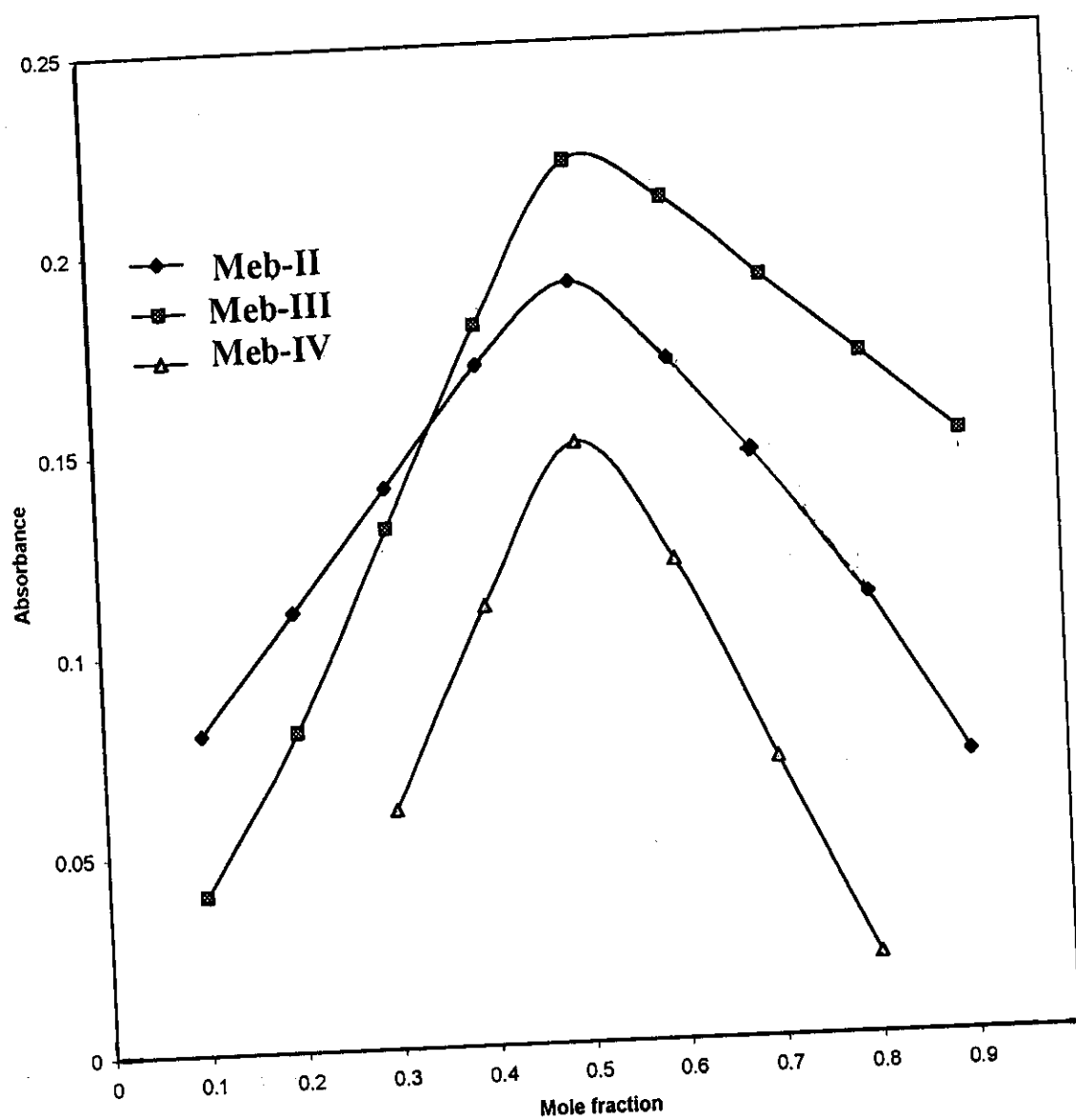


Fig. (19) Continuous variation for mebeverine HCl with reagents II, III and IV.

7. Stability constants of complexes:

The stability constants of complexes were calculated using the data of the mole ratio and continuous variation methods applying *Issa et al* equation⁽⁴⁷⁾. The conditional stability constant of the complexes, Table (7), indicated that the Meb-II complex is the most stable then Meb-III and Meb-IV.

Table (7): Stoichiometric ratios and stability constants of mebeverine-HCl complexes obtained from spectrophotometric methods.

Complex	pH	λ_{max} (nm)	<u>Mole ratio</u>		<u>Continuous variation</u>	
			Ratio	Log k	Ratio	Log k
Meb-II	4.21	525	1 : 1	1.62	1 : 1	1.79
Meb-III	4.31	428	1 : 1	1.58	1 : 1	1.77
Meb-IV	7.29	450	1 : 1	1.31	1 : 1	1.12

Where:

II, Cholranilic acid; III, 2,4 dinitrophenol and IV, picric acid

8. Validity to Beer's law:

A calibration graph was constructed using standard solutions of mebeverine ($\mu\text{g/mL}$) with constant concentration of the reagent ($1.0 \times 10^{-2} \text{ M}$). 3.0 mL buffer solution of the optimum pH value for each reagent was added in 10 mL volumetric measuring flask and the volume was completed to the mark with bidistilled water. The absorbance was measured at the recommended λ_{max} , then plotted against drug concentration as shown in Fig. (20). Limits of Beer's law, the molar absorptivity (ϵ ; $\text{L mol}^{-1} \text{cm}^{-1}$) and *Sandell*⁽⁴⁷⁾ sensitivity data are listed in Table (8) drug.

For more accurate results, *Ringbom*⁽⁴⁸⁾ method was applied by plotting $\log [C_D]$ in $\mu\text{g/mL}$ against T % as shown in Fig. (21). The linear portion of the S-shaped curve gave an accurate range of analysis. Results are listed in Table (8).

9. Interference:

The effect of the presence of additives was studied by adding an excess amount of sodium acetate, bicarbonate, magnesium stearate, talc powder, starch, glucose, fructose, sucrose and lactose to a solution containing 10 $\mu\text{g/mL}$ of mebeverine. Careful investigation showed that the presence of such ingredients do not interfere when present up to 10 %, indicating that complexation does not occur with those additives under reaction condition.

10. Accuracy and precision:

To determine the accuracy and precision of the proposed method, solutions of certain concentration were prepared and analyzed in six replicates. The RSD % and RE % were calculated and listed in Table (8). The results are considered as very satisfactory for the examined concentrations.

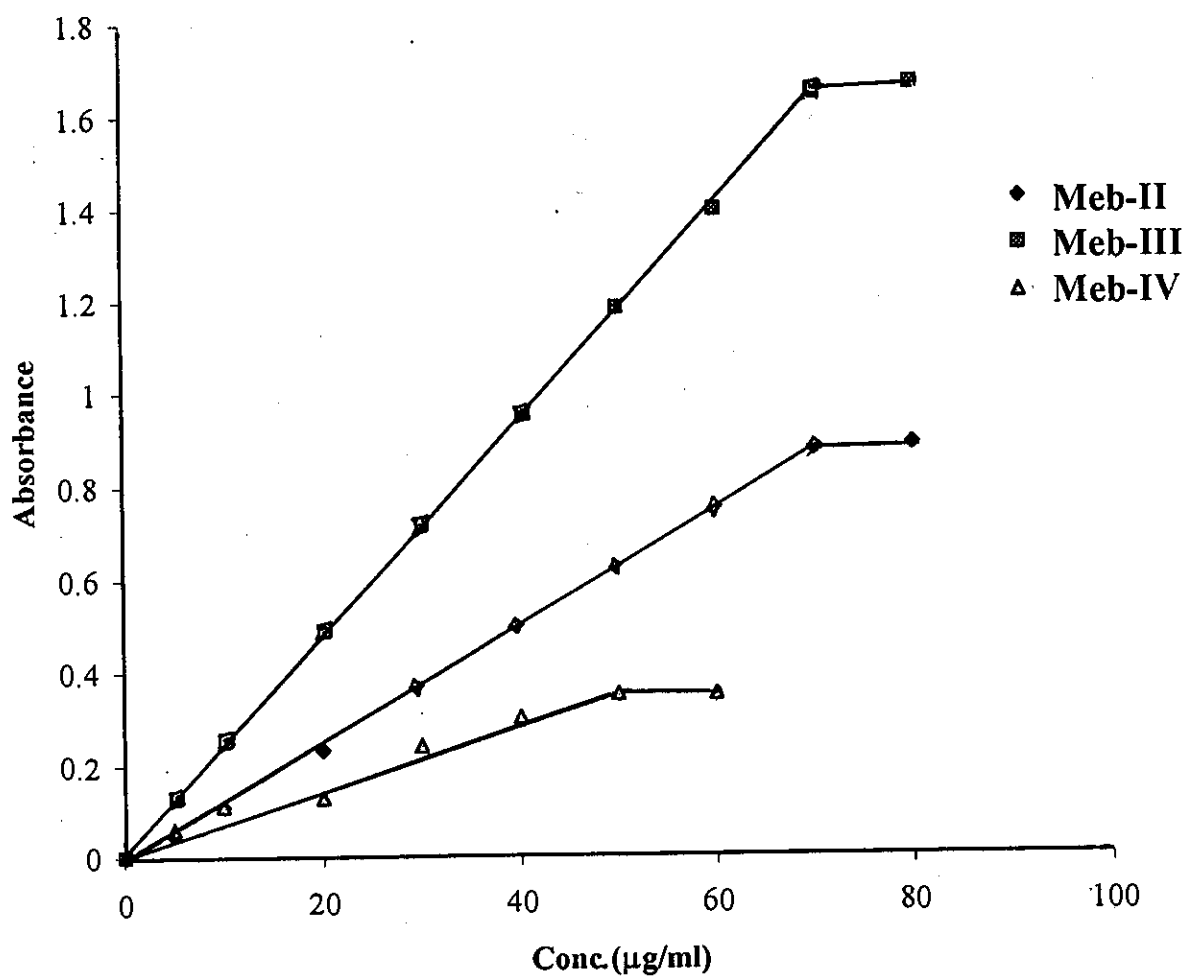


Fig. (20) Beer's assay range for mebeverine HCl with reagents II, III and IV.

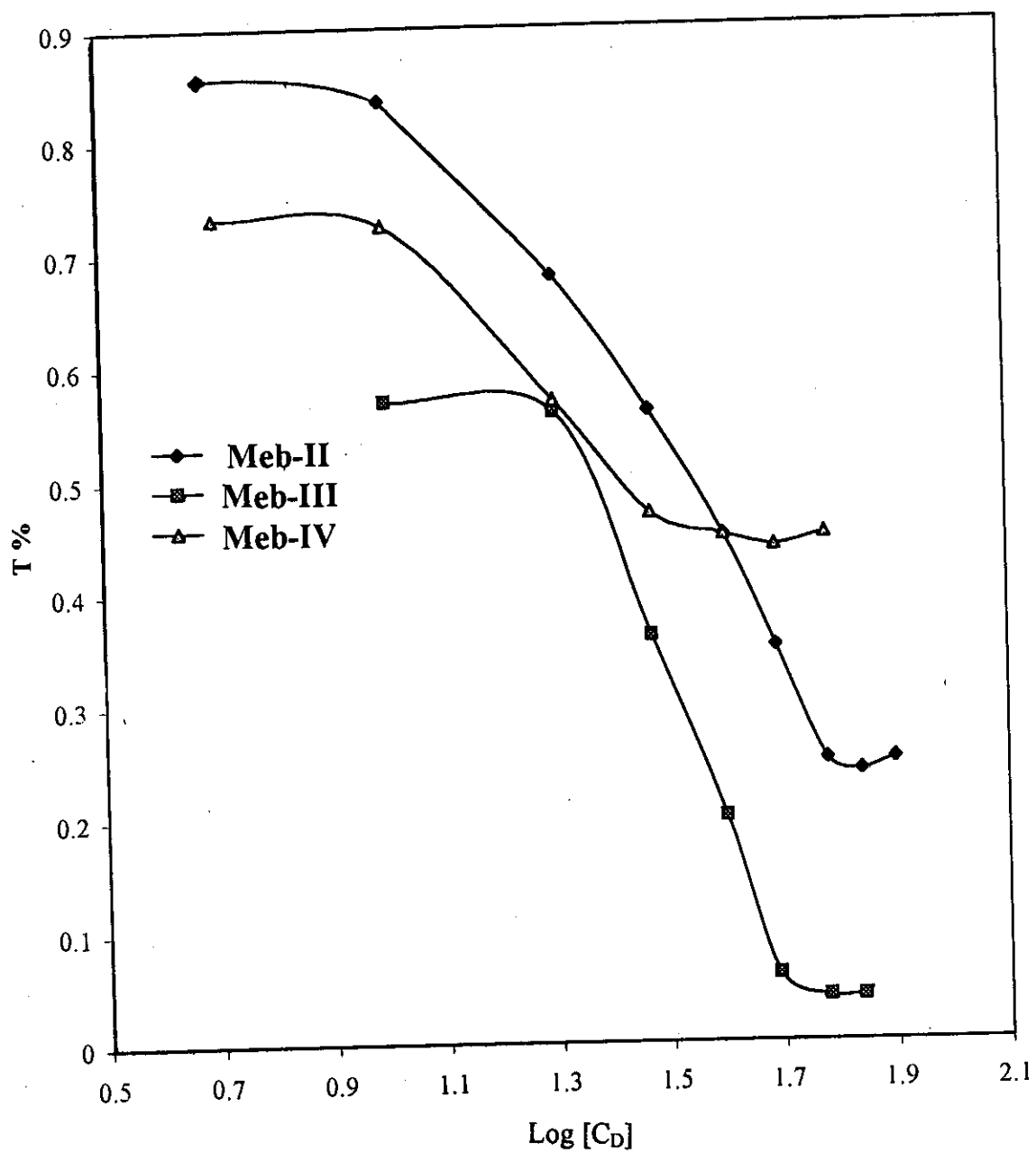


Fig. (21) Ringbom detection limit for mebeverine HCl with reagents II, III and IV.

Table(8): Spectrophotometric cumulative data for Mebeverine- HCl complexes.

Parameter	Meb-II	Meb-III	Meb-IV
pH	4.21	4.31	7.29
λ_{max} (nm)	525	428	450
Beer's limits ($\mu\text{g mL}^{-1}$)	10-70	10-60	5-30
Ringbom limits ($\mu\text{g mL}^{-1}$)	10-60	20-55	10-25
Molar absorptivity ($\text{L mol}^{-1}\text{cm}^{-1}$)	4.19×10^3	9.97×10^3	5.50×10^3
Sandell sensitivity ($\mu\text{g cm}^{-2}$)	0.111	0.046	0.084
Intercept* (A)	0.006	0.034	-0.004
Slope (B)	0.009	0.021	0.011
Correlation coefficient (r)	0.9995	0.9998	0.9991
S. D.	0.058	0.048	0.055
R. S. D. %	0.195	0.161	0.185
R. E. %	0.080	0.066	0.075

Where:

II, Chloranilic acid; III, 2,4 dinitrophenol and IV, picric acid.

*Linear Regression Equation:

$$Y = A + BX$$

11. Analytical application:

Results for the analysis of mebeverine hydrochloride tablets by the proposed method were in a good agreement with those of the British Pharmacopoeia (1998) procedure. The relative standard deviation (six determinations) and the percentage recoveries of the proposed method and pharmacopoeia procedure are recorded in Table (9).

Table (9): Evaluation of accuracy and precision of the proposed method for Mebeverine-HCl determination in Colospasmin tablets.

Reagent	Taken ($\mu\text{g/mL}$)	Found O P		Recovery %	R.S.D. %	R.E. %	t value	F value
I	30	29.90	29.80	99.33	0.300	0.313	1.79	1.37
III	30	29.90	29.85	99.50	0.389	0.408	0.79	1.24
IV	30	29.90	29.85	99.50	0.271	0.285	0.93	1.64

*Average of six determinations

$$t = 2.57$$

$$F = 5.05$$

O: Official method

P: Proposed method

➤ CONDUCTOMETRIC TITRATION STUDIES

The conductance measurement is the best physicochemical method for the determination of the stoichiometric ratios of complexes formed in solution between reagents (I, II, III and IV) and the drugs under investigation. Variations in the conductance depend on the change in the number and character of the conducting species in solution. Since the drug ions are involved in complex compounds, their conductance should be lowered as a result of decreased value of the diffusion coefficient of the particle as observed from the relation:

$$D^{\circ} = (ZF^2 / RT) \Lambda^2$$

Where:

D° , the diffusion coefficient

R , the gas constant

T , the absolute temperature

Z , Faraday constant

Λ , the conductivity

The diffusion coefficient, in turn, is related to the molar volume of the diffused particle (V_m) according to the **Stock-Einstein equation**:

$$D^{\circ} = K / (V_m)^{1/3} \eta$$

Where: η , the viscosity of the medium

The change in the type of conducting species is also an important factor that gives the direction of conductance change. This depends, in large extent, on the reaction that takes place between the drug and the reagent in solution. Hence, the conductance is directly proportional to the charge on complex and inversely proportional to both the volume of complex formed and the viscosity of the medium.

A plot of the equivalent conductance versus ml added of titrant (reagent of 1.0×10^{-2} M) gave intersected straight lines. The position of intersection indicates the stoichiometry of complex. The results obtained are shown in Figs. (22), (23) and (24).

In Fig. (22) for sulfamethoxazole (Sul), the breaks indicate the formation of one complex of ratio 1:1 with reagents I, III and IV.

In Fig. (23) for lincomycin-HCl, the breaks indicate the presence of complexes of various species 1:1 and 2:1 with reagent II and 1:1 with reagents III and IV.

In Fig. (24) for mebeverine-HCl, the breaks indicate the formation of only one complex of stoichiometric ratio 1:1 with reagents II, III and IV.

These results support those obtained by spectrophotometric methods.

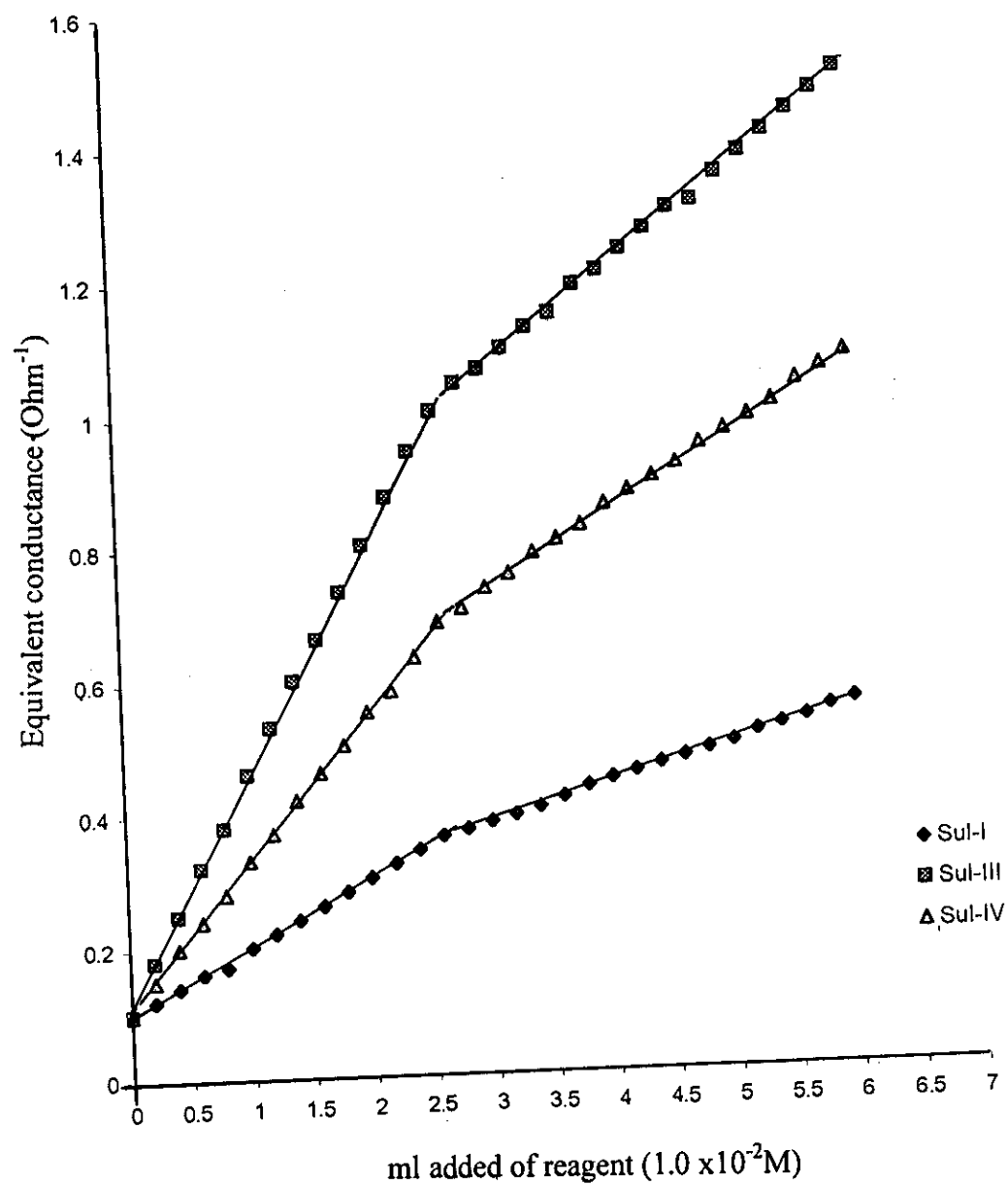


Fig. (22) Conductometric titration curves of sulfamethoxazole with reagents I, III and IV.

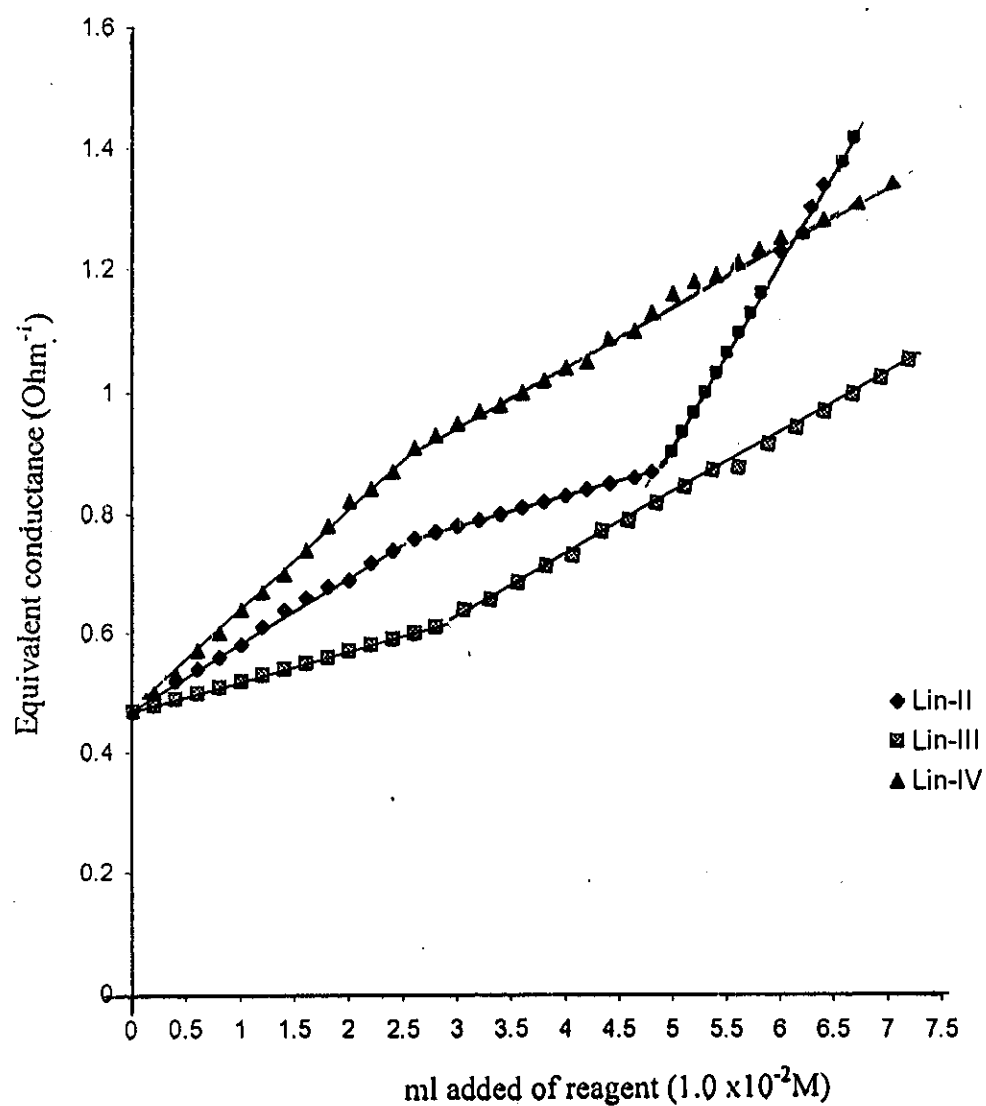


Fig. (23) Conductometric titration curves of lincomycin HCl with reagents II, III and IV.

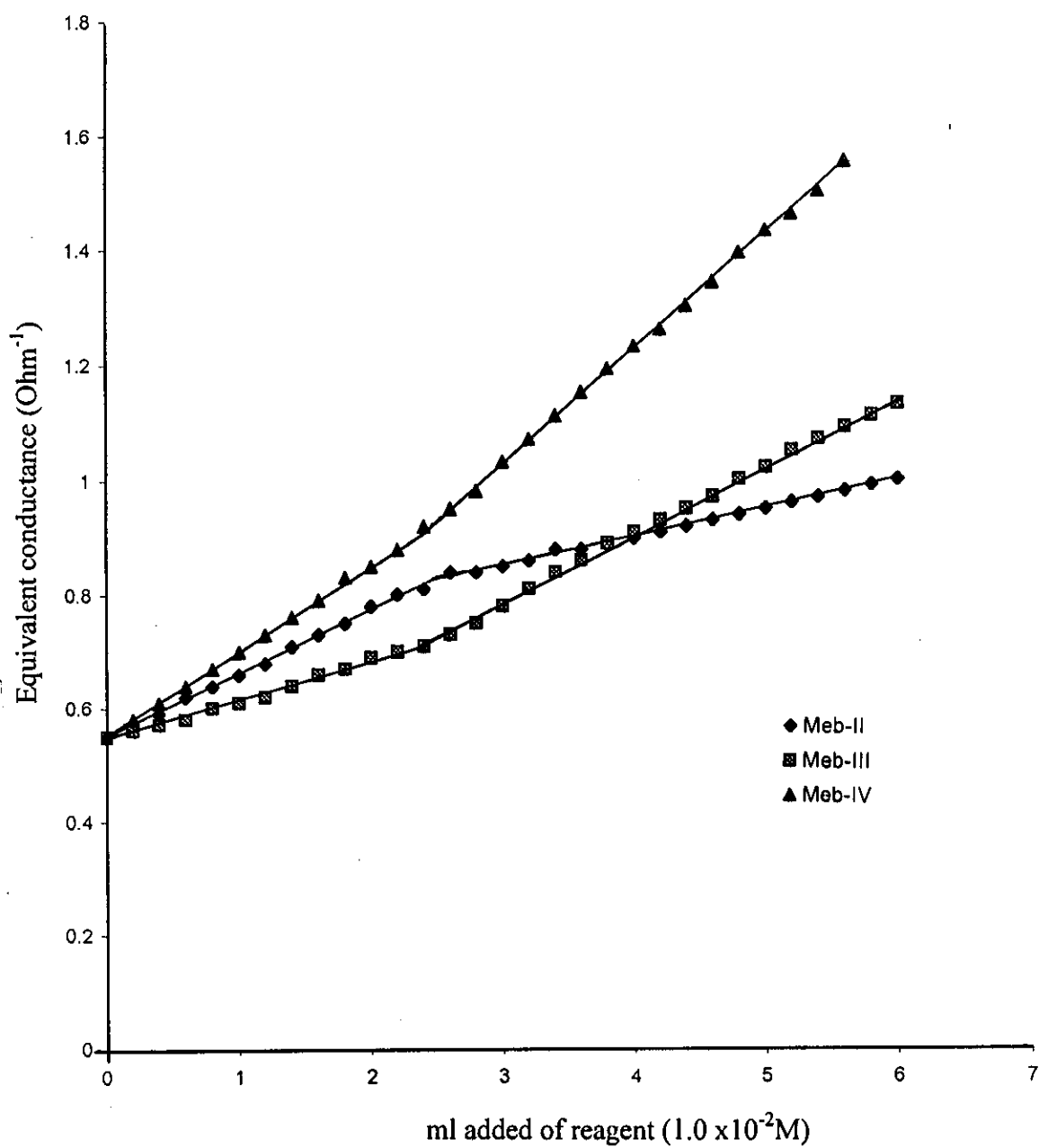


Fig. (24) Conductometric titration curves of mebeverine HCl with reagents II, III and IV.

➤ *STUDIES OF SOLID COMPLEXES*

The methods for spectrophotometric determination of the pharmaceutical compounds using reagents under investigation are based on the formation of charge transfer complexes between the drug molecule as a donor and the reagent molecule as an acceptor. The preceding study done through this thesis supported the formation of these complexes in solution. This is gathered from the change in the electronic spectra in the UV-Vis range where a new CT band is obtained, supporting the formation of a CT complex.

To ascertain the formation of the charge transfer complexes, the complexes were prepared and isolated in the solid state. Their structures were then elucidated by the following techniques:

I-Elemental analysis:

C, H and N of the prepared complexes were determined in the micro analytical center, Cairo university, Giza, Egypt. The percent composition (as cited in Table (10)) shows satisfactory agreement with the proposed formula. The colour of the prepared CT complexes, melting point and proposed tentative formula are given in Table (10).

Table(10): The elemental analysis of CT complexes of sulfamethoxazole and mebeverine HCl with reagents I, II, III, IV & V:

Complex	Colour	M. Wt.	m.p. (°C)	C%		H%		N%		Tentative Formula
				Calc.	Found	Calc.	Found	Calc.	Found	
<i>Sul-I</i>	Brownish	499.2	200-205	38.49	37.50	2.22	2.10	8.41	8.36	C ₁₆ H ₁₁ N ₃ O ₅ SCl ₄
<i>Sul-II</i>	Reddish	462.2	205-210	41.56	40.34	2.83	2.65	9.08	8.95	C ₁₆ H ₁₃ N ₃ O ₇ SCl ₂
<i>Sul-III</i>	Yellow	482.22	95-100	43.89	42.64	3.45	2.86	16.00	15.90	C ₁₆ H ₁₄ N ₆ O ₅ S
<i>Sul-IV</i>	Yellow	437.22	120-125	39.83	38.40	2.92	2.58	17.41	16.80	C ₁₆ H ₁₅ N ₅ O ₈ S
<i>Sul-V</i>	White	465.23	170-175	43.86	43.30	3.24	3.15	15.04	14.96	C ₁₇ H ₁₅ N ₅ O ₉ S
<i>Meb-I</i>	Brownish	711.56	-	52.29	52.01	5.09	4.86	1.96	1.75	C ₃₁ H ₃₆ NO ₇ Cl ₅
<i>Meb-II</i>	Reddish-brown	674.66	-	55.15	54.04	5.67	4.95	2.07	1.96	C ₃₁ H ₃₈ NO ₉ Cl ₃
<i>Meb-III</i>	Deep yellow	695.6	-	57.26	56.64	6.20	4.94	6.46	5.96	C ₃₁ H ₃₉ N ₄ O ₇ Cl
<i>Meb-IV</i>	Deep Yellow	649.76	-	53.56	52.46	5.65	5.42	8.06	7.96	C ₃₁ H ₄₀ N ₃ O ₁₀ Cl
<i>Meb-V</i>	Yellow	677.77	-	56.67	55.68	5.79	5.36	6.19	5.88	C ₃₂ H ₄₀ N ₃ O ₁₁ Cl

II-Electronic absorption spectra of CT complexes:-

The electronic absorption spectra of the pure reagents and their complexes were scanned as nujol mull within the range 250-700 nm. The spectra are shown in Figs. (25-29).

Generally, it was reported that the absorption spectra of the expected charge transfer complexes show marked shifts in λ_{\max} positions in various directions. This change in λ_{\max} results from the intermolecular charge transfer interaction taking place from the HOMO of the donor molecule as a source to the LUMO of the acceptor as a sink ($D_{\text{HOMO}} \rightarrow A_{\text{LUMO}}$). This transition will increase the electron density on the aryl moiety of the acceptor molecule (reagent molecule) while decreasing it on that of the donor molecule (drug molecule). As a result a new set of bands will appear in the absorption spectra of the CT complex; one of higher energy which is assigned to the $\pi-\pi^*$ (HOMO-LUMO) transition, while the other, the lower energy band, would be assigned to an intermolecular charge transfer of the $n-\pi^*$ type. This would probably include the transition of an electron from a non-bonding level of donor to a π^* anti-bonding orbital of the acceptor.

The electronic absorption spectra of the CT complexes display two bands within the range 250-700 nm corresponding to $\pi-\pi^*$ and $n-\pi^*$ interactions with $E_{\text{CT}} = 2.30-3.95$ eV. The existence of these bands in the electronic absorption spectra of the complexes reveals that CT complex formation occurs through $\pi-\pi^*$ and $n-\pi^*$ transition. The interaction of $n-\pi^*$ type would be of low contribution to complex formation and hence the absorption due to such electronic transition would be very low and may be masked by intense $\pi-\pi^*$ type in many cases.

Inspection of the electronic absorption spectra given in Figs. (25-29) reveals that the spectra of Sul-I complex displays two bands within the range 310-440 nm and 440-660 nm due to the π - π^* and n - π^* transitions, respectively. Similarly, Meb-V complex gives rise to two bands in the range 310-350 nm and 350-390 nm. The electronic spectra of the other complexes (Sul-II, Sul-III, Sul-IV, Sul-V) exhibit only one band in the range 250-670 nm, while (Meb-I, Meb-II, Meb-III and Meb-IV) exhibit only one band in the range 260-690 nm.

The energy of interaction [E_{CT} (eV)] of the π - π^* and n - π^* charge transfer can be calculated from λ_{max} of the electronic absorption spectra of complexes using the equation:

$$E_{CT} = 1243.667 / \lambda_{max}$$

The I_p values of the free donors are determined from their electronic absorption spectra applying the relation:

$$I_p = a + b V_o$$

Where, V_o : the energy of HOMO-LUMO (π - π^*) transition of the free donor.

(a and b) are constants having the values (4.39, 0.857), (5.15, 0.778) and (5.11, 0.701)^(52,53,54) respectively.

It is found that, the mean values of I_p calculated are equal to 8.46 and 8.56 eV for Sul and Meb, respectively.

The results obtained for E_{CT} and I_P are then used to determine the coulombic force (C) of the donor molecules using the relation given by *Briegleb*⁽⁵⁵⁾ in the form:

$$E_{CT} = (I_P - E_A) + C$$

Where:

I_P , the ionization potential of the donor.

E_A , the electron affinity of the acceptor ($E_A = 1.37, 1.10, -0.70, -0.50$ and -0.60 eV for I, II, III, IV and V⁽⁵⁶⁾, respectively).

C , the coulombic force between electron transfer and positive hole left behind^(56,57).

The coulombic forces (C), for both Sul and Meb in different complexes, are calculated from *Briegleb* equation, results are cited in Table (11).

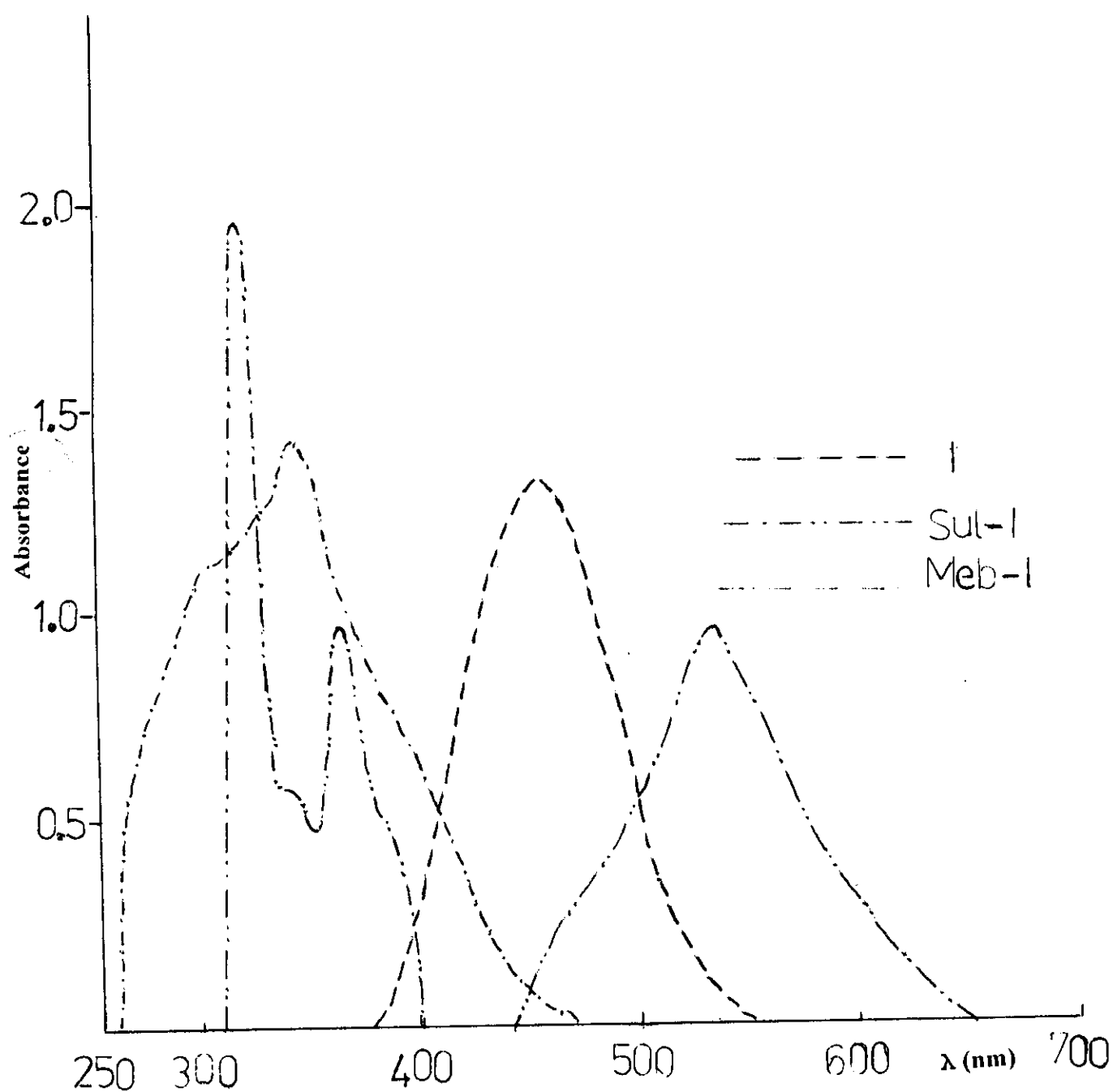


Fig. (25) The electronic absorption spectra of reagent (I) and its complexes with Sul and Meb as nujol mull.

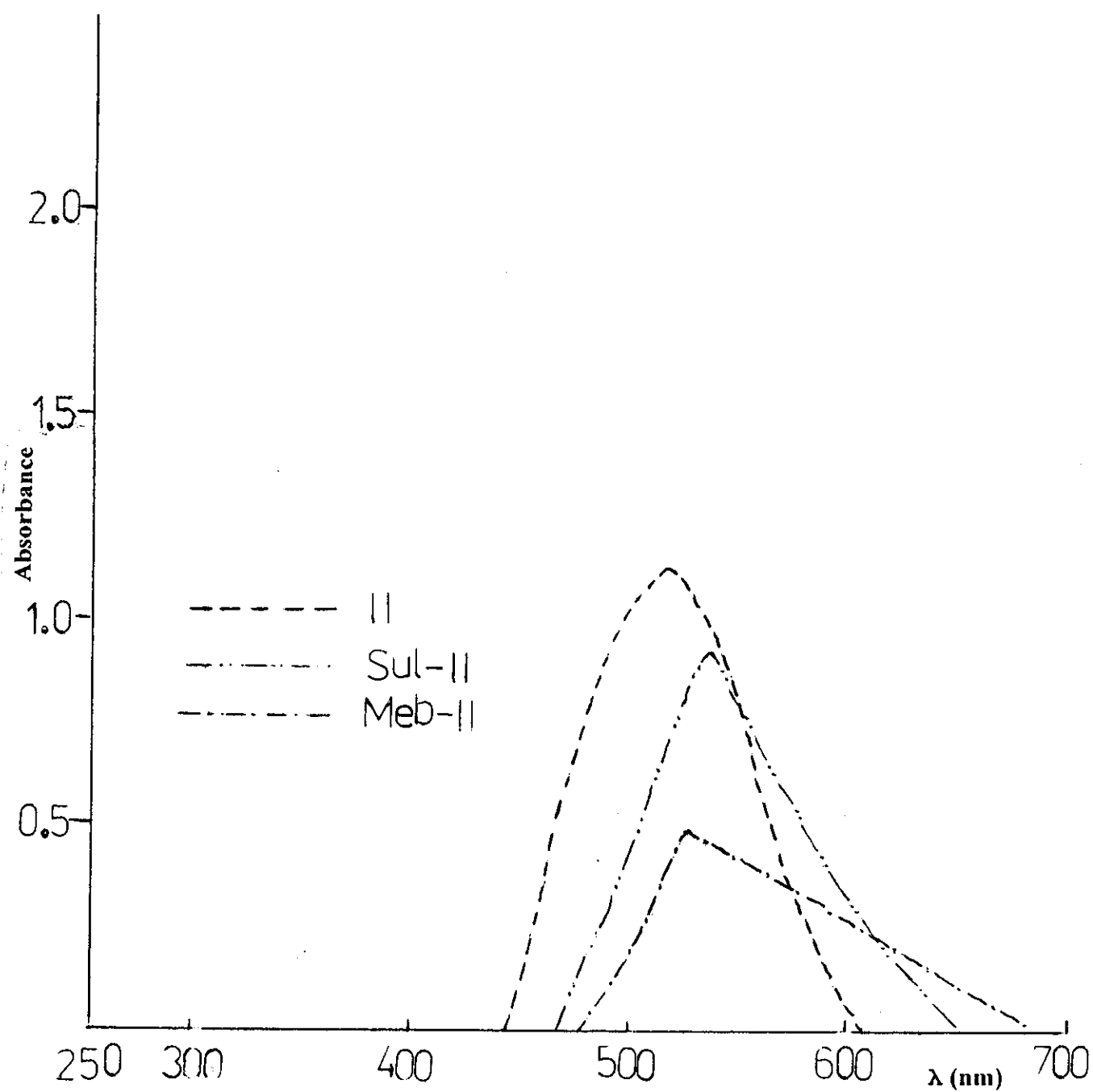


Fig. (26) *The electronic absorption spectra of reagent (II) and its complexes with Sul and Meb as nujol mull.*

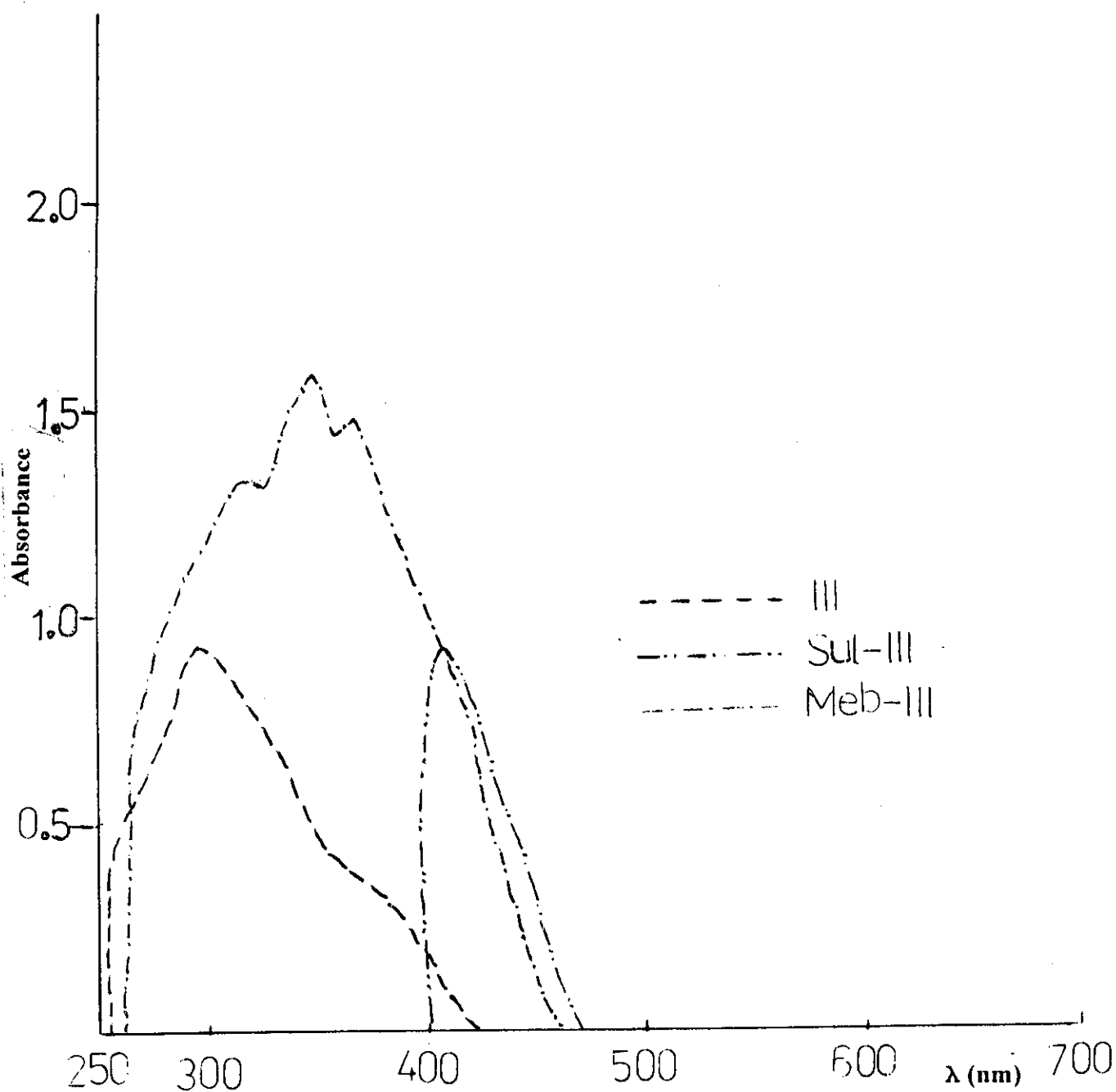


Fig. (27) *The electronic absorption spectra of reagent (III) and its complexes with Sul and Meb as nujol mull.*

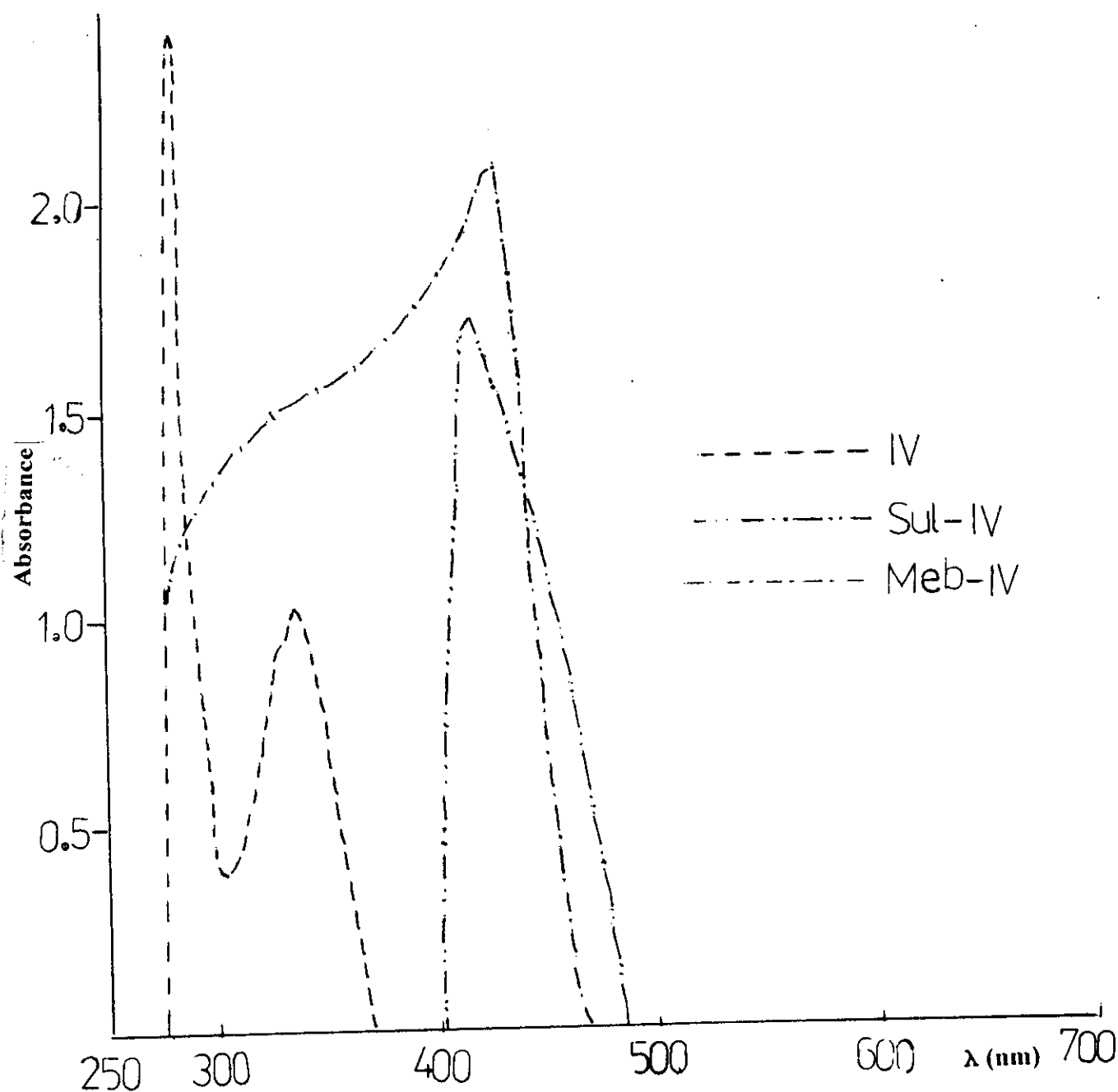


Fig. (28) *The electronic absorption spectra of reagent (IV) and its complexes with Sul and Meb as nujol mull.*

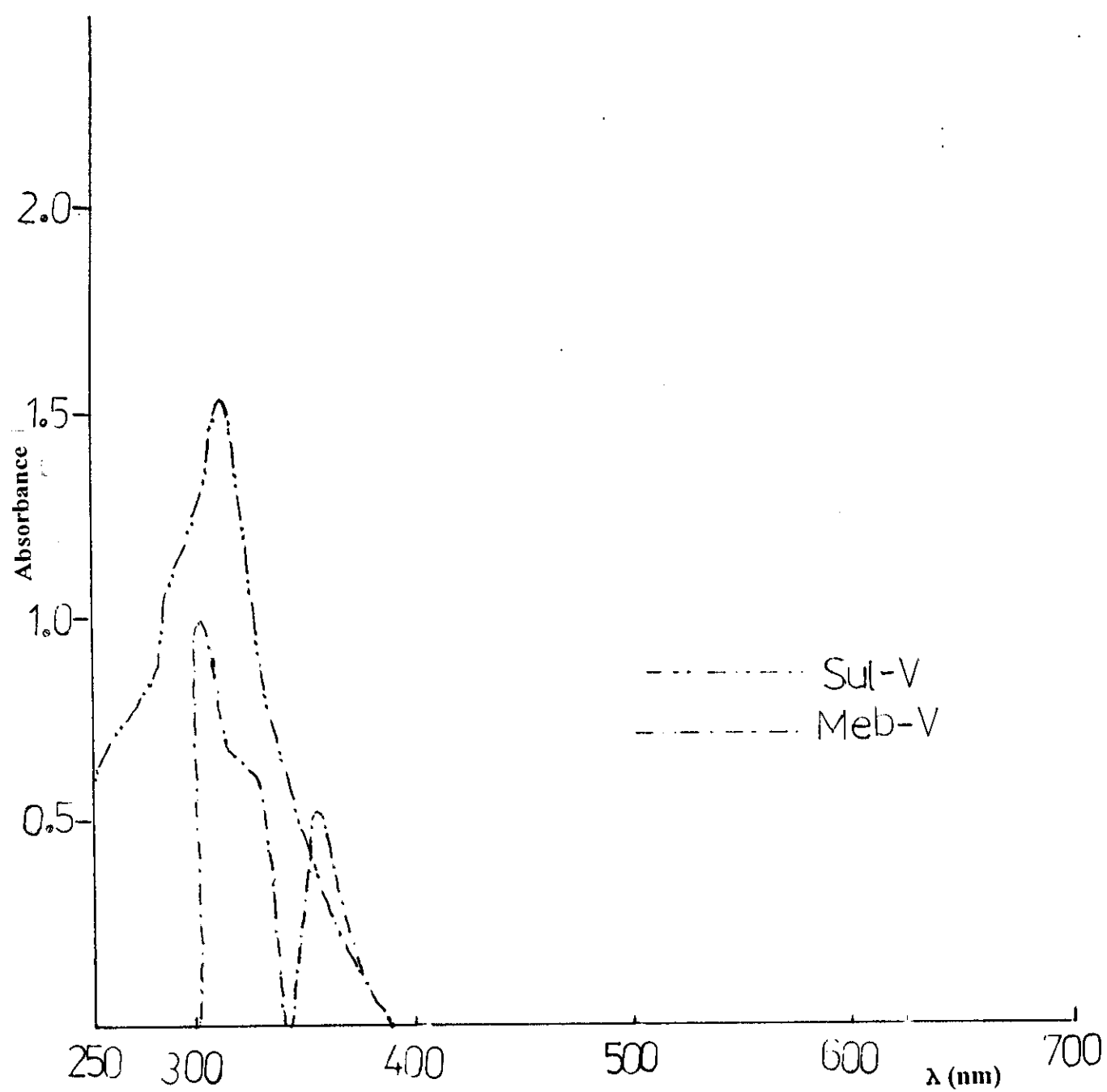


Fig. (29) The electronic absorption spectra of reagent (V) complexes with Sul and Meb as nujol mull.

III- Equilibrium studies and methods of calculations:-

Based on the important observation of *Bensi- Hildebrand*⁽⁵⁸⁾ and the subsequent interpretation of the phenomenon by *Mulliken*⁽⁵⁹⁾, several equations have been derived and tested for the evaluation of the equilibrium constant (k) and molar extinction coefficient (ϵ) of molecular complexes from spectrophotometric data.

In all these equations a single parameter, either k or ϵ and the product $k\epsilon$ appear either in the slope or in the intercept. Therefore, only one parameter can be evaluated independently while the other is obtained from the product $k\epsilon$. The reported values of K and ϵ showing a fair constancy among the values obtained by different investigators for strong complexes but deviate widely for weak ones. Although criteria for meaningful separation of many authors⁽⁶⁰⁾, necessary equation for independent evaluation of K and ϵ have not been yet reported.

Nagakura⁽⁶¹⁾, used a more simple equation applicable to the region of charge transfer bands and was given as:

$$K_{CT} = \frac{C_D (A_0 - A) + \bar{C}_D (A - A_0)}{C_D \cdot \bar{C}_D (\bar{A} - A)}$$

Where: A_0 , A and \bar{A} are the absorbances measured at fixed wave lengths, and the concentrations of the donor (drug) are C_D and \bar{C}_D respectively, while those of acceptors are equal.

Although optical measurements are often made only at wavelength for which the absorbance of the intermolecular CT band is at maximum, yet it is desirable that measurements are made over a range of wavelengths. *Liptay*⁽⁶²⁾ suggested a general method for treating such results to calculate equilibrium constants and molar absorptivities for the studied CT complexes.

The association constant (**K**) and molar extinction coefficient (**ε**) of the CT complexes studied were determined utilizing the rearranged form⁽⁶³⁾ of the *Bensi-Hildebrand* equation⁽⁵⁸⁾.

$$[A] + [D] = \frac{\epsilon L [A] [D]}{d} - \frac{1}{k}$$

Where, **[A]** and **[D]** are the initial molar concentrations of acceptor and donor respectively, (**L**) is the light path length (cm) and (**d**) the optical density.

The values of **ε** and **k**, cited in Table (11), were determined from the gradient and negative intercept of the linear plots of **[A] + [D]** against **[A] [D]/d** as shown in Fig.(30). This method enables to determine **k** and **ε** values independently for the CT complexes under the condition of constant **[A]** by taking **[D] >> [A]** (where **[D] = 10⁻² M** while **[A] = 10⁻³ M**).

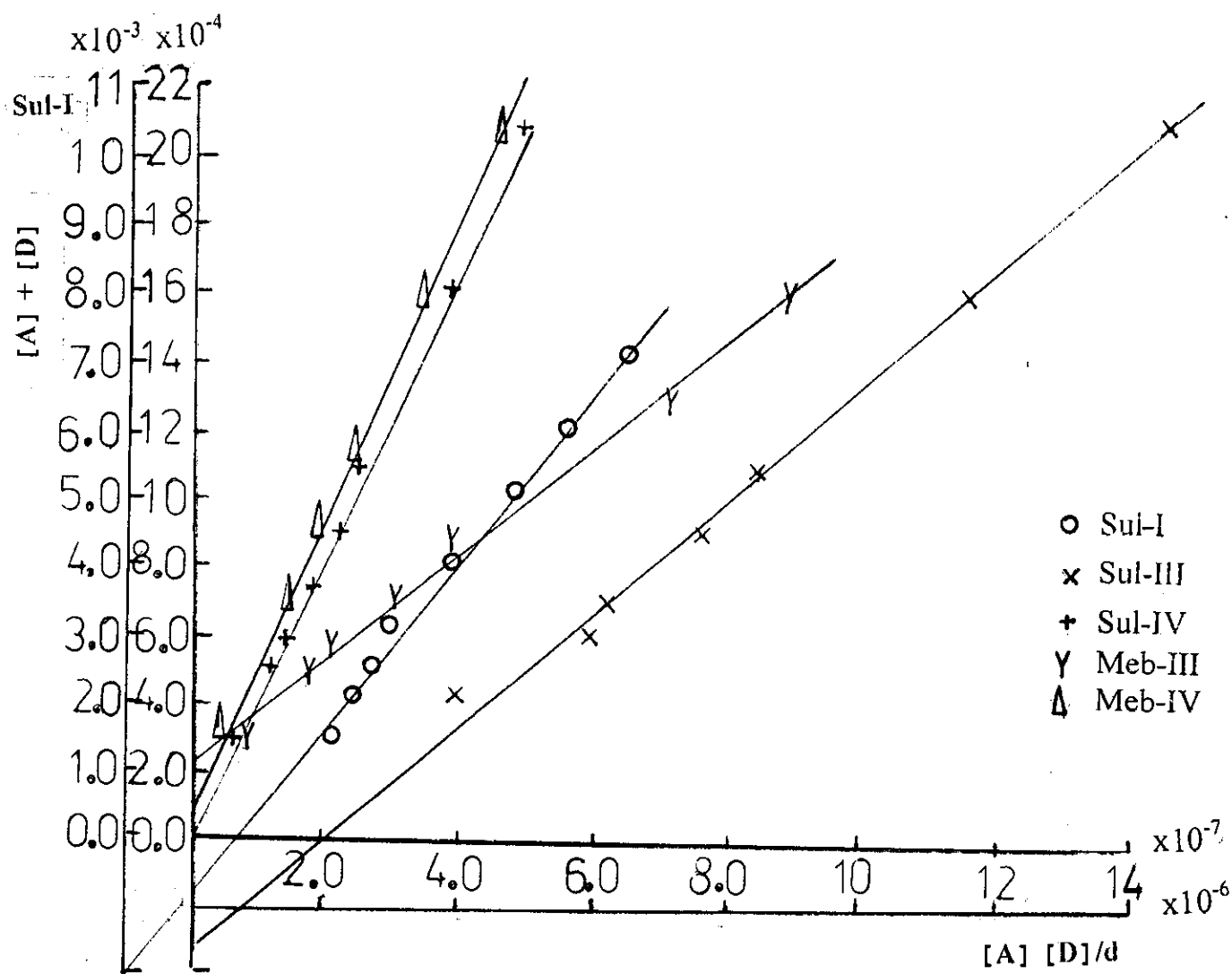


Fig. (30) Linear plot of Bensi-Hildebrand equation for some complexes.

Table (11):Spectral data for complexes of sulfamethoxazole and mebeverine-HCl complexes.

Complex	λ_{max} (nm)	C (eV)	E_{CT} (eV)	ϵ_{CT} (L mol ⁻¹ cm ⁻¹)	Log K_{CT}
<i>Sul-I</i>	540	4.09	2.30	1.14×10^3	2.69
<i>Sul-II</i>	535	4.04	2.32	-	-
<i>Sul-III</i>	405	4.59	3.07	1.66×10^3	3.52
<i>Sul-IV</i>	418	4.19	2.97	4.16×10^3	4.30
<i>Sul-V</i>	315	4.51	3.95	-	-
<i>Meb-I</i>	350	3.94	3.55	-	-
<i>Meb-II</i>	530	4.12	2.34	-	-
<i>Meb-III</i>	371	4.61	3.35	1.54×10^3	3.60
<i>Meb-IV</i>	425	4.14	2.92	4.00×10^3	4.00
<i>Meb-V</i>	364	4.55	3.41	-	-

Where:

λ_{max} , Maximum absorption wavelength of complex

E_{CT} , Transition energy

ϵ_{CT} , Molar extinction coefficient

K_{CT} , Equilibrium constant

C, The coulombic force

IV- IR spectral studies of CT complexes:

A substantial part of the knowledge concerning the mode of interaction in molecular complexes can be easily achieved by comparing the IR absorption spectra of the free components with those of the CT complexes⁽⁴¹⁾.

The IR spectra of the solid complexes formed from the electron donors, sulfamethoxazole (Sul) and mebeverine hydrochloride (Meb); with the electron acceptors, o-chloranil, chloranilic acid, 2,4 dinitrophenol, picric acid and 3,4 dinitrobenzoic acid, (I, II, III, IV and V, respectively) of stoichiometric ratio D/A (1:1) are studied and compared with those of the free drugs. The spectra are represented in Figs. (31-47), the absorption frequencies of the most important diagnostic bands are listed in Tables (12) and (13).

Inspection of the IR spectra of the pure electron donors and pure electron acceptors in comparison to those of the CT complexes reveal the following:

- 1- For the electron acceptors II, III, IV and V; the strong band observed at $3263\text{--}3093\text{ cm}^{-1}$ is due to the stretching vibration of the OH group (ν_{OH}) which disappears partially or completely from the spectra of the complexes with reagents III, IV and V. This band displayed a shift to higher frequency (3271 cm^{-1}) in case of the complex with reagent II. This is probably due to a decreased strength of the intramolecular hydrogen bond of the second OH group that not contributing in complex formation.
- 2- For the electron acceptors III, IV and V; the bands at about 1326 and 1600 cm^{-1} which are due to the symmetric and asymmetric stretching

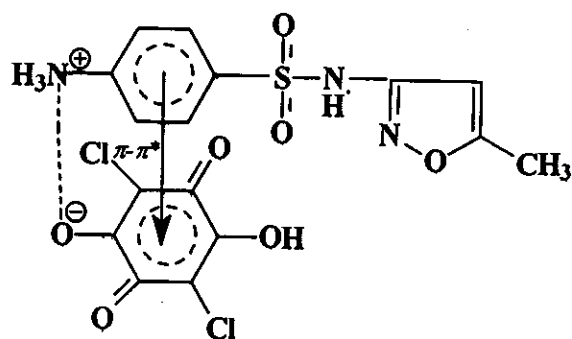
vibrations of NO_2 group (ν_{NO}) possess a shift in various directions showing different types of CT interactions.

- 3- For the electron acceptors III, IV and V; the bending vibrations of C-H ($\gamma_{\text{C-H}}$) possess shift to lower frequencies as indicating increase in electron density on the acceptors rings and hence complex formation.
- 4- For the electron donor (Sul), the sharp-medium band at 3376 cm^{-1} ; due to the stretching vibration of NH_2 group (ν_{NH}), disappears in complexes with reagents II, III, IV and V. While a new band appears within the range $2886\text{--}2537\text{ cm}^{-1}$ due to the stretching vibration of NH_3^+ group that results through proton transfer from the acceptor molecule to the NH_2 group of the donor. The bending vibration of the NH_2 group (ν_{NH}) in case of complex with reagent I exhibits a shift to higher wave number (1597 cm^{-1}) with a decrease in its intensity.
- 5- The stretching vibrations of SO_2 group ($\nu_{\text{S=O}}$) possess a shift to higher frequency at about $1366\text{--}1254$ and 1155 cm^{-1} for asymmetric and symmetric vibrations due to electron delocalization on the drug (Sul) molecule taking place through complex formation.
- 6- The strong-medium band at 900 cm^{-1} , due to the isolated hydrogen atoms on the heterocyclic ring moiety of (Sul), is shifted to $1001\text{--}913\text{ cm}^{-1}$, while the band at 830 cm^{-1} , due to the out-of-plane bending ($\gamma_{\text{C-H}}$) for two adjacent hydrogen atoms of the aromatic moiety exhibit a shift to $887\text{--}832\text{ cm}^{-1}$ due to decreased electron density on the donor rings as a result of complex formation.
- 7- For the electron donor (Meb), the stretching vibrations of both $\nu_{\text{C=O}}$ and $\nu_{\text{C=O}}$ possess a shift to higher frequency at about 1270 and 1722 cm^{-1} ,

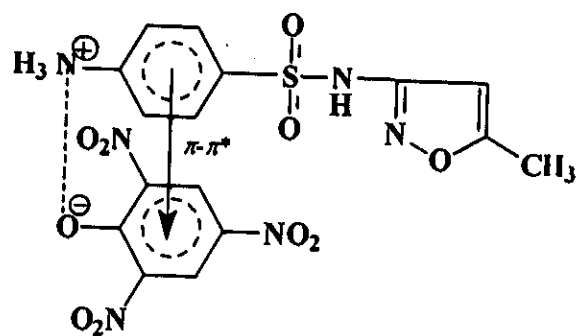
respectively indicating a decrease in the electron density on the donor molecule on complexation with acceptor V.

- 8- A new stretching vibration band specific for NH^+ group (ν_{NH^+}) appears at about $2847\text{-}2635\text{ cm}^{-1}$ due to proton transfer from the acceptor molecule during complex formation with Meb.
- 9- The stretching vibration band of $\nu_{\text{C-H}}$ of (Meb) at 2964 cm^{-1} exhibits a shift to higher frequency at about 2969 cm^{-1} .
- 10- The bending vibration of $\gamma_{\text{C-H}}$ of (Meb) possesses a shift to higher frequency near 839 cm^{-1} .

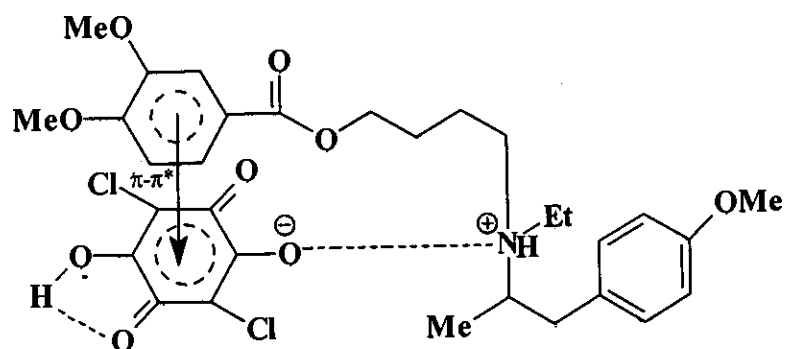
From the preceding discussion, it can be concluded that the CT complex formation for Sul-I and Meb-I takes place through $\pi\text{-}\pi^*$ transition only, while in case of other molecular complexes, the interaction takes place through both $\pi\text{-}\pi^*$ and $n\text{-}\pi^*$ transitions.



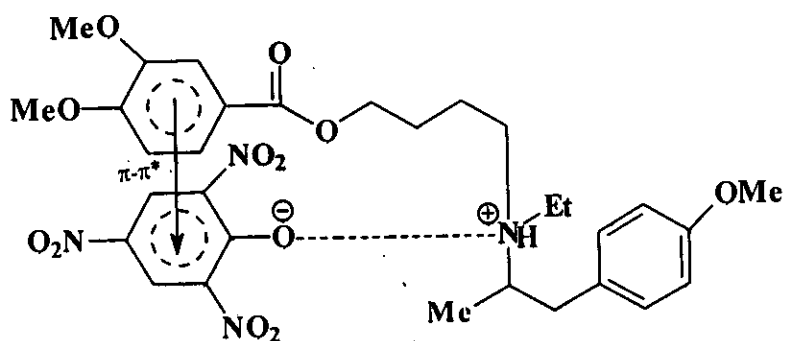
*Sul-II complex



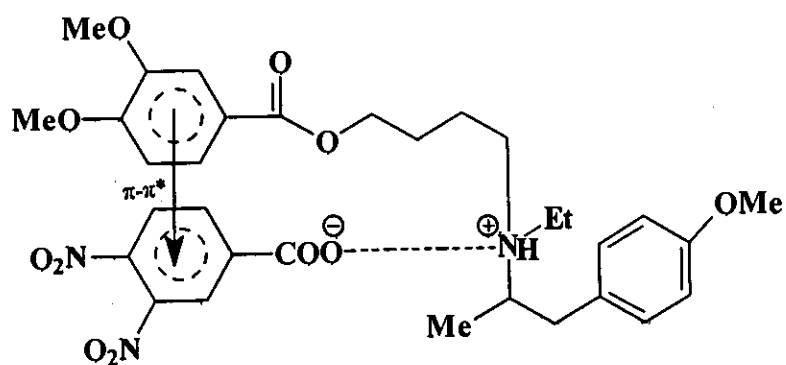
*Sul-III complex



Meb-II complex



***Meb-IV complex**



***Meb-V complex**

Table (12): IR vibrational frequencies of sulfamethoxazole and its complexes with reagents (I, II, III, IV and V).

Compound	ν_{O-H} (cm ⁻¹)	ν_{N-H}	γ_{N-H}	$\nu_{NH_3}^+$	$\nu_{S=O}$ (Asymmetric & Symmetric)	$\nu_{C=O}$	ν_{C-O}	ν_{NO} (Asymmetric & Symmetric)	γ_{C-H}	
									Adjacent H (Aromatic)	Isolated H (Heteroring)
Sul (Donor) I	-	3376	1624	-	1310, 1145	-	1088	-	830	900
(Acceptor)	-	-	-	-	-	1681	-	-	-	-
Sul-I (Complex)	-	3293	1597	2804	1392, 1161	1665	1088	-	887	1001
II	3263	-	-	-	-	1666	1259	-	-	-
Sul-II	3271	-	1619	3415	1366, 1155	1619	1254	-	851	988
III	3255	-	-	-	-	-	1253	1624, 1332	870	-
Sul-III	3262	3083	1521	2886	1339, 1155	-	1155	1629, 1339	850	920
IV	3103	-	-	-	-	-	1089	1537, 1326	909	-
Sul-IV	3088	3262	1531	2870	1328, 1150	-	1093	1644, 1328	845	913
V	3093	-	-	-	-	1707	1275	1537, 1347	850	919
Sul-V	3093	3298	-	2537	1353, 1151	1706	1285	1624, 1353	832	924

Table (13): IR vibrational frequencies of mebeverine HCl and its complexes with reagents (I, II, III, IV and V).

Compound	ν_{O-H} (cm ⁻¹)	ν_{N-H}^+	$\nu_{C=O}$	ν_{C-O}	ν_{N-O}	ν_{C-H}	γ_{C-H} Adjacent H (Aromatic)
Meb (Donor)	-	-	1717	1222	-	2964	764
I (Acceptor)	-	-	1681	-	-	-	-
Meb-I (Complex)	-	2839	1708	1270	-	2969	828
II	3263	-	1666	1259	-	-	-
Meb-II	3231	2840	1707	1270	-	2967	839
III	3255	-	-	1253	1624, 1332	-	870
Meb-III	-	2635	1707	1269	1602, 1341	2942	834
IV	3103	-	-	1089	1537, 1326	-	775
Meb-IV	3085	2847	1708	1268	1630, 1341	2927	762
V	3093	-	1707	1275	1537, 1347	-	850
Meb-V	3103	2838	1722	1270	1598, 1345	2958	817

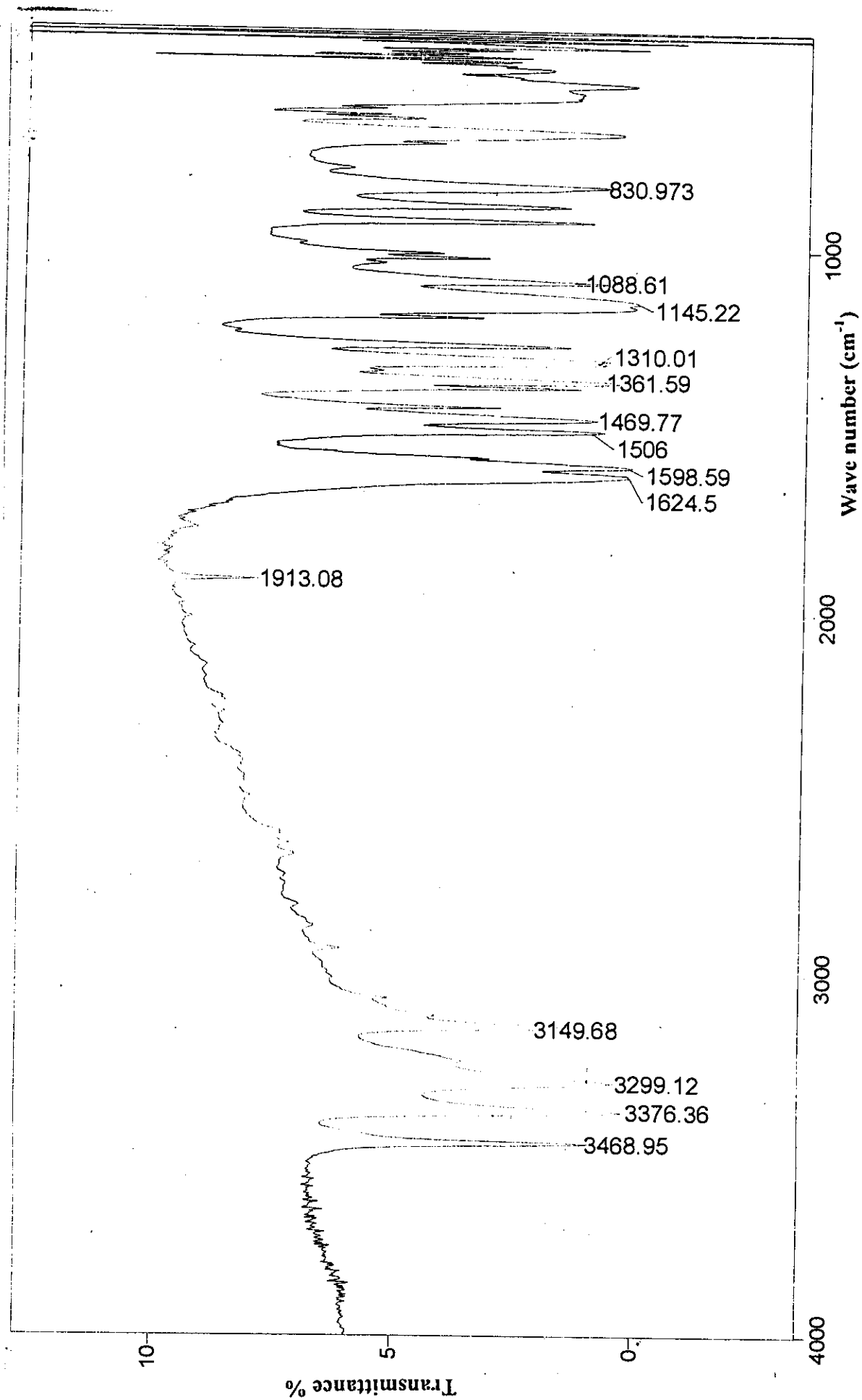


Fig. (31): IR spectra of sulfametoxazole (Sul).

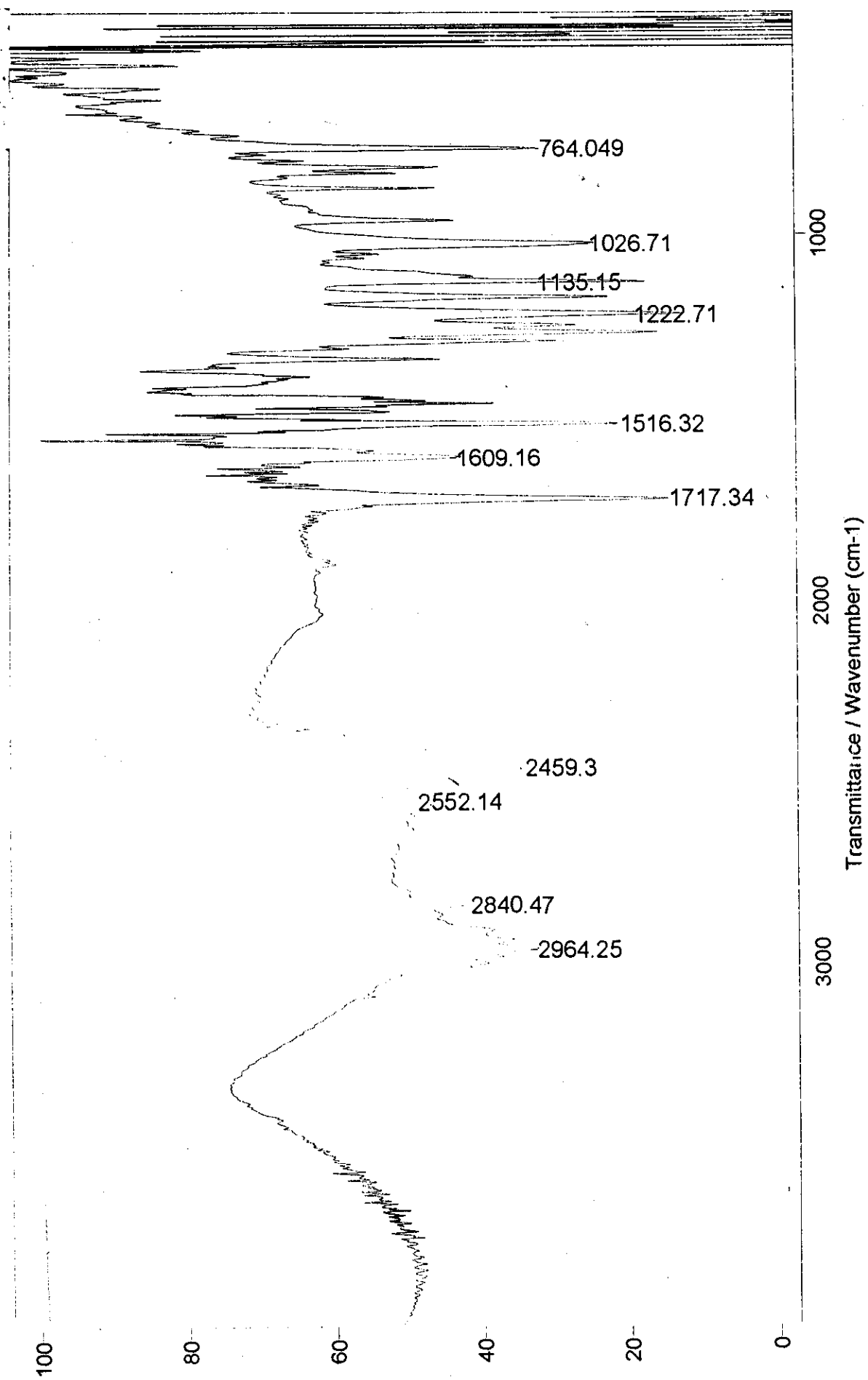


Fig. (32): IR spectra of mebeverine HCl (Meb).

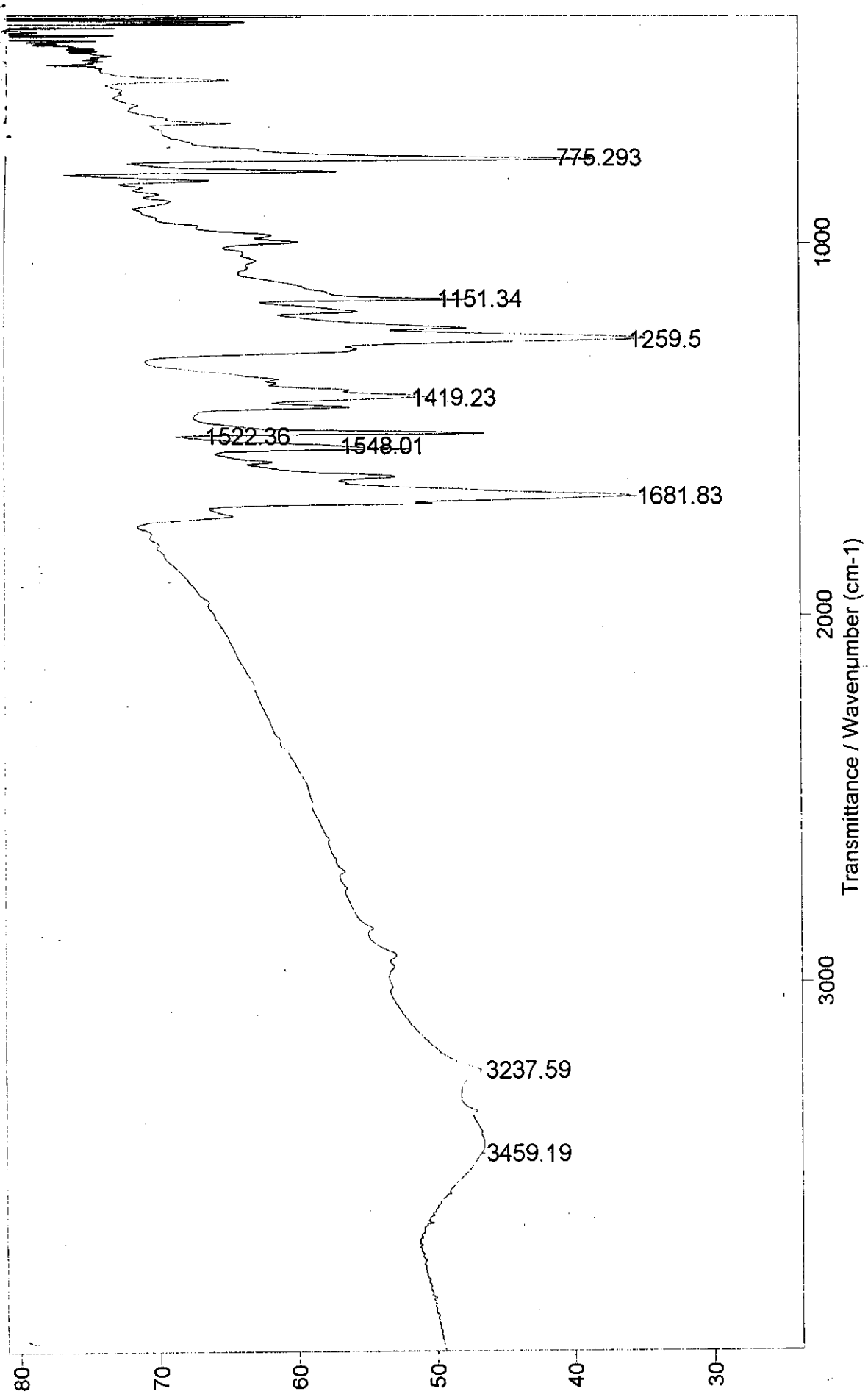


Fig. (33): IR spectra of o-chlororanil (I).

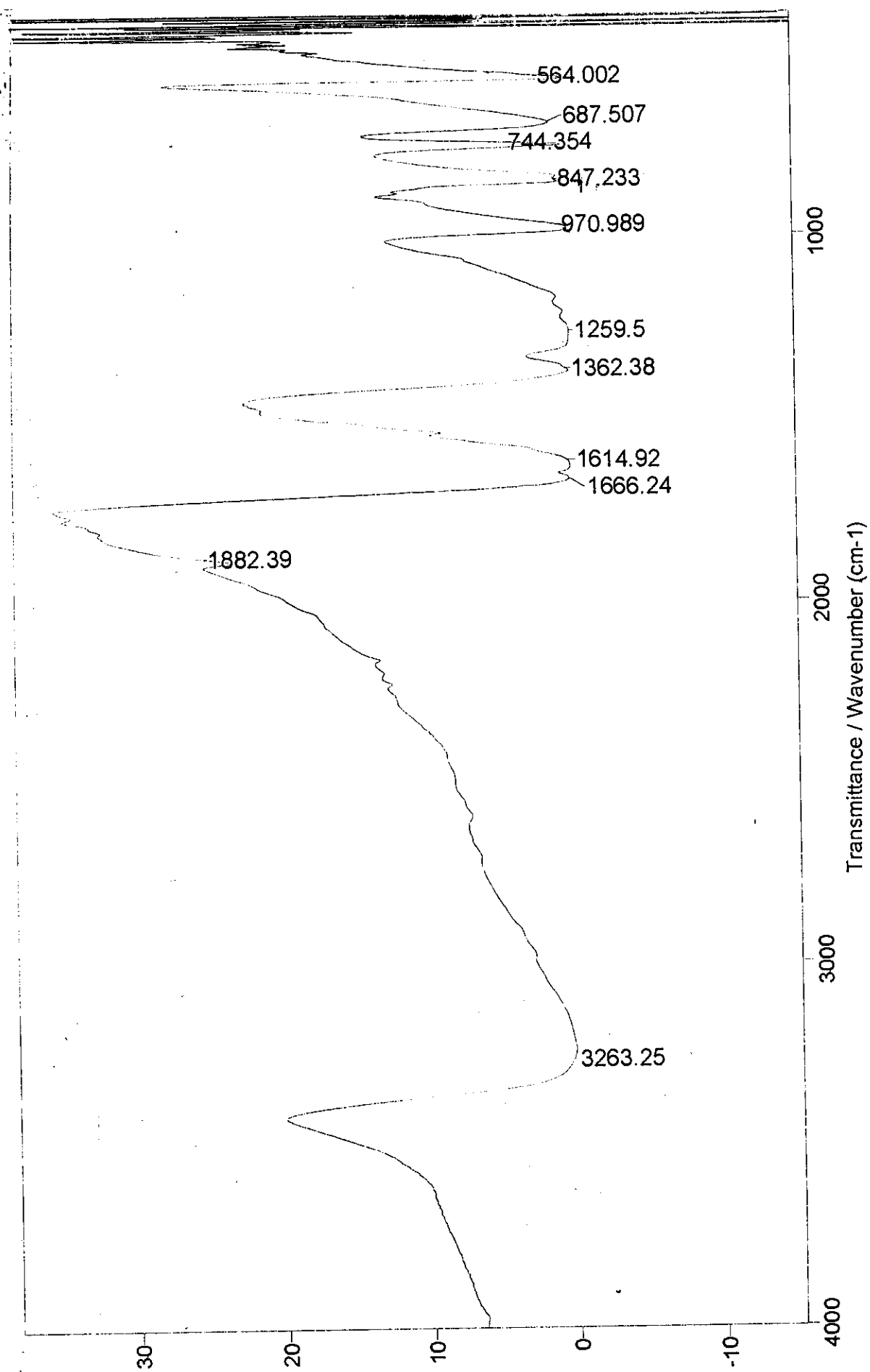


Fig. (34): IR spectra of chloranilic acid (II).

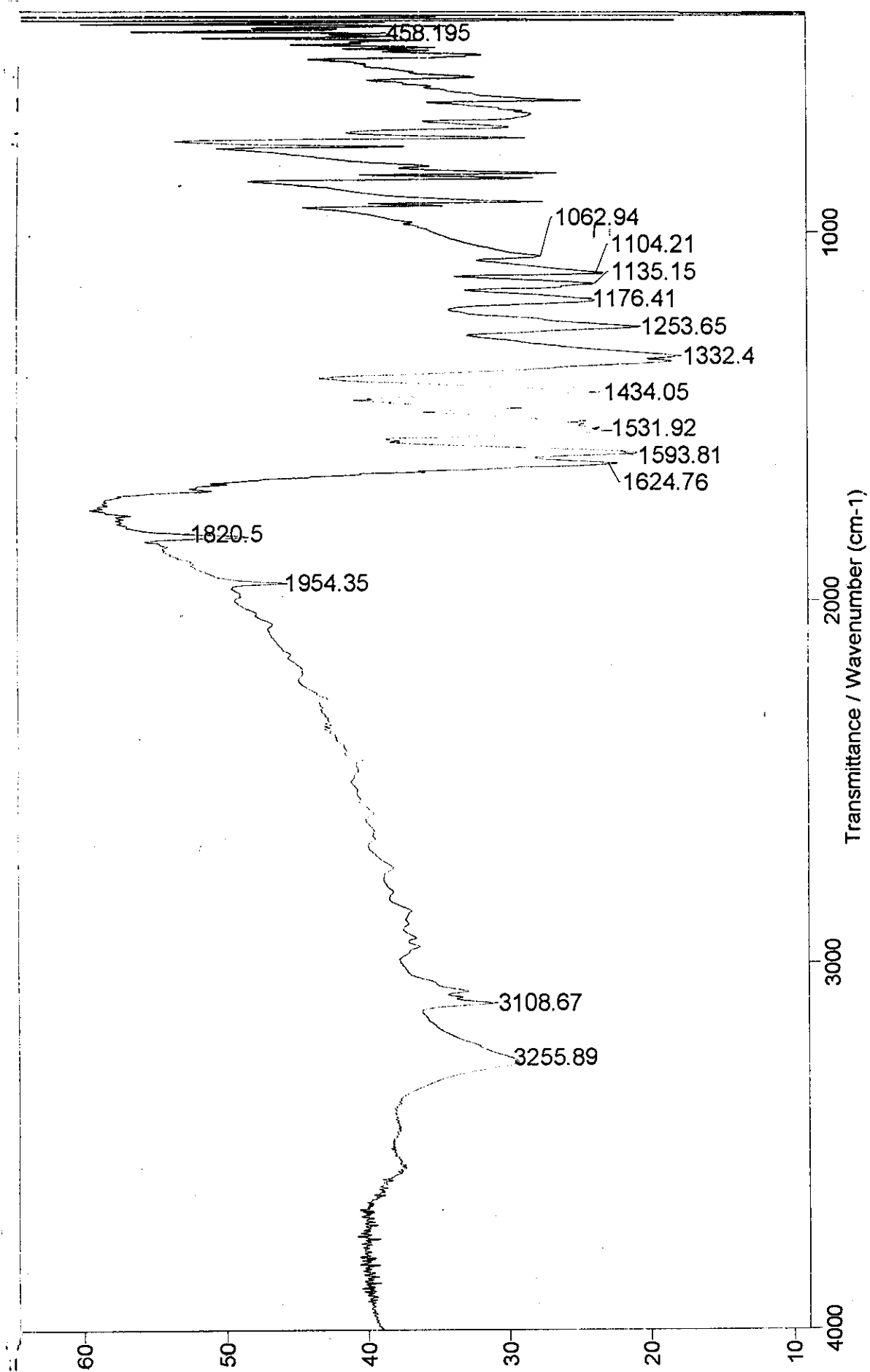


Fig. (35): IR spectra of 2,4 dinitrophenol (III).

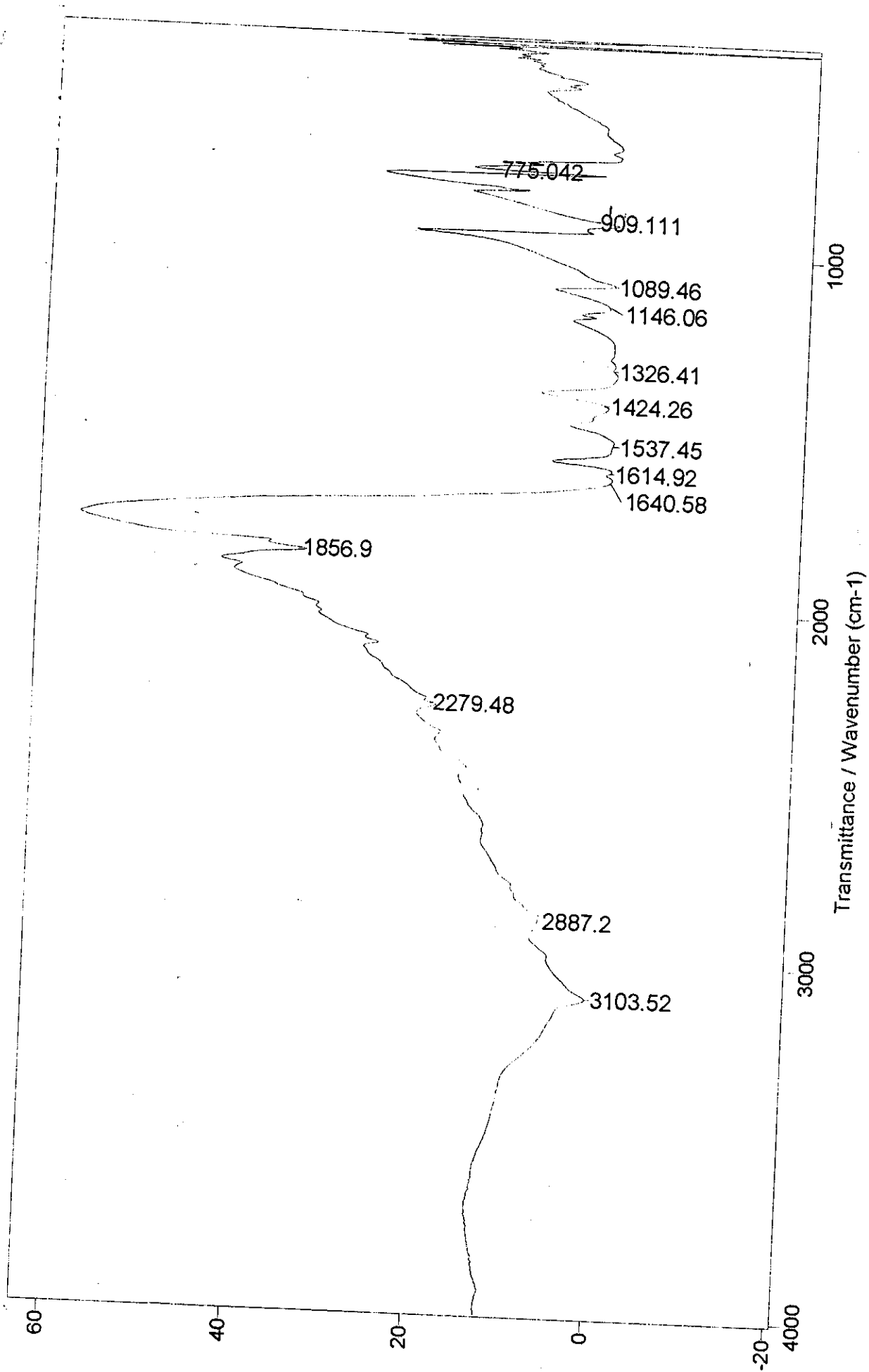


Fig. (36): IR spectra of 2,4,6 trinitrophenol (IV).

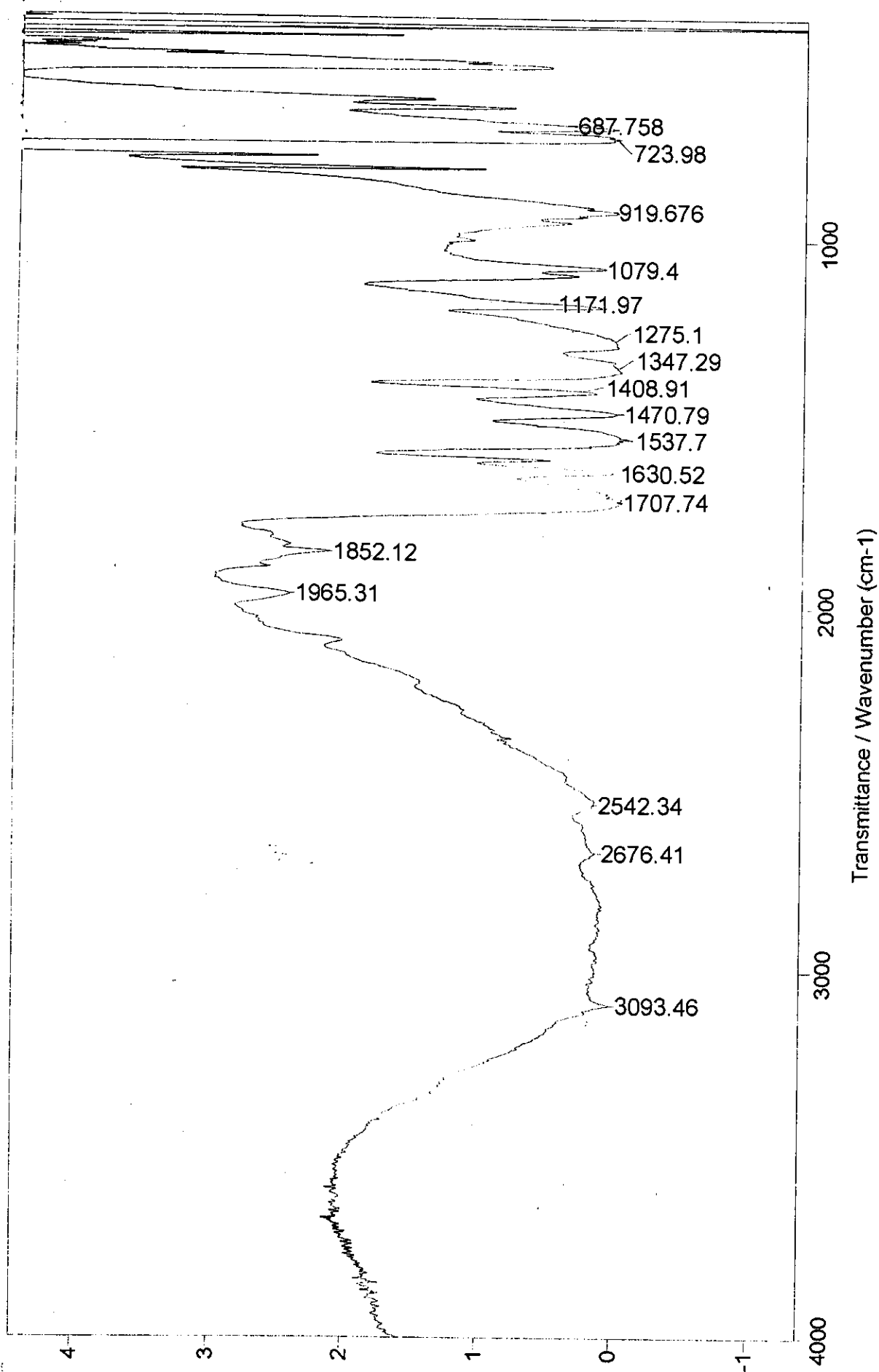


Fig. (37): IR spectra of 3,4 dinitrobenzoic acid (V):

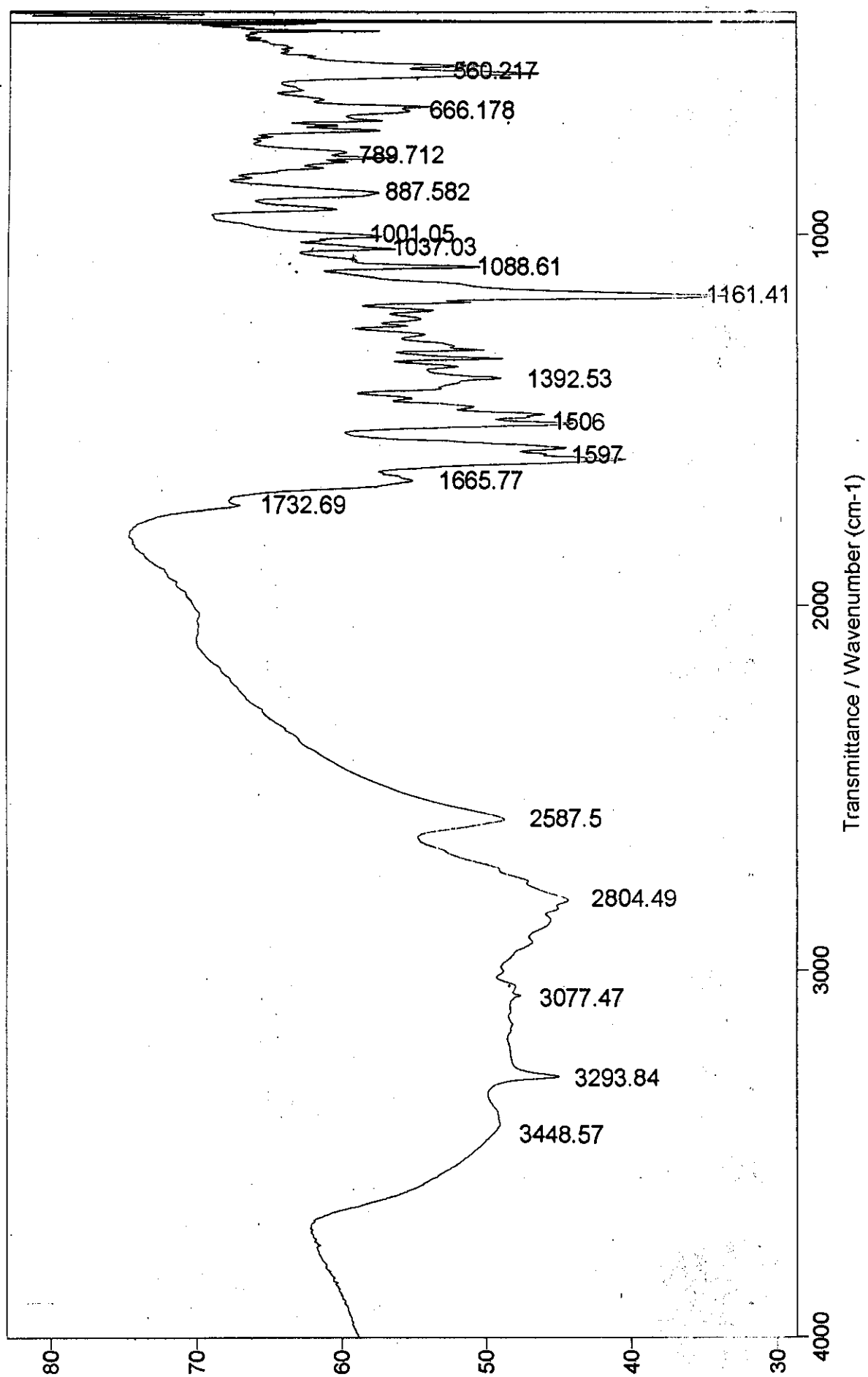


Fig. (38): IR spectra of Sul-I complex.

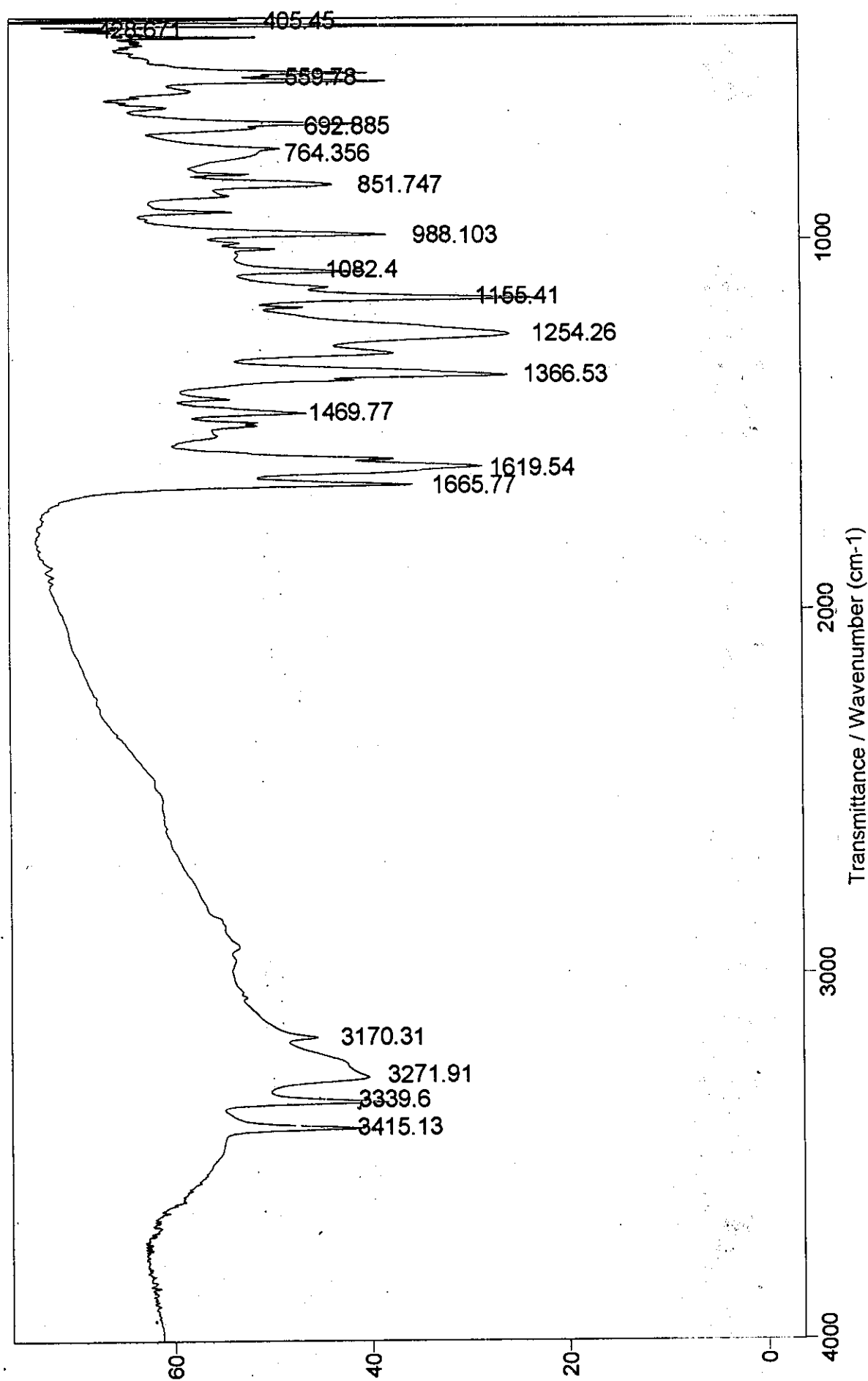


Fig. (39): IR spectra of Sul-II complex.

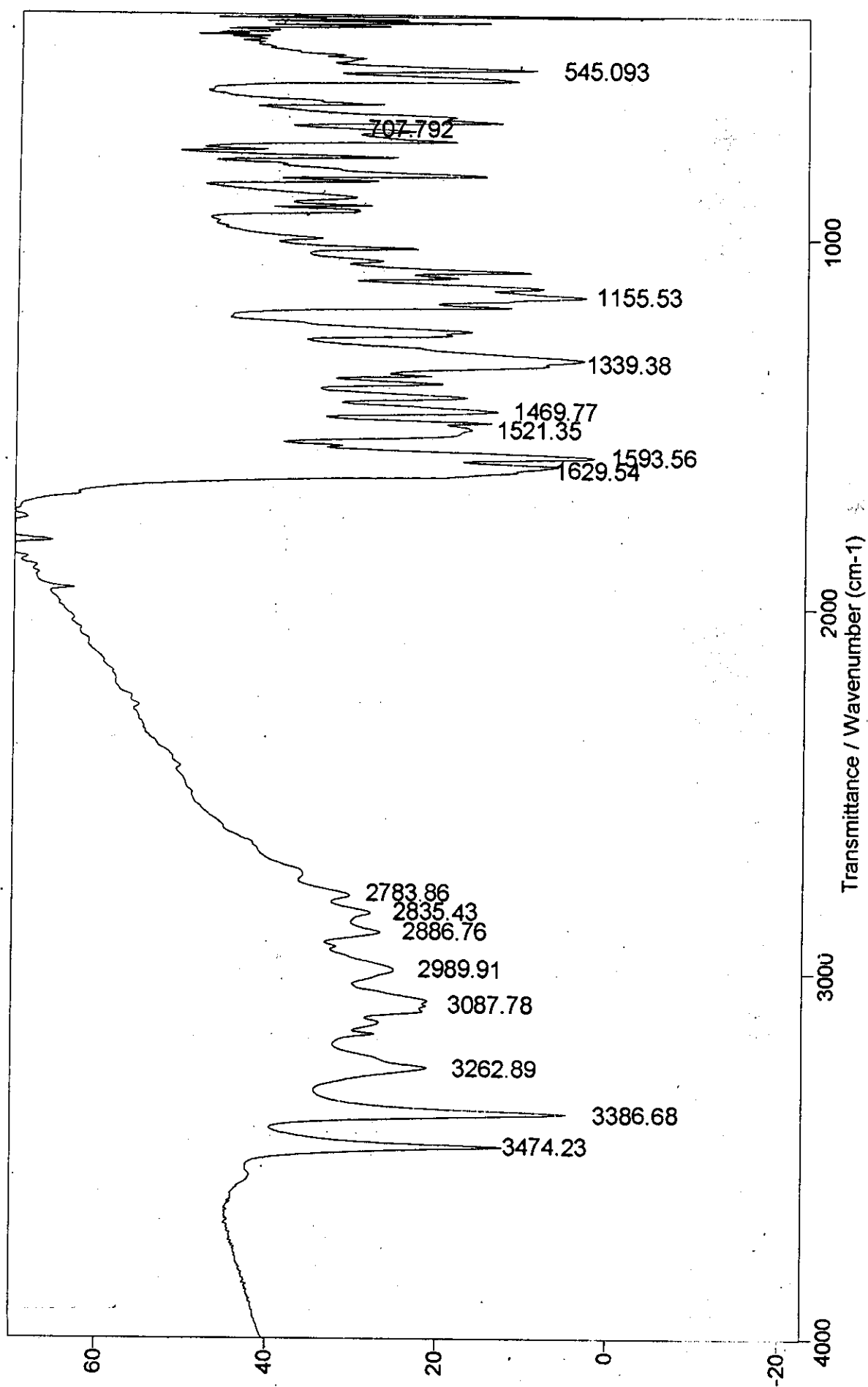


Fig. (40): IR spectra of Sul-III complex.

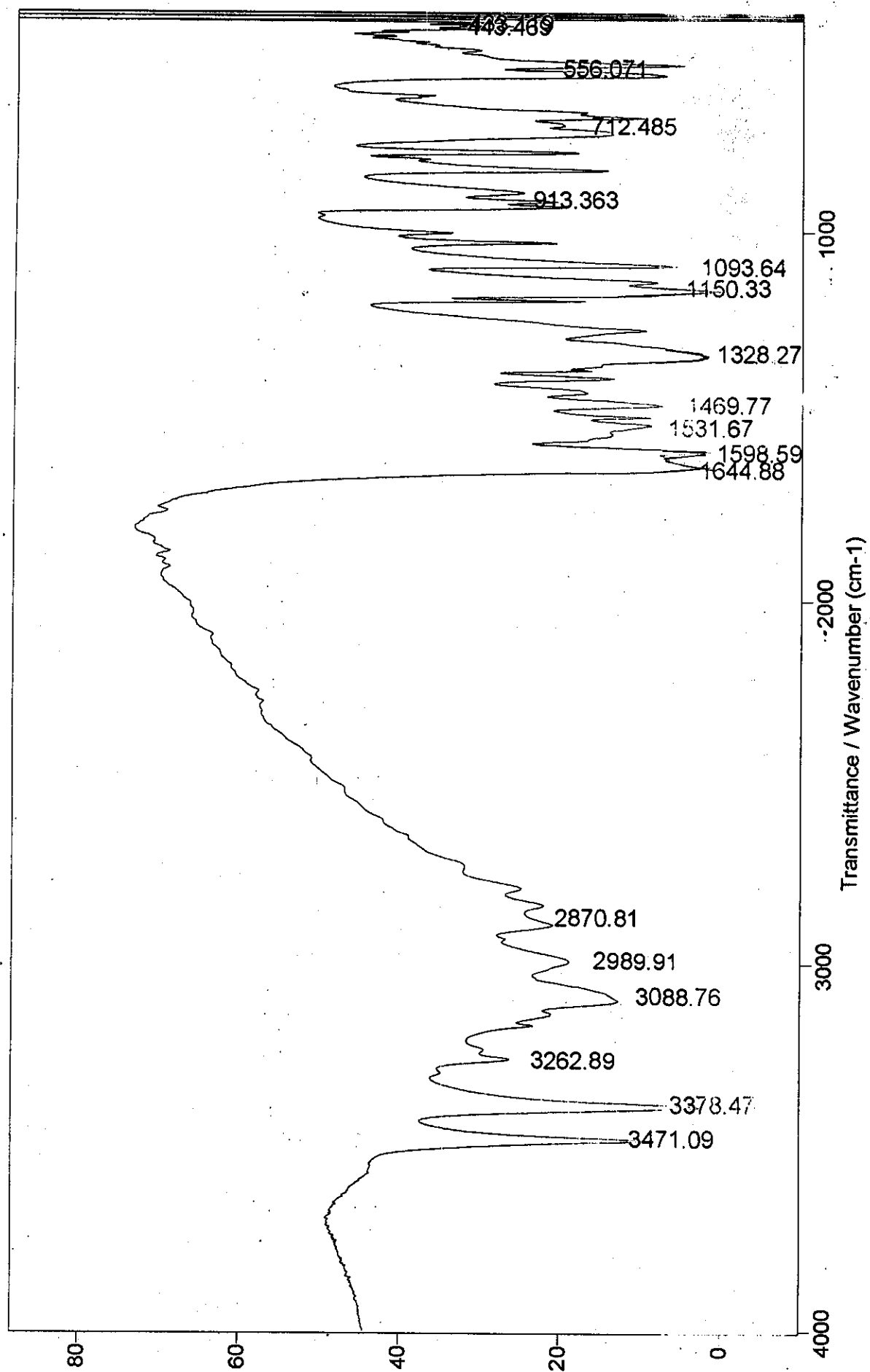


Fig. (41): IR spectra of Sul-IV complex.

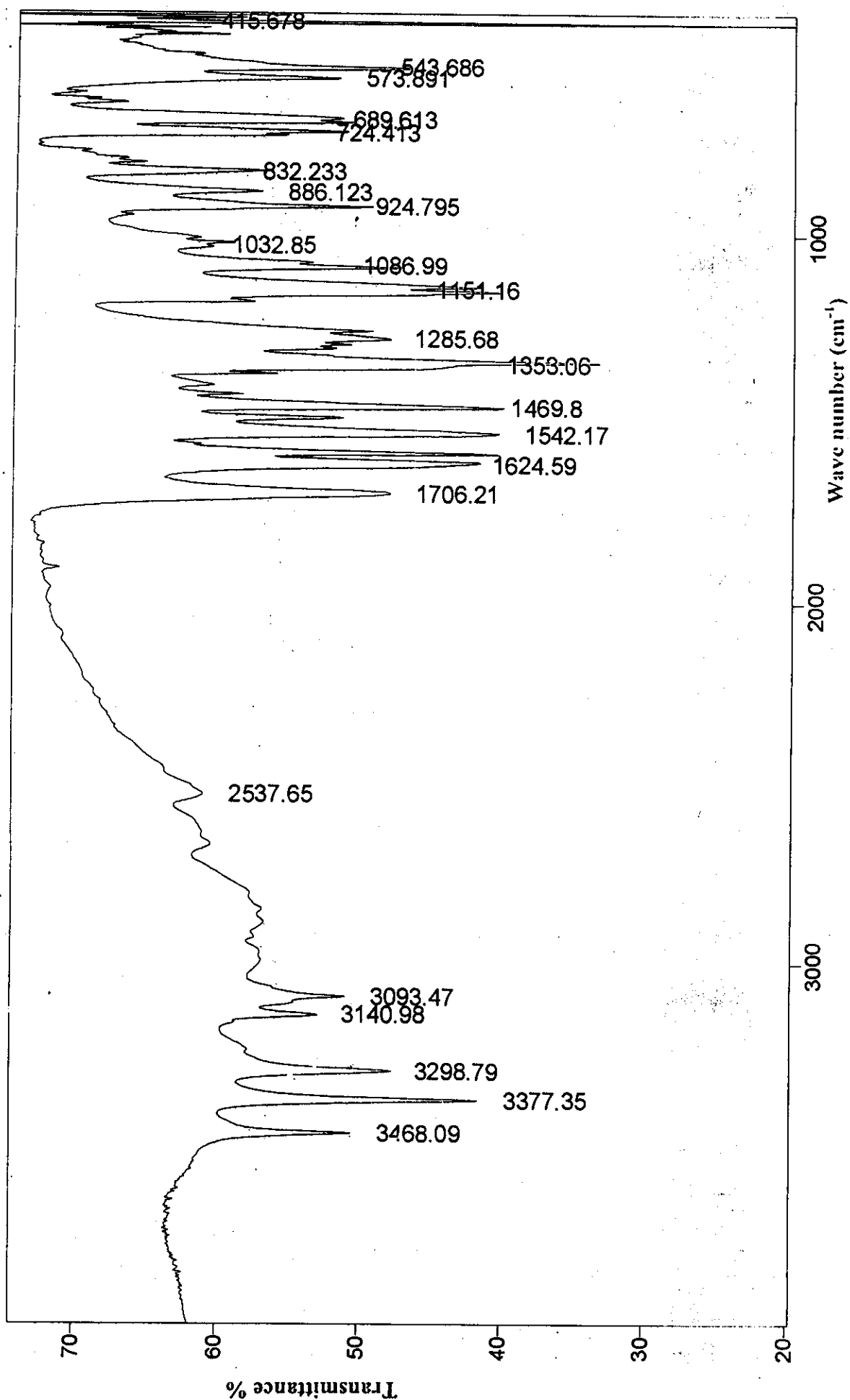


Fig. (42): IR spectra of Sul-V complex.

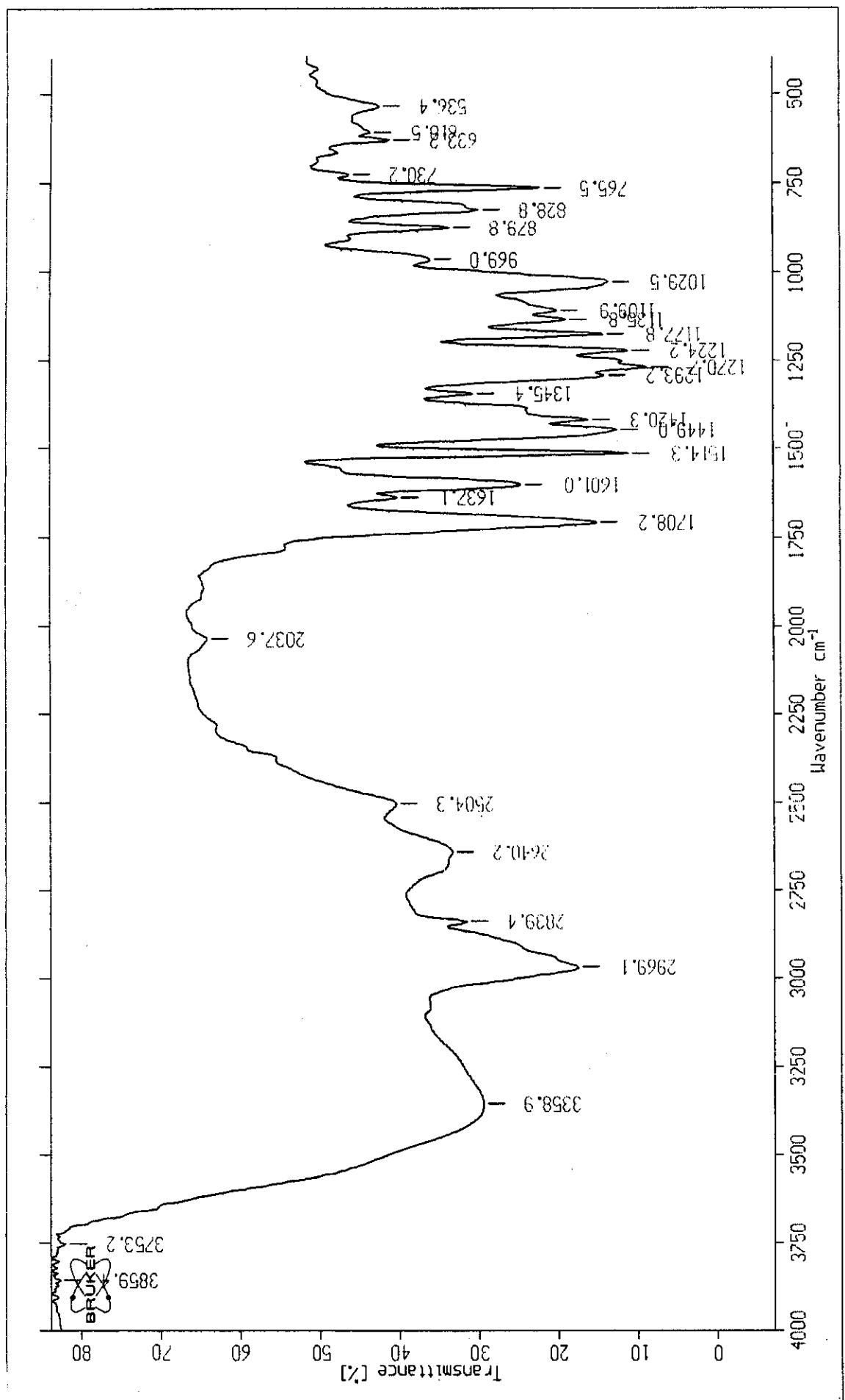


Fig. (43): IR spectra of Meb-I complex.

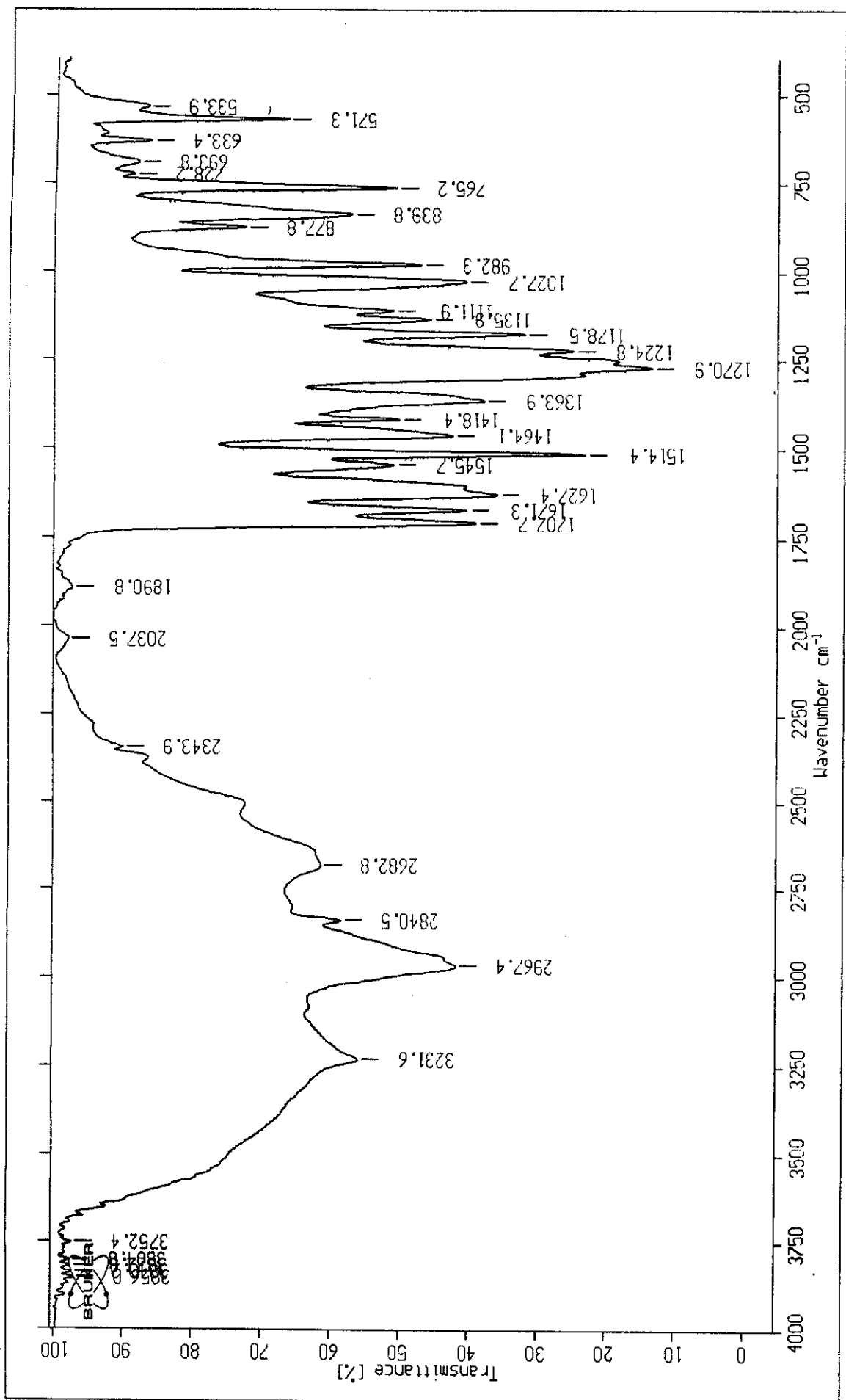


Fig. (44): IR spectra of Meb-II complex.

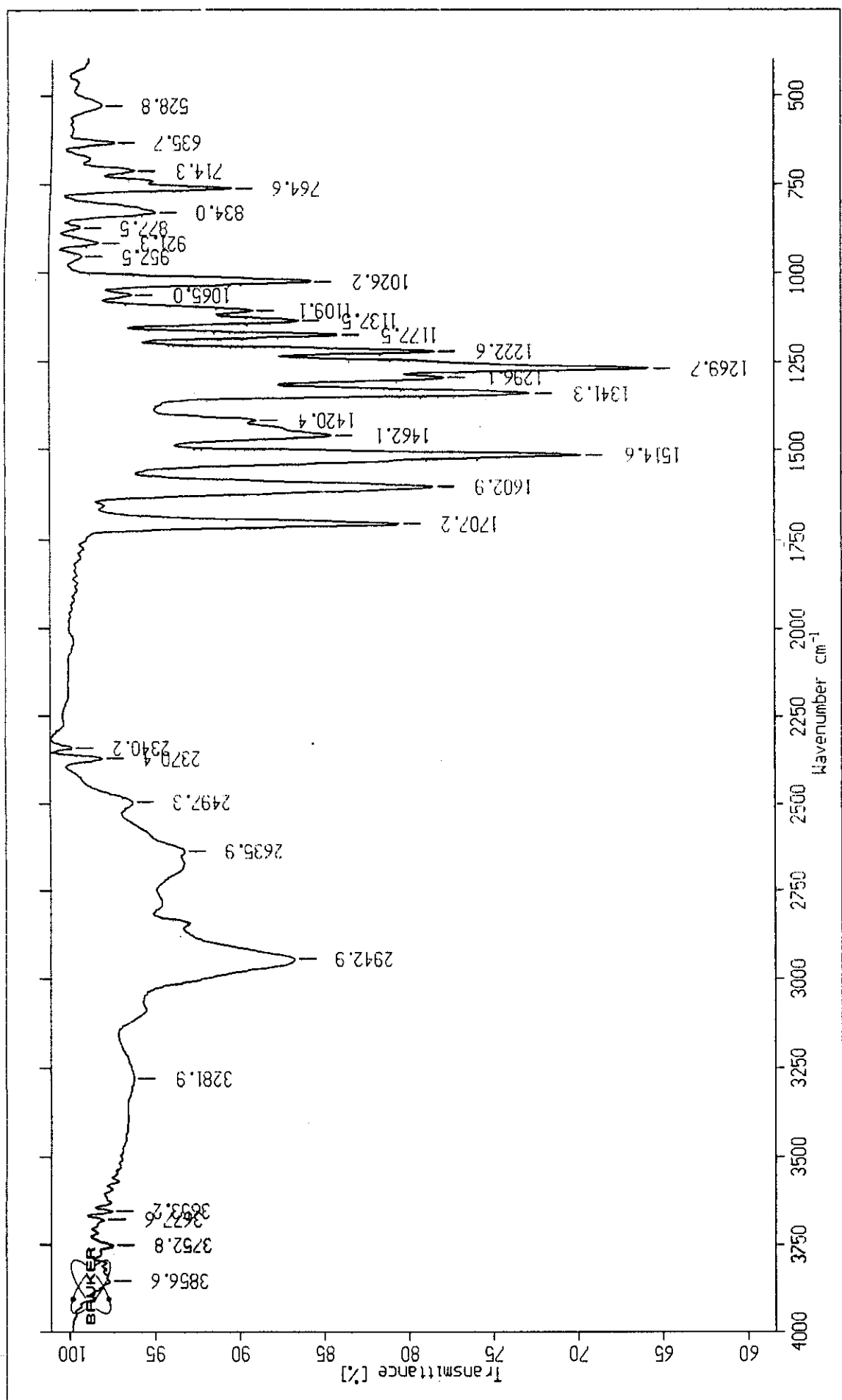


Fig. (45): IR spectra of Meb-III complex.

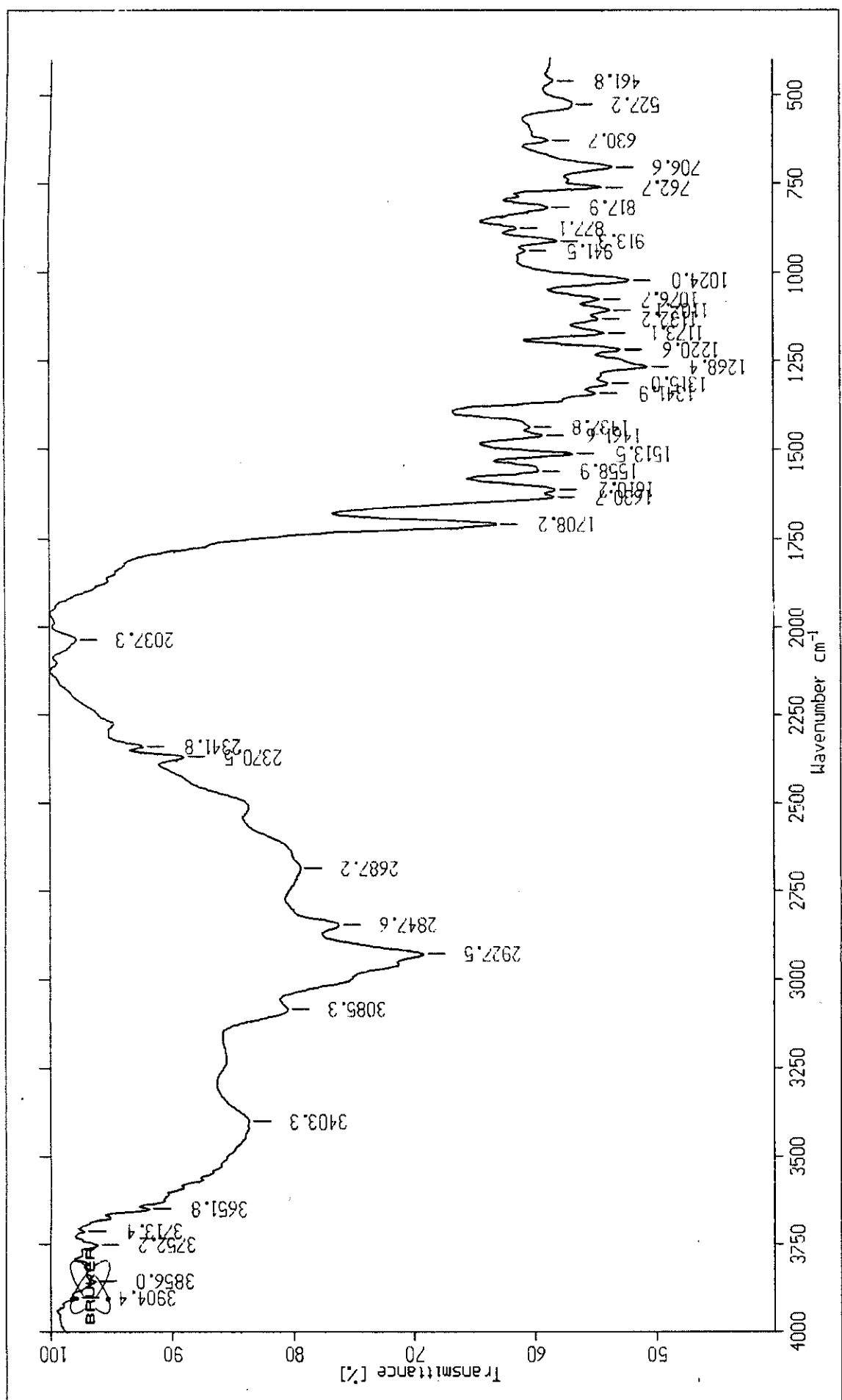


Fig. (46): IR spectra of Meb-IV complex.

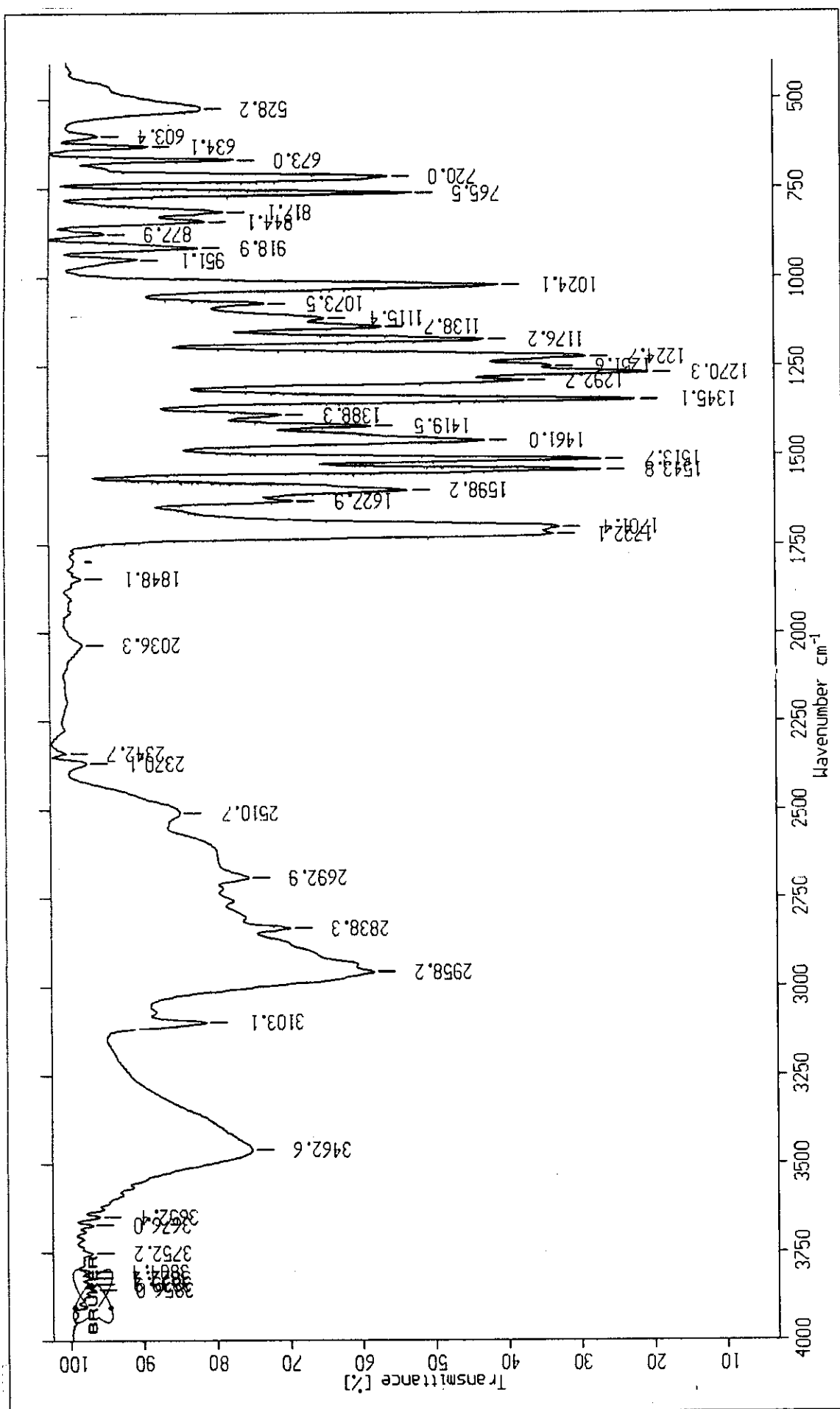


Fig. (47): IR spectra of Meb-V complex.